

RHODES UNIVERSITY
LIBRARY

Cl. No. TR 03 - 159

BRN 619174998

The Development of a Baculovirus
Expression System for the Production
of *Helicoverpa armigera stunt virus*
Capsids for use in the Encapsidation
of Foreign Molecules

Thesis submitted in fulfilment of the requirements of
Masters of Science in Micobiology
Rhodes University 2003-05-07

K. Mosisili
Supervisor: Prof. R. Dorrington

TR

03 - 159

**Dedicated to my brother Maile
(1979-2002)
Together we were indestructible**

ACKNOWLEDGEMENTS

I would like to thank my supervisor Prof. R Dorrington for her support and guidance over the past two years. I would like to especially thank her for always being able to see the positive in all negatives.

I would also like to say a big thank you to all the members of Lab 417, both past and present. Mez, thanks for all the encouragement over the past 3 years you have been a great inspiration to me. Cheryl and Lucy, tissue culture will never be the same for me without you guys.

I would also like to thank Fritz Tiedt for all his help with the EM work.

To my family, thank you for all your love and support especially over the past year. I don't know how I would have made it this far if I didn't have you on my side. This past year was a difficult one for all of us but in typical Bafokeng style we somehow pulled through. I love you all.

To all my friends and everybody else who helped make the past 3 years ones I will never forget, thank you and much love to you all.

ABSTRACT

The capsid protein of *Helicoverpa armigera stunt virus* (HaSV) a $T=4$ insect virus was expressed in *Spodoptera frugiperda* 9 cells using a baculovirus vector. When the insect cells were infected at a high MOI the expressed coat protein assembled into virus-like particles (VLPs) that spontaneously underwent maturation and were morphologically indistinguishable from wild-type HaSV. The VLPs were electron dense when viewed under EM and encapsidated their coat protein mRNA. When Sf9 cells were infected at a low multiplicity of infection (MOI) the expressed capsid protein assembled into procapsids that did not spontaneously undergo maturation. These procapsids underwent autoproteolytic maturation cleavage when they were treated with an acidic buffer. The procapsids were used in the encapsidation of a FITC labelled peptide. The peptide encapsidating VLPs showed an increase in their buoyant density that was not collaborated by an increase in the concentration of the FITC labelled peptide detected when these samples were compared to control samples with similar buoyant densities.

TABLE OF CONTENTS

Table of Contents	<i>Make your own notes. NEVER underline or write in a book.</i>	i-iii
List of Figures		iv-v
List of Tables		vi
CHAPTER 1: Literature Review		
1.1 Introduction		1
<i>Picornavirus</i> -like viruses		2
<i>Nodaviridae</i>		3
<i>Tetraviridae</i>		3
1.2 Taxonomy of <i>Tetraviridae</i>		4
1.3 <i>Nudaurelia</i> β-like viruses		6
1.4 <i>Nudaurelia</i> ω-like viruses		8
<i>Helicoverpa armigera</i> stunt virus (HaSV)		8
<i>Nudaurelia capensis</i> ω virus (N ω V)		11
1.5 Structure, Assembly and Maturation of <i>Nudaurelia</i> ω-like viruses		11
Structure		12
Assembly		14
Quasi-equivalence		14
Assembly of N ω V Capsids		15
Maturation		19
1.6 Heterologous Expression of <i>Nudaurelia</i> ω-like viruses		21
1.7 The Baculovirus Expression System		24
1.8 Biotechnological Applications of Tetraviruses		27
1.9 Project Proposal		31
CHAPTER 2: Introduction		
2.1 Introduction		33
Expression of Recombinant Genes in a Baculovirus		33
CHAPTER 3: Material and Methods		
3.1 Construction of Recombinant Plasmids		38

Construction of pFASTBACHaSV	38
Transformation and Isolation of Recombinant Bacmid DNA	41
3.2 Transfection of Insect Cells	44
3.3 Plaque Assay and Virus Titration	45
50% Tissue Culture Infectious Dose (TCID ₅₀) Assay	46
3.4 Virus Amplification	46
Passage 1 Virus Stocks	46
Passage 2 Virus Stocks	46
Passage 3 Virus Stocks	47
3.5 Baculoviral Expression of Recombinant HaSV in <i>Spodoptera frugiperda</i> cells	49
Determination of the Amount of Viral Inoculum Required for Infections at an Multiplicity of Infection of 5 and 10 using the Plaquing Technique	49
Determination of the Amount of Viral Inoculum Required for Infections at an MOI of 5 and 10 Using the End-point Dilution Method	50
VLP Purification	50
3.6 RNA Isolations and Analysis	52
3.7 Transmission Electron Microscopy (TEM) Analysis	54
3.8 Acid Maturation of Procapsids	54
3.9 FITC Encapsidation of a FITC Labelled Peptide by Recombinant HaSV VLPs	55
CHAPTER 4 Results	
4.1 Construction of Recombinant Baculovirus Expressing HaSV Capsid Precursor Protein	58
Construction of Recombinant Bacmid	58
4.2 Transfection of Insect Cells	59
Establishment of Virus Stocks	59
50% Tissue Culture Infectious Dose (TCID ₅₀) Assay	60
4.3 Baculoviral Expression of Recombinant HaSV in <i>Spodoptera frugiperda</i> cells	61
Effect of Varying MOI on HaSV Capsid Protein Expression	63
Transmission Electron Microscopy Analysis	68
RNA Isolation and Analysis	70

4.4 Encapsulation of Exogenous Molecules by FBHaSV Capsids	71
Acid Maturation	72
FITC-YVAD Encapsulation by Recombinant HaSV VLPs	76
CHAPTER 5 Discussion, Conclusion and Future Work	
Discussion	83
5.1 Construction and Isolation of Recombinant Plasmids	84
5.2 Baculoviral Expression of Recombinant HaSV VLPs in	
<i>Spodoptera frugiperda</i> cells	88
5.3 FITC-YVAD Encapsulation by Recombinant HaSV VLPs	92
5.4 Conclusion and Future Work	95
REFERENCES	97

LIST OF FIGURES

Figure 1.1	A schematic representation of the N β V genome	7
Figure 1.2	A schematic representation of HaSV genomic RNA2	9
Figure 1.3	A schematic representation of the N ω V capsid proteins	12
Figure 1.4	Surface shaded structures of N ω V (Left) and N β V (Right) viewed along a twofold axis of symmetry	13
Figure 1.5	Three dimensional, surface shaded full particle (A) and sectioned views (B) of the procapsid (Left) and the capsid (Right), of N ω V VLPs viewed down a twofold symmetry axis, with threefold (Black triangle) and quasi threefold (White triangle) axes marked	17
Figure 1.6	Schematic representation of the assembly of N ω V based on the structure of the procapsid	18
Figure 3.1	A schematic representation of the construction of pFASTBACHaSV, a recombinant baculovirus expression plasmid	40
Figure 3.2	Schematic representation of the transposition region within the bacmid contained within <i>E. coli</i> DH10Bac cells	43
Figure 4.1	Agarose gel electrophoresis of PCR products of possible recombinant bacmid DNA, FBHaSV, isolates	59
Figure 4.2	Western blot analysis of soluble and insoluble fractions of passage 3 virus stocks from Sf9 cells	62
Figure 4.3	Sucrose gradient centrifugation of VLPs expressed in Sf9 cells infected with FBHaSV at an MOI of 250 and harvested 5 days postinfection	64
Figure 4.4	Sucrose gradient centrifugation of VLPs expressed in Sf9 cells infected with FBHaSV at an MOI of 10 and harvested 5 days postinfection	66
Figure 4.5	Sucrose gradient centrifugation of VLPs expressed in Sf9 cells infected with FBHaSV at an MOI 5 and harvested 5 days postinfection	67

Figure 4.6	Sucrose gradient centrifugation of VLPs expressed in <i>Sf9</i> cells infected with FBHaSV at an MOI 5 and harvested 4 days postinfection	68
Figure 4.7	Transmission electron microscopy analysis of HaSV VLPs from <i>Sf9</i> cells infected with FBHaSV	69
Figure 4.8	(Panel A) A schematic representation of HaSV RNA2. (Panel B) Agarose gel electrophoresis of RT-PCR products of RNA extracted from wild-type HaSV and HaSV VLPs produced in <i>Sf9</i> cells	71
Figure 4.9	Western blot analysis of acid matured HaSV capsid protein diluted 1:5 (Panel A) and 1:10 (Panel B) in buffer B	73
Figure 4.10	Western blot analysis of acid matured HaSV capsid protein diluted 1:5 in buffer B	75
Figure 4.11	Resuspended sucrose pellets used in the encapsidation of FITC	77
Figure 4.12	Western blot analysis of caesium chloride (CsCl) gradient fractions of FBHaSV VLPs and FBHaSV VLPs used in the encapsidation of FITC	79
Figure 4.13	Standard curve used to calculate FITC concentrations in various FITC containing samples	81
Figure 4.14	FITC peptide concentration profiles of VLP preparations as determined using a spectrofluorometer	82

LIST OF TABLES

Table 1.1	Families of viruses infecting invertebrates	1
Table 1.2	Members of the <i>Tetrapoda</i> family	5
Table 2.1	AUG contexts of highly expressed AcMNPv proteins	33
Table 3.1	PCR protocol for the amplification of recombinant bacmid DNA	44
Table 3.2	RT-PCR protocol for the analysis of viral RNA	54
Table 3.3	Experiments and controls conducted in the determination of FITC encapsidation by FBHaSV VLPs	56
Table 4.1	Infectivity of FBHaSV as scored using the TCID ₅₀ Assay	60
Table 4.2	Spectrofluorometer readings of various FITC concentrations used to create a peak area vs FITC concentration standard curve	80

CHAPTER 1

Literature Review

1.1 Introduction

Insect viruses may have double or single stranded DNA or RNA genomes, enveloped or nonenveloped capsids and may be occluded in a protective protein matrix or nonoccluded (Tortora *et al.*, 1995). Some insects live in close association with plants and higher animals. They are able to naturally exchange viruses with them and are host to a medley of viruses. Viruses are grouped into families according to the type of genetic material they possess (van Regenmortel *et al.*, 1999). Families of DNA and RNA viruses that infect insects are listed in Table 1.1.

Table 1.1 Families of viruses infecting invertebrates. The reverse transcribing (RT) viruses and the negative (-) and positive (+) ssRNA genomes are indicated (van Regenmortel *et al.*, 1999).

Genome type and Family	
<p>dsDNA: <i>Poxviridae</i> <i>Iridoviridae</i> <i>Baculoviridae</i> <i>Polydnaviridae</i> <i>Ascoviridae</i></p> <p>ssDNA: <i>Circoviridae</i> <i>Parvoviridae</i></p>	<p>dsRNA: <i>Reoviridae</i> <i>Bimaviridae</i></p> <p>ssRNA (-): <i>Rhabdoviridae</i> <i>Bunyaviridae</i></p> <p>ssRNA (+): <i>Picornaviridae</i> <i>Togaviridae</i> <i>Raviviridae</i> <i>Tetraviridae</i> <i>Nodaviridae</i> CrP V-like</p> <p>ssRNA (RT): <i>Metaviridae</i></p>

Insect single stranded (ss) RNA viruses are usually divided into two subtypes- those that have an RNA genome that functions as mRNA and those that have

an RNA genome that functions as a template for mRNA. In the positive strand ssRNA viruses the RNA genome behaves like an mRNA molecule and the host ribosomes translate a long peptide that is later cleaved into polypeptides (Miller and Ball, 1998). The negative strand ssRNA use a virus associated RNA dependent RNA polymerase to synthesise mRNA prior to transcription. Single stranded viruses use a viral replicase to convert the viral genome into double stranded RNA. The appropriate strand then directs the synthesis of new viral genomes (Tortora *et al.*, 1995). Some positive strand ssRNA insect viruses of particular interest are discussed below.

***Picorn*a-like viruses**

The *Picorn*a-like viruses are a broadly based group of small positive strand ssRNA viruses that are found in invertebrates. They show physical similarities to the *Picornaviridae*, a family of nonenveloped, nonoccluded, ssRNA viruses that include human viruses such as the common cold virus and polio virus (Miller *et al.*, 1999). The structure of the *Infectious Flacherie virus* that infects the silkworm *Bombyx mori*, is fairly typical of *Picorn*a-like viruses, with three capsid proteins of 35kDa, 33kDa, and 31kDa, a diameter of 27nm and a buoyant density of 1.38g/ml in caesium chloride (Christian and Scotti, 1998). Other members of this family include the *Cricket paralysis virus* (CrPV) and the *Drosophila C virus* (DCV). CrPV and DCV are the best-studied members of this family as they can be grown in tissue culture. CrPV has one of the broadest natural host ranges known for insect viruses. It has been detected in 22 species in 5 insect orders (Miller *et al.*, 1999). DCV, on the other hand, seems to be limited to a few *Drosophila* species (Miller *et al.*, 1999). The *Picorn*a-like viruses are often chronic, and because of their close relationship to mammalian picornaviruses, little effort has been made to incorporate them into biological control programs (Christian and Scotti, 1998).

Nodaviridae

Nodaviruses are small, nonenveloped, and icosahedral viruses with bipartite positive strand RNA genomes (Ball and Johnson, 1998). The small ssRNA viruses in the family *Nodaviridae* are represented by two genera, alpha nodaviruses, which primarily infect insects, and beta nodaviruses that only infect fish (Miller *et al.*, 1999). *Nodaviridae* are capable of replicating in plant and vertebrate tissue cultures. A member of this family the *Nodamura Virus* (NOV), infects both insects and mammals. Other nodaviruses have been isolated from scarab beetles (*Black Beetle Virus*), from various grass grub species (*Flock House Virus*, *Boolarra Virus*, and *Manawatu Virus*), cultured *Drosophila* (*New Zealand Virus*), and dead *Lymantria ninayi* in New Guinea (Ball and Johnson, 1998).

The alpha nodaviruses are antigenically related to each other and members of this genera may be distinguished serologically (Ball and Johnson, 1998). The members of the *Nodaviridae* have an icosahedral capsid with $T=3$ quasi-symmetry. The major protein that is produced during infection is the coat protein precursor that is cleaved autoproteolytically post assembly to produce the mature capsid proteins (Gallagher and Rueckert, 1988).

Tetraviridae

The *Tetraviridae* are the only family of RNA viruses that are isolated exclusively from lepidopteran insects (Miller *et al.*, 1999). Members of this family have a positive-sense, ssRNA encased in unenveloped, icosahedral capsids that have a unique structure, $T=4$ lattice symmetry, that forms the basis of the family's name (van Regenmortel *et al.*, 2000). A disease first reported in South Africa in the 1940's, in the larvae of the emperor pine moth, *Nudaurelia cytherea capensis*, was later attributed to the tetraviruses. In the 1960's, five small RNA viruses termed *Nudaurelia* γ , δ , α , ϵ , and β viruses were isolated from the diseased larvae (Juckes, 1979). The *Nudaurelia* β virus and the *Nudaurelia* ϵ virus were found to be almost identical morphologically but were serologically distinct (Juckes, 1979). The *Nudaurelia* β virus (N β V) was the most extensively

studied and became the type virus for the group now known as the *Nudaurelia* β -like viruses (Hendry and Agrawal, 1994). Physical studies on N β V and other viruses placed in the same genus indicated that the particles had $T=4$ quasi-symmetry in their capsid structure resulting in the group being named the *Tetraviridae* (Hanzlik and Gordon, 1997). Members of this family were found to have a monopartite genome, however encapsidation of subgenomic RNA corresponding to the 3' region of the genomic RNA was observed (Gordon, *et al.*, 1999). A virus that was similar to the N β V in its biophysical properties but differed from it by having a second genomic RNA strand was later isolated from *Nudaurelia* larvae co-infected with *Nudaurelia* β virus (Hendry *et al.*, 1985). This virus was named the *Nudaurelia* ω virus (N ω V), and became the type virus for a second genus within the *Tetraviridae*, the *Nudaurelia* ω -like viruses. The N ω V was later joined by a virus similar to it isolated from Australia, the *Helicoverpa armigera* stunt virus (Hanzlik *et al.*, 1993).

1.2 Taxonomy of *Tetraviridae*

Table 1.2 lists the recognised as well as the possible members of the *Tetraviridae* family (Ball *et al.*, 2000)

Viruses are classified as tetraviruses if they are serologically related to, or have capsids and protein subunits of similar sizes to, recognised members of this family. Tetraviruses are not unique in having a ss (+)RNA genome encapsidated in an unenveloped icosahedral capsid. Once it has been established that an icosahedral capsid contains a ss (+)RNA genome, two strong indicators of the virus being a tetravirus are a particle diameter of 35-41nm and a density in caesium chloride of <1.30 g/ml. As these are not definitive, members of the *Tetraviridae* family are distinguished from similar RNA viruses on the basis of their being an insect virus with a major coat protein component of $M_R >60\ 000$, and the production of a coat protein from a separate RNA (Hanzlik and Gordon, 1999; Gordon and Hanzlik, 1998).

Table 1.2 Members of the *Tetraividae* family (Ball *et al.*, 2000)

Virus Name	Family of Host	Origin
Genus: <i>Nudaurelia</i> β-like viruses		
<i>Nudaurelia capensis</i> β virus	<i>Saturniidae</i>	South Africa
<i>Antheraea eucalypti</i> virus	<i>Saturniidae</i>	Australia
<i>Darna trima</i> Virus	<i>Limacodidae</i>	Malaysia
<i>Dasychira pudibunda</i> virus	<i>Lymantriidae</i>	United Kingdom
<i>Euprosterna elaeasa</i> virus		
<i>Philosamia cynthia x ricini</i> virus	<i>Saturniidae</i>	United Kingdom
<i>Pseudoplusia includens</i> virus	<i>Noctuidae</i>	United States
<i>Setothosea asigna</i> virus	<i>Limacocidae</i>	Malaysia
<i>Thosea asigna</i> virus	<i>Limacodidae</i>	Malaysia
<i>Trichoplusia ni</i> virus	<i>Noctuidae</i>	United States
<i>Calliteara pudibunda</i> virus		
<i>Providence</i> virus	<i>Noctuidae</i>	United States
Genus: <i>Nudaurelia</i> ω-like virus		
<i>Nudaurelia capensis</i> ω virus	<i>Saturniidae</i>	South Africa
<i>Helicoverpa armigera</i> stunt virus	<i>Noctuidae</i>	Australia
Unassigned possible members:		
<i>Acherontia atropas</i> virus	<i>Sphingidae</i>	Canary Islands
<i>Agraulis vanillae</i> virus	<i>Nymphalidae</i>	Argentina
<i>Callimorpha quadripunctata</i> virus	<i>Arctiidae</i>	United Kingdom
<i>Eucoytis meeki</i> virus	<i>Cocyiidae</i>	Papua New Guinea
<i>Euploea corea</i> virus	<i>Danadidae</i>	Australia/ Germany
<i>Hyalophora crecopia</i> virus		
<i>Saturnia pavonia</i> virus		
<i>Setora nitens</i> virus		
<i>Hypocrita jacobaeae</i> virus	<i>Arctiidae</i>	United Kingdom
<i>Lymantria ninayi</i> virus	<i>Lymantriidae</i>	Papua New Guinea
<i>Nudaurelia</i> ϵ virus	<i>Saturniidae</i>	South Africa

Thosea asigna virus (TaV) was classified as a *Nudaurelia* β -like virus based on its physical characteristics (Pringle *et al.*, 1999). However TaV has a 55kDa major capsid protein which is smaller than the 60kDa minimum size required for classification as a tetravirus. Based on the size of its major coat protein and also the lack of sequence similarities between TaV and the type strains of the *Tetraviridae*, TaV does not qualify to be classified as a tetravirus (Pringle *et al.*, 1999). *Euprosterina elaeasa virus* (EeV) has also been classified as a member of the tetraviral family based on its structural and genomic organisation. The replicases of TaV and EeV however lack the methyltransferase and helicase domains of the *Tetraviridae* type strains (Gorbalenya *et al.*, 2002). These differences at sequence level between members of the same family suggest that structure based classification of viruses is no longer sufficient (Gorbalenya *et al.*, 2002)

1.3 *Nudaurelia* β -like Viruses

The members of this genus are listed in Table 1.2. The physical and serological relationships among the *Nudaurelia* β -like viruses have been used to classify members of this genus as each member has a positive serological reaction to at least one other member of the genus (Gordon and Hanzlik, 1998). The serological relationships amongst members of this genus are however not reflected at the sequence level, as members of this genus have a very low sequence similarity (Pringle *et al.*, 1999).

Nudaurelia β -like viruses have a monopartite genome, with both the replicase and the capsid genes found on the single RNA molecule. The genomic RNA is 6.6 kb in size and contains two open reading frames (ORFs), one at the 5' end and the other at the 3' end (Gordon *et al.*, 1999). A second RNA may be found in *Nudaurelia* β -like viruses and this is due to the virus coencapsidating the β -like subgenomic mRNA for the capsid protein. The subgenomic mRNA has been postulated as one method of translating the capsid gene. Another method involves the internal initiation of translation on genomic RNA (Gordon *et al.*,

1999). The subgenomic RNA is not capable of being replicated, as only one species of double stranded RNA the length of the genomic strand is extracted from larvae infected with N β V (Hanzlik and Gordon, 1997).

Nudarelia capensis β virus (N β V) is the best-characterised member of the *Nudaurelia* β -like viruses and it is also the type strain of this genus (Gordon *et al.*, 1999). N β V will therefore be used as an example in describing the structure and genome organisation of this genus.

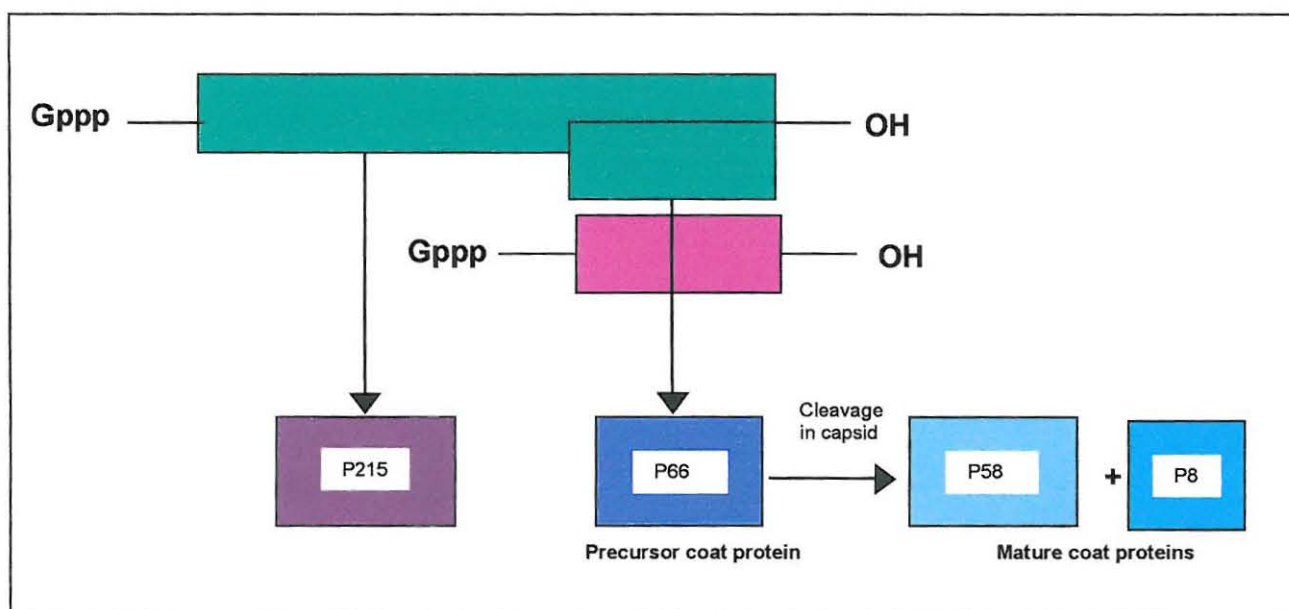


Figure 1.1 A schematic representation of the N β V genome. The two ORFs are represented as green rectangles and the subgenomic RNA as a pink rectangle. The functional protein of the larger ORF is represented as a purple rectangle enclosing its molecular weight. The functional proteins of the second ORF are represented as rectangles in different shades of blue enclosing their molecular weights.

The 5' end ORF of N β V's genomic RNA is made up of 5778 nucleotides and encodes a 215kDa protein that contains three functional domains characteristic of viral replicase (Figure 1.1). The 3' ORF overlaps the replicase gene by more than 99% and is composed of 1836 nucleotides (Gordon *et al.*, 1999). The 3' ORF encodes the 612 residue, 66kDa precursor capsid protein. The precursor capsid protein is thought to be expressed via the 2656 nucleotide subgenomic

mRNA (Figure 1.1) (Gordon *et al.*, 1999). The distance of the capsid gene from the 5' end of the genomic RNA makes it highly unlikely that this gene is translated from the genomic RNA by ribosomes leaking through the start of the replicase gene. The precursor protein is cleaved between the residues Asparagine536 and Glycine537 to produce the 58kDa and 8kDa mature capsid proteins (Gordon *et al.*, 1999).

1.4 *Nudaurelia* ω -like Viruses

Nudaurelia ω -like viruses are highly similar to the *Nudaurelia* β -like viruses in all measured physiochemical characteristics, including their $T=4$ symmetry. The two genera are differentiated from each other by their genomes- *Nudaurelia* ω -like viruses have bipartite genomes and the *Nudaurelia* β -like viruses have monopartite genomes (Hanzlik and Gordon, 1997). The *Nudaurelia* ω -like viruses may have evolved from a virus with an unsegmented genome, as found in the β -type viruses, through the evolution of the subgenomic RNA into a separate component, with the accompanying loss of the capsid gene from the longer genomic RNA (Gordon *et al.*, 1999). The two members of the ω -like viruses, *Nudaurelia capensis* ω virus and the *Helicoverpa armigera* stunt virus, are highly similar at the sequence level but show no serological relationship (Hanzlik *et al.*, 1995).

***Helicoverpa armigera* stunt virus (HaSV)**

HaSV was first isolated from laboratory bred larvae of *Helicoverpa armigera* (Hanzlik *et al.*, 1993). Symptoms of infection with HaSV range from negligible weight loss and stunting in *H. armigera* larvae to severe stunting that may be accompanied by the disintegration of the midguts of the larvae resulting in the larvae starving to death (Hanzlik and Gordon, 1997).

HaSV particles are isometric and 38nm in diameter. In caesium chloride at pH 7.4, HaSV particles have a buoyant density of 1.296g/ml. The viral capsid has two major non-glycosylated protein components with M_{RS} of 65 000 and 6 000.

HaSV particles contains a genome composed of two non-polyadenylated single stranded RNA molecules with lengths of 2.4 kb (RNA2) and 5.3 kb (RNA1) (Hanzlik *et al.*, 1993).

RNA1 of HaSV is composed of a single ORF of 1704 codons that covers 96% of the total length, and encodes a 187kDa protein. Analysis of the sequence of the protein encoded by RNA1 indicated that it contained three domains conserved in RNA-dependent RNA polymerases (replicases) of RNA viruses in the alpha-like superfamily. The 3' end of RNA1 contains three smaller ORFs that are out of frame with the replicase ORF and that encode proteins of 11kDa, 15kDa and 8kDa. No evidence for a subgenomic RNA that could express these proteins has been found. There has also been no discernible relationship to other proteins to indicate the function of these proteins (Gordon *et al.*, 1995).

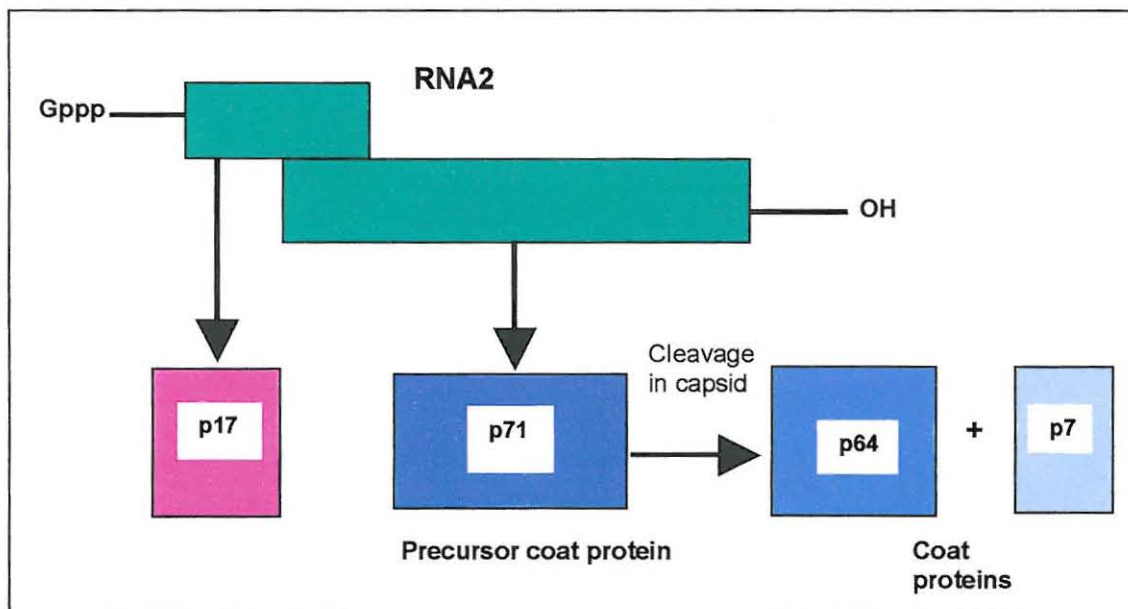


Figure 1.2 Schematic representation of HaSV genomic RNA2. The two ORFs are represented as green rectangles. The protein product of the first ORF is represented as a pink rectangle enclosing its molecular weight. The functional proteins of the second ORF are represented as rectangles in different shades of blue enclosing their molecular weights.

RNA2 of HaSV has two overlapping ORFs that are out of frame with each other (Hanzlik *et al.*, 1995). A 'leaky scanning' mechanism for ribosomal translation is postulated to be the most probable method of both genes being expressed from the same RNA. The first gene has its initiating AUG at base 283 in poor context for translation initiation. Most ribosomes are thought to scan through to the second AUG in good context at base 366, initiating translation of the second gene. The first ORF encodes a 17kDa protein (p17) of unknown function, although there has been evidence implicating it in strand synthesis regulation. The second ORF of RNA2 encodes the 647 residue, 71kDa coat protein precursor (p71). P71 is cleaved at an Asparagine-Phenylalanine site into the mature coat proteins, P64 and P7 Figure 1.2 (Hanzlik *et al.*, 1995).

RNA1 and RNA2 of HaSV have two areas that share similarities in their sequences. These areas form two secondary structures, one at each terminus (Gordon *et al.*, 1995; Hanzlik *et al.*, 1995). The 5' termini of both RNA1 and RNA2 may fold into stem-loop structures and have a hexamer sequence GGUAAA. The stem of the RNA1 hairpin is shorter than that of RNA2, it terminates just upstream of the AUG codon that initiates the long ORF for the viral replicase. The sequences at the 5' termini of viral RNA's have been implicated in RNA replication (Gordon *et al.*, 1995; Hanzlik *et al.*, 1995).

The 3' termini of RNA1 and RNA2 may fold into distinct tRNA-like structures. The 108 nucleotides of the 3' termini that form the tRNA-like structures show 79% contiguous sequence identity between the two RNAs. The tRNA-like structure of HasV forms without a pseudoknot and has a Valine anticodon. The lack of a pseudoknot during the formation of the HaSV tRNA-like structure differentiates it from tRNA-like structures that are found on some plant viruses. The tRNA-like structure of HaSV therefore resembles the authentic tRNA^{Val} more closely than the plant viral structures. HaSV is the first virus for which the presence of a tRNA-like structure lacking a pseudoknot has been reported (Gordon *et al.*, 1995; Hanzlik *et al.*, 1995).

***Nudaurelia capensis* ω virus (N ω V)**

N ω V was first isolated from larvae of *Nudaurelia cytherea capensis* co-infected with N β V (Hendry *et al.*, 1985). N ω V particles have a 40nm diameter and a buoyant density of 1.285 g/ml in caesium chloride at a pH of 7.5 (Hendry *et al.*, 1985). The capsids contain two species of ssRNA of different sizes. The larger RNA (RNA1) has been estimated to be slightly larger than 5kb, and the smaller RNA (RNA2) is 2.5kb. While only a partial sequence of RNA1 is available, it is similar to the RNA1 of HaSV and thought to encode the viral replicase (Agrawal and Johnson, 1992).

The 2.5kb RNA2 of N ω V contains two overlapping ORFs. The first smaller ORF is the coding region for a very hydrophobic peptide, and terminates a base from the initiation codon of the second much longer ORF. The long ORF encodes the 644 residue, 70kDa precursor capsid protein. RNA2 has 366 untranslated bases at the 5' end and 150 noncoding bases at the 3'end. A small protein associated with the capsid protein is also encoded by RNA2. The amino terminal sequence of this protein corresponds to a portion of the long ORF beginning at codon 571 (Agrawal and Johnson, 1992). As there is no initiation codon found near this sequence, the small protein is thought to be a cleavage product from the 70kDa precursor protein. The capsid protein of N ω V is initially composed of a 70kDa precursor capsid protein, that is cleaved post-translation into the 62kDa and 8kDa capsid proteins (Agrawal and Johnson, 1995).

1.5 Structure, Assembly and Maturation of *Nudaurelia* ω -like Virus Capsids

Many aspects of the virus life cycle such as the assembly of progeny virions, particle maturation, or interaction with the cellular receptor involve either the virion or its building blocks (Liljas, 1999). The assembly of virus particles is a relatively complex process that involves a large number of protein subunits interacting both with each other and with the viral nucleic acid (Liljas, 1999). The assembly process is thought to have a role in ensuring that viral nucleic

acid is specifically recognised packaged so as to avoid the packaging of cellular RNA (Johnson and Chiu, 2000).

Structure

N_ωV is the only *Nudaurelia ω*-like virus that to date has had its T=4 virus capsid structure determined at atomic resolution (Munshi *et al.*, 1996). This virus will be used as a model for the description of the T=4 virus capsid structure of *Nudaurelia ω*-like viruses.

The T=4 particle is formed by 240 copies of a single subunit type. The subunit is composed of a helical inner domain that contains residues preceding and following a canonical, viral eight-stranded β-sandwich that forms the contiguous shell. Inserted between two strands of the shell domain are 133 residues with an immunoglobulin c-type (Ig-like) fold (Figure 1.3) (Munshi *et al.*, 1996).

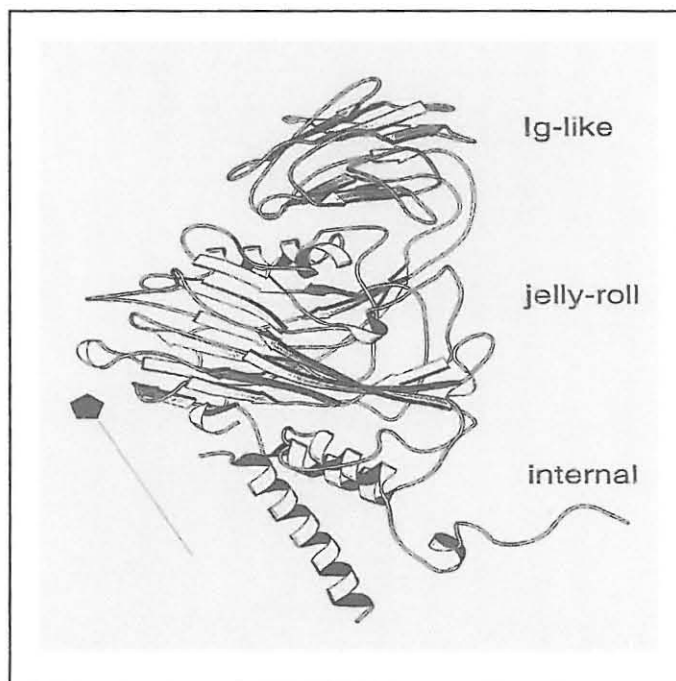


Figure 1.3 A schematic representation of the N_ωV capsid proteins. The capsid protein subunit with the 3 domains indicated on the side (Hanzlik and Gordon, 1999)

Figure 1.4 contains image reconstructions of frozen hydrated *Nudaurelia capensis virus*. Each triangular face of both the N β V and the N ω V viruses is composed of 12 capsid protein subunits that are arranged in four Y-shaped trimeric aggregates. The subunits are packed such that each face is nearly planar, is separated from neighbouring faces by deep grooves and in the case of the N β V contains three deep pits (Hanzlik and Gordon, 1999). The subunits of N β V consist two domains. The smaller domains form the contiguous capsid shell and the larger cylindrical domains that associate with similar neighbouring domains to form trimeric aggregates in the outer capsid surface.

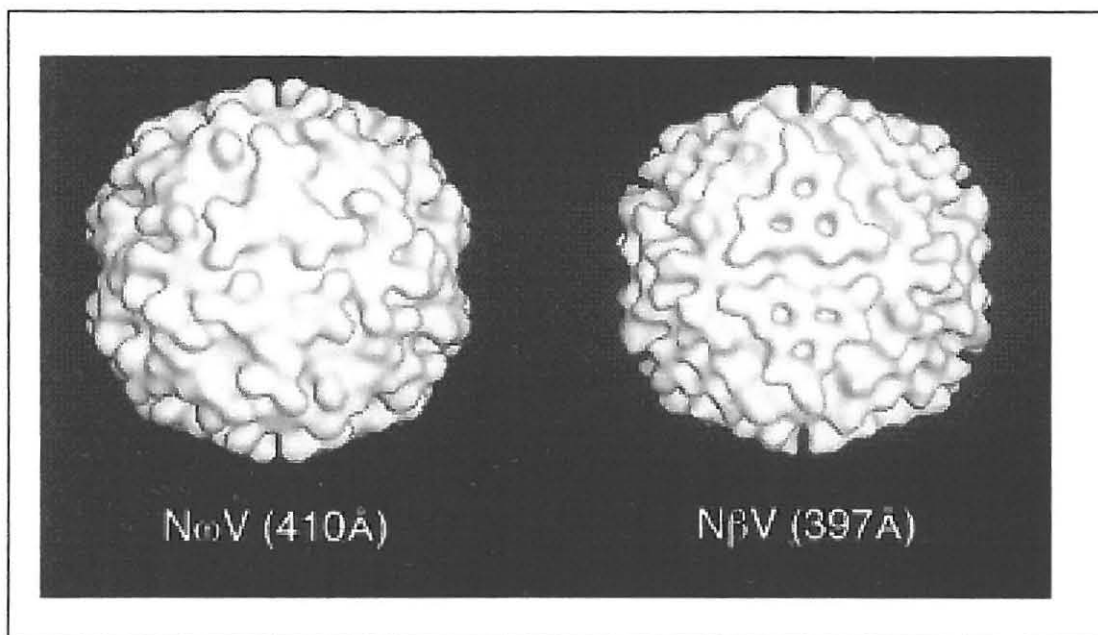


Figure 1.4 Surface shaded structures of N ω V (left) and N β V (right) viewed along a twofold axis of symmetry. The Ig-like domain forms knobs on the surface of the N ω V capsid. Three deep pits are found on the each face of the N β V (Baker *et al.*, 1999).

Sequence comparison of the N ω V capsid protein with that of HaSV shows over 67% sequence homology apart from three regions on the primary sequence. The two terminal regions, amino acids 1-48 and 601-647, have 40% and 53% identity respectively and correspond to the interior domain. The 165 amino acid region in the middle of the primary sequence, amino acids 274-439, have only

33% identity. The 133 residues in this area, with 33% identity, make up the exterior Ig-like domain (Hanzlik *et al.*, 1995). The Ig-like domain dominates the surface of the virus particle. The lack of any detectable serological relationship between N_ωV and HaSV suggests that the Ig-like domain is the dominant antigenic determinant for the viruses. The Ig-like domain is thought to function as the viral acceptor protein involved in virus-host cell recognition (Munshi *et al.*, 1996).

Assembly

Viral capsid shells usually consist of multiple copies of one protein. The viral nucleic acid is therefore encapsidated by multiple copies of the same protein, necessitating that all the protein subunits be in identical environments (Liljas, 1999). The need for identical environments limits the possible assembly to the Platonic solids. Platonic solids are polyhedra that may be made from polygons with equal sides and angles using the same number of polygons at each vertex and the same angle between each edge (Rossmann and Erickson, 1985).

There are only 5 possible Platonic solids, namely the tetrahedron, the cube, the octahedron, the dodecahedron and the icosahedron (Casjens, 1985).

Icosahedral particles are common because they form the largest envelope in which all subunits are in identical environments, and also allow the viral nucleic acid to be covered by the largest number of subunits (Liljas, 1999). Many of the capsid shells appear to self-assemble or spontaneously polymerise in the host cell environment. Assembly may sometimes be assisted by scaffolding proteins that assemble with the capsid proteins to form a precursor shell, but are removed before maturation of the capsid proteins (Berger *et al.*, 1994).

Quasi-equivalence

Explanation of the assembly process has largely focused on the icosahedral symmetry through the Caspar and Klug theory of quasi-equivalence (Reddy *et al.*, 1998). This theory classifies icosahedral virus shells whose protein subunits all have similar (quasi-equivalent) neighbourhoods and form hexamers and pentamers in the virus shell (Berger *et al.*, 1994). The 12 pentamers are always

exact and located at positions equivalent to the vertices of an icosahedron (Rossmann and Erickson, 1985). On the other hand, the hexamers may form sixfold symmetrical associations that are almost precise or they may form trimers and dimers (Reddy *et al.*, 1998; Munshi *et al.*, 1996). The theory of quasi-equivalence as described by Caspar and Klug classifies icosahedral shells according to their T number, with the T number defined as the number of subunits per corner of each triangular face (Rossmann and Erickson, 1985; Berger *et al.*, 1994). Based on the quasi-equivalence theory, icosahedral structures can therefore only have certain multiples of 60 identical subunits, for example a virus can have $60T$ subunits with T as an integer greater than 1 (Berger *et al.*, 1994). To occupy their quasi-equivalent positions in the capsid shell, the subunits are required to maintain their basic bonding properties, but remain flexible enough to allow slight deformations that would enable them to occupy slightly different environments (Reddy *et al.*, 1998). The construction of quasi-equivalent capsids requires that subunits contain molecular switches that facilitate polymorphic association into hexameric and pentameric oligomers. The switching mechanism that is usually multifaceted and different for each virus group, is a major determinant of the geometry of the hexamer structure (Johnson and Chiu, 2000).

Assembly of $N_{\omega}V$ Capsids

$N_{\omega}V$ is a $T=4$ icosahedral virus, and therefore according to the theory of quasi-equivalence each triangular subunit exists in four different environments. The viral capsids assemble from 240 copies of the 70kDa (α) capsid protein precursor, which adopts four slightly different conformations in the capsid, designated A, B, C, and D (Canady *et al.*, 2000). The capsid subunits of $N_{\omega}V$ first assemble into procapsids that are morphologically distinct from the wild-type virus at neutral pH. The procapsid is 16% larger, has a rounder shape and is perforated by holes at all of the symmetry axes (Figure 1.5, Panels A and B) (Canady *et al.*, 2000; 2001). The Ig-like domains of the subunits form conspicuous dumbbell-shaped dimers on the exterior of the procapsid (Canady *et al.*, 2000). When the pH of the procapsids is lowered to pH 5.0, the structure

of the procapsids changes and forms capsids that resembles the wild-type virus. These capsids are smaller, solid and have a polyhedral shape. The Ig-like domains on the exterior of the capsid are trimeric and result in a smoother surface, Figure 1.5, Panels A and B. (Canady *et al.*, 2000; Taylor *et al.*, 2002). The conformational change from procapsids to capsids is thought to be initiated by a reduction in electrostatic repulsions in the interior of the capsid (Canady *et al.*, 2001). The initial conformational change from a procapsid to a capsid occurs rapidly and may be reversible. The initial conformational is followed by a slower irreversible change. Autoproteolytic maturation cleavage has therefore been postulated as being responsible for structural changes that cause ionisable groups to be repositioned thus preventing the expansion of the capsid (Canady *et al.*, 2001). The densities of the procapsid and capsid differ (Figure 1.5, Panel C). The procapsid has a density that corresponds to three domains, as in the β -sheets, Ig-like domain and the internal domain. The capsid has a density that corresponds to two domains- the β -sheets and the Ig-like domain (Canady *et al.*, 2000). The additional internal domain in the procapsid is triskelion-shaped and found on the inner surface at both the 3-fold and quasi 3-fold axes. In the capsid the internal domains lose their trimeric interactions and become less distinct as domains (Canady *et al.*, 2000). The internal structure of the procapsid suggests that the internal domain is required for stabilising the structure of the procapsid, and also for determining its curvature. Rearrangement of the internal domain would have to be complete prior to the onset of autoproteolytic cleavage, although it would be possible for further rearrangement to occur during maturation, (Canady *et al.*, 2000; 2001).

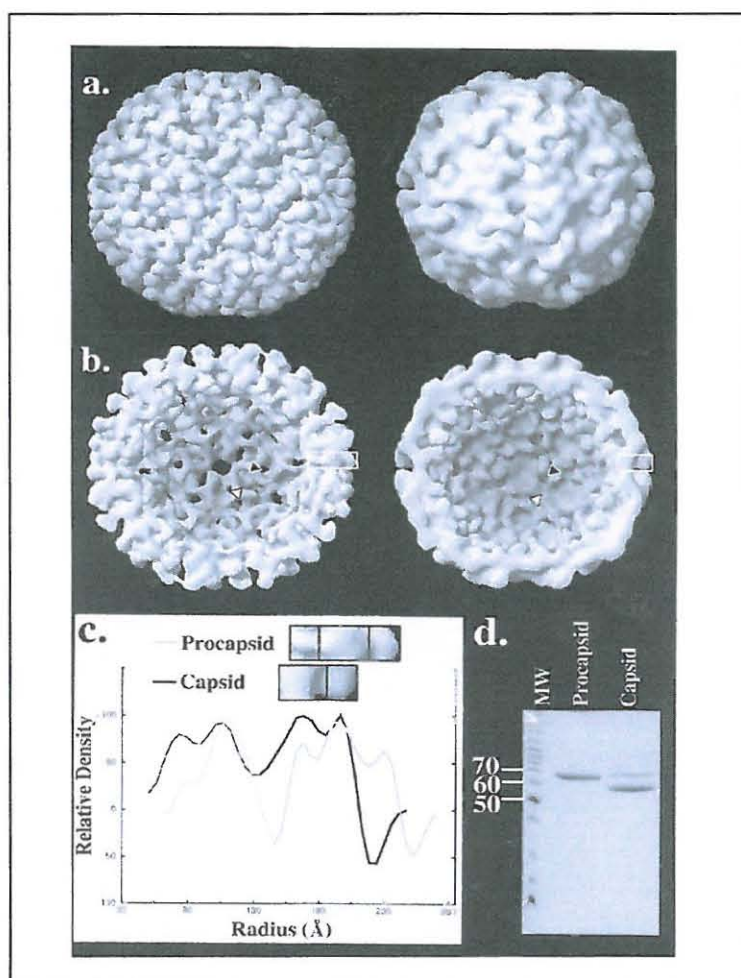


Figure 1.5 Three dimensional, surface shaded full particle (A) and sectioned views (B) of the procapsid, Left, and the capsid, Right, of N ω V VLPs viewed down a twofold symmetry axis, with threefold (black triangle) and quasi threefold (white triangle) axes marked. The procapsid is larger, rounded and porous. The capsid is smaller, solid and more angular. **Panel C.** The radial density plots of the procapsid (grey line) and the capsid (black line) indicating that the procapsid has a thickness of 83 \AA and comprised three domains. The capsid was 62 \AA thick and was comprised of two domains. **Panel D.** SDS-PAGE analysis of the procapsid and capsid indicating the precursor capsid protein (70kDa) and the mature capsid proteins 62kDa and 8kDa, data not shown (Canady *et al.*, 2000)

Figure 1.6 shows a schematic representation of the conformational changes involved in the assembly of N ω V. Protein dimers AB and CD dominate the structure of the procapsid, while the capsid is dominated by the ABC and DDD trimers. The AB and CD dimers are approximately equivalent in the procapsid

and contribute equally to the curvature of the rounded particle (Canady *et al.*, 2000). The N and C termini of the subunits are found in the interior of the procapsid, they therefore probably comprise the internal domain of the subunits (Munshi *et al.*, 1996).

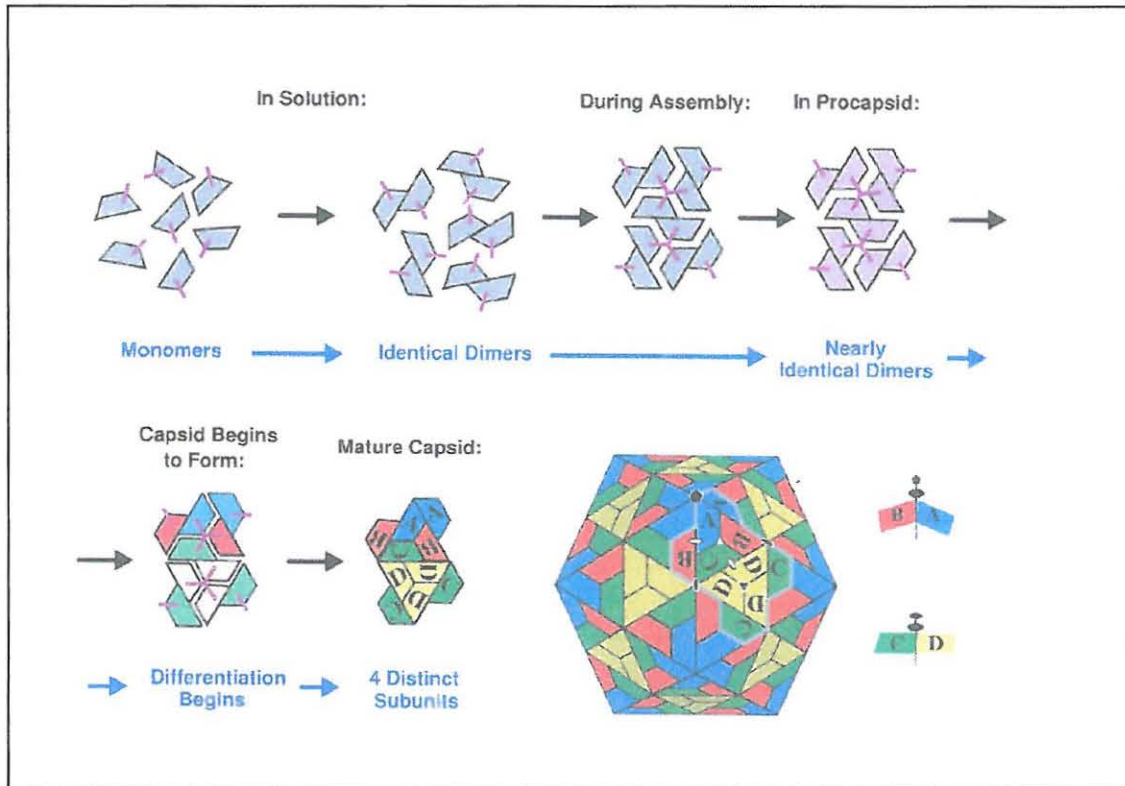


Figure 1.6 Schematic representation of the assembly of N ω V based on the structure of the procapsid. Dimers (grey) are thought to be the building blocks of assembly, due to their tight associations in the procapsid. The dimers exist in the non-differentiating environment of the cytoplasm. The dimers form associations with other dimers via their N and C terminal regions, which form the trimeric internal domain (purple lines which become triskelions). The dimers remain closely similar in the procapsid, but they may have altered slightly from their structure in solution, as shown by a colour change from grey to purple. As the procapsid shrinks and capsid begins to form, the subunits differentiate as they adjust to their slightly different environments. Four distinct subunits are found in the $T=4$ polyhedral capsid. The internal domain becomes the molecular switch that differentiates the AB and CD dimers in the mature capsid (shown to the right of the $T=4$ icosahedron) (Canady *et al.*, 2000)

In the procapsid all the subunits have almost equivalent structures, and the N and c termini of the subunits are ordered. In the capsid the N and C termini of the A and B subunits are not ordered. The transition of the N and C termini from the ordered state in the procapsid to the disordered state in the capsid leads to a rotation of the A and B subunits. This rotation places the A and B subunits in slightly different environments and differentiates them from the CD dimers leading to a bent contact between the facets of the polyhedral capsid. The changes in the state of the N and C termini are also depicted by the lack of a detectable internal domain in the mature capsid (Munshi *et al.*, 1996; Canady *et al.*, 2000).

Maturation

Many viruses undergo maturation events after assembly that are required for infectivity (Liljas, 1999). In tetraviruses and other icosahedral viruses (nodaviruses and picornaviruses) these events are autoproteolytic and dependent upon proper particle assembly (Johnson, 1996; Oliviera *et al.*, 2000). In the *Nodaviridae*, autoproteolytic maturation occurs only after the completion of assembly of the capsid shell that results in increased stability and infectivity of the virus (Gallagher and Rueckert, 1988). The maturation of the nodaviruses also targets the virus particles towards simultaneous dissociation and unfolding that leaves the virus particle in a metastable state. This metastable state of the mature virus particle is thought to have a role during infection (Oliviera *et al.*, 2000).

N_ωV undergoes a post-assembly cleavage that releases a small C terminal peptide. The site for autoproteolytic cleavage in N_ωV is found in the internal helical domain at Asparagine570-Phenylalanine571 and is inaccessible to cellular enzymes (Agrawal and Johnson, 1992 ; 1995). The capsid protein precursor is cleaved autoproteolytically to produce the mature capsid proteins, α (644) → β (1-570) + γ (571-644) (Agrawal and Johnson 1995; Munshi *et al.*, 1996). Autoproteolytic maturation cleavage does not occur when Asp570 is replaced with other residues in particles that have undergone the assembly

transition from procapsid to capsid. The presence of Asp570 has consequently been thought essential for cleavage to occur (Taylor *et al.*, 2002).

Maturation usually occurs in the extracellular environment and probably corresponds to the release of a 'safety switch' that prevents the particle from reinfecting the cell of its origin. The release of VLPs from N ω V infected cells is not essential for maturation to occur but facilitates the maturation process (Agrawal and Johnson, 1995). When N ω V VLPs are expressed in *Spodoptera frugiperda* cells, they produce procapsids that are structurally distinct from wild-type viruses and that do not undergo maturation at neutral pH. When the pH of the VLPs is lowered to 5.0, they undergo a structural change from procapsids to capsids that are morphologically indistinguishable from the wild-type virus. The transition in the structure of the VLPs from procapsid to capsid occurs within seconds, however autoproteolytic cleavage requires hours for completion (Canady *et al.*, 2000; Taylor *et al.*, 2002). The autoproteolytic active site is found in each subunit at the interface between the 5-fold (A) and the quasi 6-fold (B, C, and D), placing each cleavage site in a different environment (Canady *et al.*, 2000). The differences in the environments of the cleavage sites results in 80% of the subunits being cleaved at a relatively fast rate, with a half-life of approximately 2.5 hours, and the remaining 20% being cleaved at a slower rate, with a half life of approximately 13 hours (Cheng *et al.*, 1994; Taylor *et al.*, 2002).

The autoproteolytic maturation cleavage is thought to be catalysed by the intrasubunit Glutamine103 that forms a hydrogen bond to the C terminus of the mature capsid protein β (Munshi *et al.*, 1996). The catalysis of autoproteolytic cleavage by Glu103 is thought to be similar to the dependence of autoproteolytic maturation on a single Aspartic acid residue (Asp75) in nodaviruses (Zlotnick *et al.*, 1994). The replacement of Glu103 with a different residue affects ability of N ω V to assemble, however its role in cleavage has not been independently established (Taylor *et al.*, 2002). The rearrangement that occurs in the N and C termini of the subunits of procapsids during their

transition to capsids is thought to be sufficient for activating autoproteolysis (Canady *et al.*, 2000; 2001). Procapsid assembly is thought to have a role in the stabilisation of the hydrophobic cleavage site altering the pK_a of Glu103 and adding strain to the scissile bond of Asn570-Phe571. The pK_a of Glu103 may be shifted up by its environment, allowing it to be protonated at physiological pH and potentially making it a proton donor in the catalysis of cleavage (Zlotnick *et al.*, 1994; Munshi *et al.*, 1996).

Autoproteolytic maturation cleavage in $T=4$ particles, like in $T=3$ particles, may together with stabilising the virus capsid, facilitate the release of a pentameric helical bundle for translocation of RNA (Cheng *et al.*, 1994; Munshi *et al.*, 1996; Oliviera *et al.*, 2000). Although there are 4 identical gene products within the asymmetric unit, the helical bundles in $N\omega V$ are only formed when the γ peptide residues 571-595, associated with the A subunits, aggregate about the fivefold axes. These bundles have sufficient length to span a membrane bilayer and are of sufficient size to accommodate ssRNA (Munshi *et al.*, 1996). A similar process has been identified in *Nodaviridae*. A pentameric helical bundle is formed by the γ peptides of nodaviruses following proteolytic cleavage of their precursor capsid proteins. These bundles were found to release RNA when virus particles were heated to 65°C and then exposed to pH 4.0 buffer (Cheng *et al.*, 1994). The pentameric helical bundles of $N\omega V$ are thought to be inserted in and across the membrane bilayer by a pH drop in the endosome following receptor binding. Continued uncoating of the RNA would then be facilitated by translation when the ribosome binding site was exposed in the cytosol (Munshi *et al.*, 1996).

1.6 Heterologous Expression of *Nudaurelia* ω -like viruses

The expression of recombinant proteins in heterologous systems is invaluable in the determination of the biochemical and structural properties of the expressed proteins (Kost and Condreay, 1999). The expression of recombinant proteins commonly involves the overexpression of the proteins in question from

multicopy plasmids in the bacterium *Escherichia coli*. The expression of recombinant proteins in bacteria may yield inappropriately folded and/ or glycosylated proteins (Morton and Potter, 2000). The problems encountered with bacterial expression of recombinant proteins have been overcome by the development of expression systems such as those in yeast, plants and insects (Morton and Potter, 2000). The expression of the coat proteins of many simple viruses can form virus-like particles when they are produced in a suitable expression system, indicating that these protein components have all the properties that are required for the formation of large particles (Johnson, 1996). The dispensation of the viral replicase in the production of VLPs was indicated by the production of *Flock house virus* VLPs that were morphologically indistinguishable from wild-type virus. The *Flock house virus* capsid gene was expressed in *Spodoptera frugiperda* cells in the absence of the viral replicase gene (Schneemann *et al.*, 1993).

Bacterial expression of the N_ωV and HaSV coat protein genes has been found to result in the production of the capsid precursor protein that does not undergo autoproteolytic maturation cleavage (Agrawal and Johnson, 1995; Hanzlik *et al.*, 1995). The lack of maturation in the expressed capsid proteins and the absence of any ordered structures that resembled VLPs was an indication that bacterial expression of the tetra-viral capsid genes did not result in assembly of the capsid protein subunits (Agrawal and Johnson, 1995; Hanzlik *et al.*, 1995).

The expression of the coat protein ORF of HaSV in *Saccharomyces cerevisiae* resulted in the production of the precursor capsid protein. A great fraction of the expressed protein was however insoluble, indicating that the protein had formed aggregates. The capsid protein that remained soluble did not undergo spontaneous autoproteolytic maturation cleavage (Venter, 2001). A very low amount of the expressed precursor coat protein underwent autoproteolytic maturation cleavage when cleavage was induced *in vitro* by lowering the pH of the procapsids to pH 5.0. The ability of some of the expressed protein to

undergo acid induced maturation cleavage indicated that capsid protein assembly had occurred (Gallagher and Rueckert, 1988; Venter, 2001).

The HaSV coat protein ORF in combination with the viral genomic RNA has been transiently expressed in plant protoplasts. The expressed capsid protein formed VLPs that selectively encapsidated the viral genomic RNA and were infectious as they caused stunting in neonate larvae fed with the plant protoplasts (Hanzlik and Gordon, 1998; Gordon *et al.*, 2001). The expression of the coat protein ORF in plant protoplasts in the absence of the viral genomic RNA also resulted in the production of VLPs that underwent autoproteolytic maturation cleavage and were indistinguishable from wild-type virus. The expressed VLPs did not replicate, indicating that virus replication was not necessary for viral assembly to occur. The expression of the coat protein in the absence of viral genomic RNA did not produce infectious particles, indicating that the viral genomic RNA represented an infective form of the virus (Gordon *et al.*, 2001).

The expression of the coat protein ORFs of *N_oV* and HaSV in insect cells using baculovirus vectors resulted in the formation of VLPs (Agrawal and Johnson, 1995; Hanzlik and Gordon, 1998). The produced VLPs were morphologically indistinguishable from wild-type virus and displayed post assembly autoproteolytic cleavage of the precursor coat proteins. The expressed VLPs were found to selectively encapsidate the mRNA's for their coat proteins in a cellular environment that contained numerous other RNA species (Agrawal and Johnson, 1995; Gordon and Hanzlik, 1998). The selective encapsidation of its mRNA suggests that at least one of the signals required for the encapsidation of viral RNAs is found within the coat protein ORF (Agrawal and Johnson, 1995; Gordon and Hanzlik, 1998). The selectivity of the tetraviral VLPs was in contrast with what had been previously observed for *Flock house virus*, a nodavirus. The *Flock house virus* coat protein lacked selectivity for viral RNA's under conditions of heterologous baculovirus expression (Schneemann *et al.*, 1993). Recombinant expression of tetraviral structural proteins in insect cells provides

an efficient system in which to study four distinct functions required of capsid proteins: (1) The specific requirement of viral nucleic acid (2) Assembly around the nucleic acid into a stable form (3) Specific recognition of and binding to a susceptible cell, and (4) Release of the nucleic acid into a cellular environment that will support replication (Agrawal and Johnson, 1995). The stable form of the virus particle must be able to exist in the variety of environments and retain the ability to become unstable again in the type cell where it was initially assembled in order to release the viral RNA for translation.

1.7 The Baculovirus Expression System

Baculoviridae are a group of invertebrate-specific viruses. Baculoviruses are a family of rod shaped double stranded DNA viruses. The virus particles have a diameter of 40-50nm (Miller *et al.*, 1999). *Baculoviridae* are divided into the genera *Nucleopolyhedroviridae* and *Granuloviridae*. The nucleopolyhedrovirus are found mainly in insects but there have also been reports of their infections in crustaceans. Nucleopolyhedroviruses form large occlusion bodies that contain many virus particles. The occlusion bodies are used to protect the virions during their transmission from host to host. Granuloviruses in contrast to the nucleopolyhedroviruses are found only in insects and their occlusion bodies contain one virus particle. Baculoviruses have two distinct morphologies, the budded form and the occluded form. The budded virus comprises a single virus particle surrounded by a lipid envelope (O'Reilly *et al.*, 1992; Miller *et al.*, 1999).

The baculoviruses enter their hosts via the ingestion of food contaminated with baculoviral occlusion bodies. The occlusion bodies are solubilised in the alkaline midguts of the insect cells releasing the virus particles. The virus particles enter the midgut cells by fusion with the membrane of the microvilli (O'Reilly *et al.*, 1992). Following infection of a cell, the viral DNA is uncoated in the nucleus and a set of genes known as the early genes are expressed. These genes encode proteins that are required for the replication of the viral DNA. A second set of genes known as the late genes are expressed concurrent with the onset of DNA replication. The late genes encode the viral structural proteins.

The viral structural proteins combine with the replicated DNA molecules to form virus particles. The virus particles bud from the infected cells, resulting in the production of the budded virus. The budded virus is infectious and is responsible for the cell to cell spread of the virus (O'Reilly *et al.* , 1992; Luque and O'Reilly, 1999).

The biology of the infection process in the insect larvae underlies the utility of baculoviruses as expression vectors. The budded form of the baculoviruses is used in the infection of cell cultures (Luque and O'Reilly, 1999). The *polyhedrin* gene (*polh*) is nonessential for replication in cell culture, yet it is expressed in high levels during the late stages of infection (O'Reilly *et al.* , 1992). The basic design of the first baculovirus gene expression vectors therefore involved placing the heterologous genes under the transcriptional control of the strong *polh* promoter (Kost and Condreay, 1999). These recombinant viruses were however found to be unable to form occlusion bodies due to their lack of the *polyhedrin* gene (O'Reilly *et al.* , 1992). The majority of vectors in use are based on replacing the *polyhedrin* gene with the heterologous gene of interest (Kost and Condreay, 1999).

Autographa californica nucleopolyhedrovirus (AcNPV) is the most commonly used baculovirus as an expression vector (Luque and O'Reilly, 1999). The genome of AcNPV is comprised of circular double stranded DNA of about 134 kb (O'Reilly *et al.* , 1992). Due to its large size, direct manipulation of the viral DNA by simply digesting it with restriction endonucleases and ligating in the heterologous gene proved to be difficult. Most recombinant viruses have therefore been generated by *in vivo* recombination (Kost and Condreay, 1999). The target gene is initially cloned into an appropriate transfer vector, which usually contains sequences homologous to the viral *polyhedrin* locus in order to allow recombination. The insect cells are then cotransfected with the viral DNA and the modified transfer vector. Homologous recombination between the viral DNA and the modified transfer vector DNAs results in the transfer of the target gene to the viral genome (Kost and Condreay, 1999). Recombinant viruses are

thus identified based on the formation of occlusion negative plaques. However occlusion negative plaques are not easily identifiable among the background of nonrecombinant occlusion positive plaques. In addition recombinant viruses are produced at a low frequency (0.1-1%), and their identification and isolation is time consuming and laborious (O'Reilly *et al.*, 1992; Luque and O'Reilly, 1999).

A fast and efficient method called the Bac-to-Bac[®] Baculovirus Expression System that does not involve the generation of recombinant baculoviruses in insect cells has been developed by researchers at Monsanto (Luckow *et al.*, 1993). This method involves site-specific transposition of the heterologous gene into a bacmid generated in *Escherichia coli*. The recombinant DNA that is isolated is not mixed with parental nonrecombinant virus and therefore does not require plaque purification, decreasing the time required for the identification of recombinant virus from 4-6 weeks to 7-10 days (O'Reilly *et al.*, 1992; Luckow *et al.*, 1993).

The Bac-to-Bac[®] Baculovirus Expression System is based on site specific transposition of an expression cassette into a baculovirus shuttle vector (bacmid) generated in *E. coli* DH10Bac[™]. The bacmid contains the low copy number mini-F replicon, a kanamycin resistance marker, and a portion of DNA that encodes the *lacZ* α peptide from a pUC-based cloning vector. The attachment site for the bacterial transposon Tn7 (mini-attTn7) that does not disrupt the reading frame of the *lacZ* α gene, is inserted into the N-terminus of the *lacZ* α gene. The bacmid may complement a *lacZ* deletion found on the chromosome of the *E. coli* DH10Bac[™] cells, to form colonies that are blue in the presence of a chromogenic substrate such as Bluo-gal or X-gal and the inducer IPTG. The *E. coli* DH10Bac[™] cells also contain a helper plasmid that contains the tetracycline resistance gene and encodes the Tn7 transposase (Luckow *et al.*, 1993).

A series of pFASTBAC[™] donor plasmids that share common features have also been generated. These vectors contain a baculovirus-specific promoter

from AcMNPV for the expression of heterologous proteins in insect cells. The donor plasmids contain a mini-Tn7 element that contains an expression cassette consisting of a gentamycin resistance gene, a baculovirus-specific promoter, a multiple cloning site, and an SV40 poly A signal that is inserted between the left and right arms of Tn7. Genes to be expressed are cloned into the multiple cloning site of the donor plasmid downstream from the baculovirus-specific promoter. Recombination occurs between the donor plasmid and the bacmid contained in *E. coli* DH10Bac™ when the mini-Tn7 element from a donor plasmid is transposed into the mini-attTn7 attachment site on the bacmid with the helper plasmid providing the transposition functions *in trans*. Insertion of the mini-Tn7 into the mini-attTn7 attachment site on the bacmid disrupts the expression of the *lacZ* α peptide, and colonies that contain the recombinant bacmid are white in the background of blue colonies that contain the undisrupted bacmid. The recombinant bacmid DNA may then be used to transfect insect cells (Luckow *et al.*, 1993).

1.8 Biotechnological Applications of Tetraviruses

Insects cause a third of all agricultural losses recorded annually. Attempts to minimise these losses through insect control measures are mainly based on the use of chemical pesticides (Miller *et al.*, 1999). However there are serious problems with pests developing resistance to these chemical control measures in many parts of the world. There is also increasing concern about the impact of these chemicals on the environment. These problems have led to a rise of interest in biological control agents, including the use of insect specific micro-organisms for pest control (Miller, *et al.*, 1999). Among these micro-organisms are the viral pathogens of insects. Desirable attributes of any ideal viral insecticide would include a specific host range, an ability to cause virulent infections in the field and a rapid rate of kill. Any ideal agent should also be easy to produce and should show stability both in storage and in the environment once released (Hanzlik and Gordon, 1997).

Tetraviruses and other small RNA viruses have generally been used very little as biological pest control agents. The lack of their use has been generally due to three major reasons. (1) Most tetraviruses show a lower pathogenicity toward their hosts than other viruses such as those belonging to the *Baculoviridae* family that are highly virulent when traditional methods are used to infect their hosts. Tetraviruses are also not as effective as chemical agents thus have been neglected by the agricultural industry where rapidly acting agents are required. (2) Members of the *Tetraviridae* family were originally thought to cross-react with vertebrate sera, However these cross-reactions have been shown to be non-specific interactions. (3) The cost of production of infectious particles is not economically feasible (Gordon and Hanzlik, 1998). Despite all these obstacles, tetraviruses have been utilised as pest control agents, with much success in developing countries (Gordon *et al.*, 2001). Their ability to be transmitted both horizontally and vertically and their high levels of persistence in the environment have made them targets for use as biological pest control agents. Their ability to be propagated in non-host systems such as plants and insect cells has also decreased the cost of production of infectious VLPs (Gordon and Hanzlik, 1998).

The ability of recombinant N_oV and HaSV VLPs expressed in insect cells to selectively encapsidate the mRNA of their coat proteins has made them potential vectors for the targeted delivery of specific RNAs to specific cells (Agrawal and Johnson, 1995; Hanzlik and Gordon, 1997). Manipulation of gene content, so that the particles contain translatable mRNA for a specific gene, and cell targeting, through the manipulation of the Ig-like domain so that the particles have altered binding specificity for a particular cell surface antigen, would allow these particles to function as vectors for specific gene delivery to targeted cells (Gordon and Hanzlik, 1998).

These vectors would be used in medicine and agriculture. The use of these vectors in medicine would include targeting toxin genes at cancer cells, with this approach having the potential to be more specific than the presently composed

immunotoxins. The ability of RNA1 to self replicate in the absence of RNA2 (Ball, 1995; Gordon *et al.*, 2001) suggests that VLPs containing RNA1 modified to contain toxin genes could be targeted at specific cells and the self-replication ability of RNA1 utilised to increase the concentration of the toxin genes in the targeted cells. These VLPs would not be able to form progeny thus could not be transmitted to other individuals (Gordon *et al.*, 2001). The tetraviral vectors would have an advantage over those presently in use, such as those of alphaviruses, in that they would not require replicons for the trans-encapsidation of the modified RNA (Frolov *et al.*, 1996; Gordon *et al.*, 2001). In agriculture, insect specific toxins could be more quickly targeted to a particular insect thus precluding the need to find a virus for every insect pest (Hanzlik and Gordon, 1997; Gordon and Hanzlik, 1998).

Some virus particles are able to assemble into empty virion particles *in vitro*. If the empty virus particles are able to behave as hemicarcerands they may then be utilised as delivery vehicles of exogenous molecules (Douglas and Young, 1998; Houk *et al.*, 1996). Hemicarcerands are molecules that have the ability to form stable complexes with smaller molecules entrapped by them (Houk *et al.*, 1996). The smaller entrapped guest molecules are able to move in and out of the hemicarcerand via openings on the hemicarcerand that may be reversibly opened or closed (gating) (Houk *et al.*, 1996). Without gating the molecules would only be allowed to move into the host molecule during synthesis but would never be able to leave (Houk *et al.*, 1996). The gating mechanism that is observed in hemicarcerands is also observed in $T=3$ plant viruses (Robinson *et al.*, 1982; Speir *et al.*, 1995). Many $T=3$ viruses swell when their pH is raised in the absence of cations resulting in the formation of pores in the virus capsid. When the pH is dropped the swelling reverses resulting in the closure of the pores (Speir *et al.*, 1995). Douglas and Young (1998) used the ability of the *Cowpea chlorotic mottle virus* (CCMV) to open and close pores in its capsid in a reversible manner that is pH dependent to encapsidate an anionic organic polymer. The ingress and egress of the guest molecule was controlled by gating of the CCMV pores at different pHs (Douglas and Young, 1998). The ability of

plant viruses to behave as hemicarcerands therefore allows the virus particles to be utilised as delivery vectors for exogenous molecules such as peptides, radioisotopes and other small molecules (Douglas and Young, 1998).

N_ωV VLPs form porous procapsids when the VLPs are harvested at neutral pH. Upon lowering of the procapsid pH to 5.0, the porous procapsids form solid shelled capsids that are indistinguishable from the wild-type virus capsid (Canady *et al*, 2000). The conformational change from porous procapsids to non-porous capsids is reversible until autoproteolytic maturation cleavage has occurred in at least 15% of the subunits at pH 5.0 (Taylor *et al*, 2002). The ability of the tetraviral capsids to open and close pores on its capsid surface may in a manner that may be controlled implies that tetraviral capsids may also be able to function as hemicarcerands. The use of virus capsids as delivery vehicles of exogenous molecules coupled with the retargeting of the virus towards different cells via the manipulation of the Ig-like domain to have altered binding specificity for a particular cell surface antigen, would have an astounding impact in the treatment of complex diseases and not so complex diseases (Smith, 1995; Douglas and Young, 1998).

1.9 Project Proposal

N_ωV undergoes pH dependent conformational changes from a porous procapsid to a nonporous capsid (Canady *et al.*, 2000). This conformational change is reversible until the capsid proteins undergo autoproteolytic maturation cleavage that locks the virus particles in the mature capsid conformation (Canady *et al.*, 2001; Taylor *et al.*, 2002). The ability of N_ωV to open and close its capsid pores in a controlled manner implied that they too, like the CCMV particles, could behave as hemicarcerands (Houk *et al.*, 1996; Douglas and Young, 1998). The N_ωV particles could therefore be utilised as delivery vectors for exogenous molecules. These particles would also have an advantage over plant virus vectors in that they could behave as both hemicarcerands and carcerands. Carcerands unlike hemicarcerands do not allow the ingress and egress of guest molecules, but lock the guest molecule within their interior once they have formed stable complexes with them (Houk *et al.*, 1996). Prior to the occurrence of autoproteolytic maturation cleavage the N_ωV particles would behave as hemicarcerands allowing the guest molecules to ingress and egress from the virus capsids as the pH of the virus particles was altered to allow the opening and closing of the capsid pores (Houk, *et al.*, 1996, Canady *et al.*, 2001; Taylor *et al.*, 2002). Once autoproteolytic maturation cleavage had occurred the N_ωV particles would become carcerands as they would prohibit the egress of the guest molecule from the virus capsids (Houk, *et al.*, 1996, Canady *et al.*, 2001; Taylor *et al.*, 2002). Due to the high degree of similarity between the *Nudaurelia ω*-like viruses at both structural and sequential levels (Hanzlik *et al.*, 1993; 1995) it was understood that HaSV particles would behave in a manner similar to that of N_ωV particles and could therefore also be used as hemicarcerand and carcerand delivery vectors.

The objectives of this project were:

- To express the HaSV coat protein ORF in a baculovirus expression system.

- To determine if the expressed VLPs were morphologically identical to wild-type virus and if they underwent spontaneous autoproteolytic maturation cleavage of their precursor coat protein.
- To determine if the expressed VLPs encapsidated coat protein mRNA.
- To determine if it was possible to load the expressed procapsids *in vitro* with an exogenous molecule and trap the molecule within the capsids by acid maturation.

CHAPTER 2

2.1 Introduction

The baculovirus expression vector system is one of the major eukaryote recombinant DNA expression systems used today for the production of a wide variety of heterologous proteins (Ailor and Betenbaugh, 1999). Among the advantages of the baculovirus expression system are the high quantities of proteins produced due to the strength of the viral promoters used to drive the expression of the target genes. Insect cells also carry out most eukaryotic post-translation modifications in an authentic manner (O'Reilly *et al.*, 1992).

Eukaryotic proteins expressed in insect cells usually have the same biological activity and immunological reactivity as the authentic protein (Ailor and Betenbaugh, 1999).

Expression of Recombinant Genes in a Baculovirus Expression System

The immediate context of the translation initiation codon of the heterologous protein has been found to be important in the optimisation of gene expression in the mammalian expression system. The context of the nucleotides in the vicinity of the AUG start codon were very important in the initiation of translation in cultured monkey cells (Kozak, 1991). The AUG contexts of the highly expressed AcMNPV proteins have also been determined as they are also thought to be important for translation and are listed in Table 2.1 (O'Reilly *et al.*, 1992).

Table 2.1 AUG contexts of highly expressed AcMNPV proteins (O'Reilly *et al.*, 1992)

Gene	AUG Context
<i>polh</i>	CCUAUAAAUAUGCCGG
<i>p10</i>	UUUACAAAUAUGUCA
<i>p6.9</i>	AAUUUAAACAUGGUUU
<i>vp39</i>	GGCAACAAUAUGGCGC
Consensus	A YAUG Y

Y - pyrimidines

The consensus sequence was found to indicate that A was found at the -3 position relative to the AUG at +1, +2, +3, and pyrimidines are found at -1 and +5 (O'Reilly *et al.*, 1992). The consensus sequence for the initiation of translation in AcMNPV is very similar to that found for mammalian cells where an A/G are found at position -3 relative to the AUG, Table 2.1. Agrawal and Johnson (1995) found that the recombinant expression of the capsid protein of N ω V in *Spodoptera frugiperda* insect cells was affected by the context of the AUG and a long untranslated leader sequence on the N ω V insert. A decrease in the length of the untranslated leader sequence and a change in the context of the initiation codon to that of the consensus sequence for translation in mammalian cells, resulted in an increase in the levels of coat protein expressed (Agrawal and Johnson, 1995).

N ω V capsid protein expressed in *Spodoptera frugiperda* cells underwent spontaneous autoproteolytic maturation cleavage of the precursor protein resulting in the formation of mature virus like particles, VLPs. The expressed VLPs selectively encapsidated the coat protein mRNA (Agrawal and Johnson, 1995). The expression of the *Flock House virus* (FHV), a nodavirus, capsid protein in *Spodoptera frugiperda* cells also resulted in the production of precursor capsid protein that underwent spontaneous autoproteolytic maturation cleavage resulting in the production of mature VLPs. The FHV VLPs however did not selectively encapsidate their coat protein mRNA but also encapsidated cellular mRNA (Schneemann *et al.*, 1993). Recombinant baculoviral expression of N ω V capsid protein in *Spodoptera frugiperda* cells also resulted in the production of immature capsids, procapsids that did not spontaneously undergo maturation at neutral pH. Autoproteolytic maturation cleavage of the precursor capsid protein could however be induced by lowering the pH of the VLPs to 5.0 (Canady *et al.*, 2000; Taylor *et al.*, 2002). The expression of N ω V procapsids in insect cells using a recombinant baculoviral expression system by Canady *et al.* (2000) and Taylor *et al.* (2002) was however in contrast with the results obtained by Agrawal and Johnson (1995). When Agrawal and Johnson (1995)

expressed the N_ωV capsid protein in insect cells using a recombinant baculoviral expression system only capsid protein that spontaneously underwent autoproteolytic maturation cleavage at neutral pH was expressed. Glover (2002) found that the reason for the difference in the VLP product expressed at neutral pH by Agrawal and Johnson (1995) and Canady *et al.* (2000) was due to differences in the cDNA sequence utilised by both groups.

Many virions such as most $T=3$ plant viruses, herpesviruses and some bacteriophages undergo reversible structural changes that open or close pores on the surface of the capsid thus allowing access to their interior that may be switched on and off (Taylor *et al.*, 2002). Douglas and Young (1998) used this ability of viral capsids to open and close pores on the surfaces of their capsids to encapsulate an anionic polymer (poly-anethosulphonic acid) inside the capsid of the *Cowpea chlorotic mottle virus* (CCMV). CCMV undergoes a reversible pH-dependent swelling which results in an increase in the dimension of the virus. The increase in the viral dimension is as a result of the formation of pores in the capsid of the virus. When the pH of the CCMV VLPs is increased above 6.5, the virus capsids form pores that allow the virus particles to selectively entrap and release particles from within the central cavity. When the pH of the virus particles is dropped to below 6.5, the virus particles undergo a structural change that closes the pores and prohibits any exchange of material between the virus capsid and its environment (Douglas and Young, 1998).

The ability of virus particles to encapsulate exogenous particles makes them great targets for use as drug delivery vectors. Virus hosts equipped with the ability to undergo reversible structural conformations resulting in the opening and closing of pores on their capsid surfaces may form very stable complexes with a variety of exogenous particles under readily achievable conditions (Houk *et al.*, 1996). Modification of the outer surface protein of these virus hosts would facilitate specific biological targeting and surface interaction (Hanzlik and Gordon, 1997; Douglas and Young, 1998).

N ω V undergoes a pH-dependent conformational change from a porous procapsid to a nonporous capsid when viral coat proteins are expressed in *Spodoptera frugiperda* cells using a recombinant baculovirus expression system (Canady *et al.*, 2000; Taylor *et al.*, 2002). The procapsids are formed when the viral coat proteins are allowed to assemble at a neutral pH. These procapsids are stable and do not undergo autoproteolytic maturation cleavage. When the pH of the procapsids is lowered to 5.0, they undergo a structural change that closes the pores in less than 100 milliseconds. Autoproteolytic maturation cleavage then proceeds slowly and has a half-life of several hours. Autoproteolytic maturation cleavage irreversibly locks the VLPs in their mature state (Taylor *et al.*, 2002). The substitution of Asparagine570 with Threonine results in the production of procapsids that are able to undergo conformational changes to form capsids that are unable to undergo autoproteolytic maturation cleavage. The conformational change is therefore reversible. However the capsids that re-expand to form procapsids show different properties to the original capsids thus indicating that they may be unstable (Taylor *et al.* 2002).

Virus capsids have been used as delivery vectors for non-native nucleic acids as the range of viral morphology and size allow great flexibility in the adaptation of their capsids for their use as delivery vectors (Smith, 1995). Viruses have evolved efficient mechanisms used in the introduction and expression of their nucleic acids into recipient cells. Viral host cells have in return evolved mechanisms to rid themselves of the pathogens (Smith, 1995). The limiting factor in the use of viral capsids as delivery vectors has been in obtaining access to the interior of the capsid, and in maintaining efficient and often extended expression of the exogenous material while evading the host defences (Smith, 1995; Douglas and Young, 1998).

Based upon the similarities between the *Nudovirelia* ω -like viruses, discussed earlier in this chapter it was understood that HaSV would also form porous procapsids at neutral pH. These procapsids could therefore be used in a manner similar to that of swollen porous CCMV to entrap exogenous particles

within the virus shell (Douglas and Young, 1998). The exogenous particles would then be locked within the HaSV VLPs when they underwent conformational structural changes from a porous procapsid to a solid shell capsid when the pH was dropped to 5.0 (Canady *et al.*, 2000).

Chapter 3

Materials and Methods

3.1 Construction of Recombinant Plasmids

All enzymes used below were used according to the manufacturers instructions, and all recombinant DNA techniques were as described by Sambrook *et al* (1989), unless otherwise specified.

Construction of pFASTBACHaSV

A multi-copy yeast expression vector, pAV3, that contains the HaSV *p71* open reading frame (ORF) was obtained from Dr. Arno Venter (Rhodes University, South Africa) (Figure 3.1). The HaSV *p71* ORF was excised from pAV3 using the restriction enzymes *Sac I* and *Xba I* (USB Amersham). pFASTBAC1 (GIBCO/BRL) a baculovirus expression vector with a *polh* promoter was linearised using the restriction enzymes *Sac I* and *Xba I* (Figure 3.1). Restriction fragments were separated by electrophoresis in 1% agarose and visualised by staining with ethidium bromide and destaining with TAE buffer [242g Tris base, 57.1ml glacial acetic acid, 37.2g EDTA, made to 1L in triple distilled water (dddH₂O)]. The fragments containing the pFASTBAC1 vector backbone and the HaSV *p71* ORF were excised from the gel, and purified using the GENECLEAN II Kit (bio101).

The gel purified DNA fragments were ligated using T4 DNA Ligase (Promega), to produce pFASTBACHaSV (pFBHaSV) (Figure 3.1). The ligations were incubated overnight at 4 °C and the DNA transformed into competent *E. coli* DH5 α cells. The *E. coli* DH5 α cells were made competent as follows: a single colony of the *E. coli* DH5 α cells was inoculated into 5ml tubes of Luria broth and incubated overnight at 37°C. 4x100ml Luria broth flasks were then inoculated with 1.5ml, 1.0ml, 0.7ml and 0.3ml of the overnight culture. The inoculated Luria broth flasks were incubated at 37°C for not longer than 2 hours. When the optical density 600 (OD₆₀₀) in the flask inoculated with 1.5ml pre-inoculum reached 0.6-0.8 units the cells were harvested. The flasks were cooled for 5-10

minutes on ice and the cells centrifuged in a Beckman JA10 rotor at 5000rpm for 10 minutes at 4°C. The supernatant was decanted and the pellet resuspended in 50ml RF1 [100mM Potassium Chloride, 50mM Magnesium chloride, 30mM Potassium Carbonate, 15%*m/v* Glycerol]. The resuspended pellets were incubated on ice for 20 minutes and then pooled to make 2x100ml resuspensions. The pooled resuspended pellets were then centrifuged in a Beckman JA10 rotor at 5000rpm for 10 minutes. The supernants were decanted and the pellets resuspended in 4ml RF2 [10mM MOPS, 10mM Potassium chloride, 75mM Calcium chloride, 15%*m/v* Glycerol]. 100µl aliquots of the resuspended pellets were made and stored at -80°C. The transformed *E. coli* DH5α cells were then plated onto Luria agar plates (10g tryptone, 5g yeast extract, 5g sodium chloride, 15g agar, and made to 1L with dddH₂O) containing ampicillin (100µg/ml) and gentamycin (7µg/ml) and incubated at 37°C overnight. Colonies on the plates were inoculated into 5ml tubes of Luria broth (10g tryptone, 5g yeast extract, 5g sodium chloride, and made to 1L with dddH₂O) containing ampicillin (100µg/ml) and gentamycin (7µg/ml) and incubated overnight at 37°C.

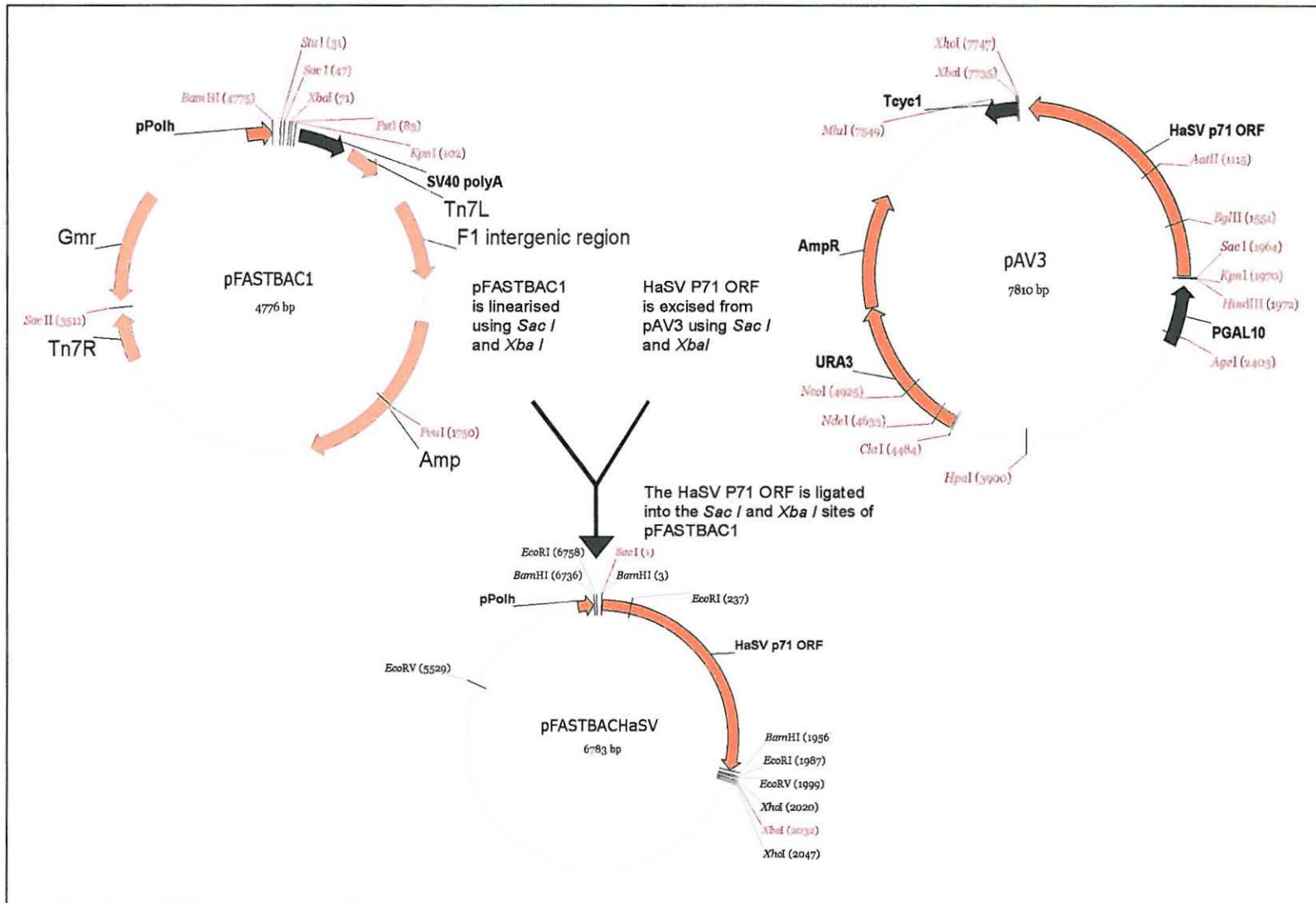


Figure 3.1 A schematic representation of the construction of pFASTBACHaSV a recombinant baculovirus expression plasmid.

Plasmid DNA extracted from the overnight cultures essentially according to the Easyprep method of Berghammer and Auer (1993) as follows: overnight cultures were microfuged in a Heraeus microfuge for 5 minutes at 13 00rpm. The supernatant was decanted and the pellet resuspended in 50µl smart buffer (10mM Tris pH 8.0, 1mM EDTA pH 8.0, 15%w/v sucrose, 200µg/ml Dnase-free Rnase, 2mg/ml lysozyme) and incubated at 37°C for 30 minutes. The samples were boiled for 1 minute and then incubated on ice for 15 minutes. The samples were microfuged at 13 000rpm in a Heraeus microfuge for 10 minutes and the supernatant transferred to a clean Eppendorf. The isolated plasmids contained in the supernatant were screened for pFBHaSV using the restriction enzymes *Sac I* and *Xba I* as these enzymes would result in the excision of the HaSV *p71* ORF from the pFASTBAC1 vector if the isolated DNA contained the pFBHaSV construct. A single possible positive recombinant colony was picked and screened further using the restriction enzymes *Eco RI*, *Eco RV* (Roche), *Xho I*, *Bam HI* and *Hinc II* (USB, Amersham).

The nucleotide sequence of the 5' end of the HaSV *p71* ORF contained in the pFBHaSV construct was determined with the primer polhF (TTTTCGTAACAGTTTTGTAATAAAA) that binds within the *polyhedrin* promoter of pFASTBAC1 using the ABI3100 automated sequencing system.

Transformation and Isolation of Recombinant Bacmid DNA

The transformation of pFBHaSV into *E.coli* DH10Bac™ cells and the isolation of recombinant bacmid DNA was essentially carried out as described in the Bac to Bac Manual (GIBCO BRL).

pFBHaSV was transformed into *E. coli* DH10Bac™ cells using the heat-shock method as described by Sambrook *et al* (1989), and cells incubated at 37°C for 4 hours to allow recombination to occur. The cells were then plated onto Luria agar plates containing kanamycin (50µg/ml), gentamycin (7µg/ml), tetracycline (10µg/ml), X-gal (100µg/ml) and IPTG (40µg/ml). The plates were incubated at

37°C for 48 Hrs. Colonies containing recombinant bacmid DNA were selected as white colonies vs. blue colonies. The white colonies indicated the disruption of *lacZ* α peptide due to recombination and the insertion of the HaSV *p71* ORF sequence into the bacmid. Both blue and white colonies were inoculated into 5ml tubes of Luria broth containing kanamycin (50 μ g/ml), gentamycin (7 μ g/ml) and tetracycline (10 μ g/ml). Isolation of the recombinant bacmid DNA was as performed as described in the Bac to Bac Manual (GIBCO BRL). 1.5ml of the overnight cultures was microfuged at 13 000 rpm for 5 minutes in a Heraeus microfuge. The supernatant was removed and the pellets resuspended in 300 μ l Solution 1 (High Pure Plasmid Isolation kit, Roche). 300 μ l of Solution 2 (High Pure isolation kit, Roche) was added to the samples and they were incubated at room temperature for 5 minutes. 300 μ l of Solution 3 was added to the samples and they were incubated on ice for 10 minutes. The samples were centrifuged at 13 000 rpm for 10 minutes, and the supernatant removed and placed in an Eppendorf tube containing 800 μ l of absolute isopropanol. The samples were incubated at -20°C for 20 minutes and then centrifuged at 13 000 rpm for 15 minutes. The supernatant was removed and 500 μ l of ice cold 70% ethanol added to the pellets. The samples were centrifuged at 13 000 rpm for 5 minutes and the supernatant removed. The supernatant was removed and the pellet air-dried at 37°C for 10 minutes. The DNA was dissolved in 40 μ l sterile dddH₂O.

Verification of the insertion of the HaSV *p71* ORF into the bacmid DNA was done by polymerase chain reaction (PCR) analysis of the isolated bacmid DNA using the primers pucF (CGCCAGGGTTTTCCCAGTCACGAC) and pucR (TCACACAGGAAACAGCTATGAC) that bind within the *lacZ* α gene to regions which flank the points of recombination (Figure 3.2). The use of these primers would result in the amplification of an approximately 4.3Kb fragment if the correct recombinant bacmid, FBHaSV, had been isolated.

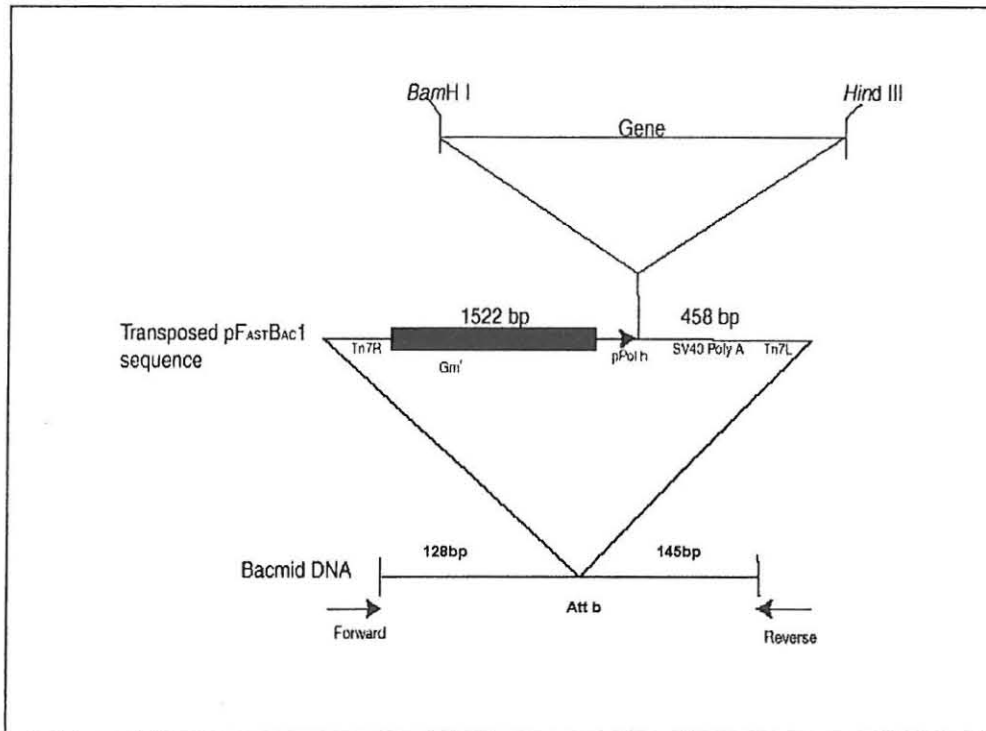


Figure 3.2 Schematic representation of the transposition region within the bacmid contained in *E. coli* DH10Bac cells. For PCR amplification the forward primer is pUCF and the reverse primer is pUCR

The PCR reactions were set up as follows: 1 μ l of template DNA, 2.5 μ l of 10x PCR buffer (Roche), 0.5 μ l of 10mM dNTP mix, 1.25 μ l of 10 μ M pucF, 1.25 μ L of 10 μ M pucR, 1.25U of *Taq* polymerase (Roche) and 18.25 μ l of sterile dddH₂O. The PCR reaction was carried out in a Hybaid PCR sprint machine. The PCR protocol used is outlined in Table 3.1.

Table 3.1 PCR Protocol for the Amplification of Recombinant Bacmid DNA

Temperature (°C)	Time	No. of Cycles
93	3 minutes	1
94	45 seconds	30
55	45 seconds	
72	5 minutes	

3.2 Transfection of Insect Cells

The protocols used below were adapted from the Bac to Bac Manual, GIBCO BRL and the Growth and Maintenance of Insect Cell Lines Manual, Invitrogen. All insect cells used were grown in Grace's complete insect medium (545ml Grace's insect medium, 50ml Foetal Bovine Serum, and 5ml 100x Antibiotic Antimycotic (Highveld Biological Pty Ltd.), as monolayers.

35mm 6 well Tissue Culture dishes were seeded with 1×10^6 cells/well and incubated at room temperature for 1 hour to allow the cells to attach. The growth medium was removed and replaced with 2ml of fresh Grace's complete insect medium. Recombinant baculovirus DNA, FBHaSV, and bacmid vector DNA was then transfected into the cells as follows: Solution A: 5 μ l Fugene reagent (Roche) was added drop wise to 95 μ l of Grace's insect medium, and incubated at room temperature for 5 minutes. Solution B: 6 μ l of the recombinant bacmid DNA was diluted to a final volume of 25 μ l using Grace's insect medium. Solution A was added drop wise to solution B to a final volume of 100 μ l. The solutions were mixed and incubated at room temperature for 30 minutes. The mixed solutions were added drop wise to the seeded wells. The 35mm dishes were placed in a plastic container with wet paper towels to prevent the wells from drying up during incubation, and incubated at 27°C for 4 days. After 4 days the transfection supernatants that contained the virus were transferred to sterile Eppendorf tubes and microfuged at 2000 rpm for 2 minutes in a Heraeus

microfuge to pellet the cells and debris, with the recombinant baculovirus remaining in the supernatant.

3.3 Plaque Assay and Virus Titration

35mm 6 well Tissue Culture dishes were seeded with Sf9 cells at 1×10^6 cells/well, and incubated at room temperature for 1 hour to allow the cells to attach. A ten-fold dilution series of the viral supernatant was prepared in Grace's complete insect medium. The growth medium was removed from the seeded wells and replaced with 1ml of the 10^{-1} , 10^{-2} , 10^{-3} , 10^{-4} , 10^{-5} , 10^{-6} , 10^{-7} , 10^{-8} and 10^{-9} dilutions. The dilutions were added to the seeded wells by gently running them down the side of the wells to avoid disturbing the cell monolayer. The dishes were then incubated at 27°C for 2 hours with gentle agitation. The virus dilutions were removed and the infected cells overlaid with sterile 2% Seakem ME agarose diluted to a final concentration of 0.5% with Grace's complete insect medium heated to 60°C. The agarose overlay was cooled to 40°C prior to it being added to the wells. The 6 well dishes were incubated at 27°C for 4 days. After 4 days incubation 1ml of Neutral Red, diluted to 100µg/ml in Grace's insect medium, was added to each well and incubated for 5 hours at 27°C. The Neutral Red solution was then removed and the dishes incubated overnight at 27°C. Following the overnight incubation, the precise position of each plaque was marked on the bottom of the plate.

For the determination of the virus stock titre the number of plaques present was counted, with the most reliable counts being presumed to be those of wells containing between 10 and 100 plaques. For plaque purification, a marked plaque was removed as a plug of agarose and placed in 1ml Grace's complete insect medium. The mixture was then vortexed to remove the virus from the plug.

50% Tissue culture infectious dose (TCID₅₀) Assay

The virus titre of FBHaSV was also determined using the TCID₅₀ assay (O'Reilly *et al.*, 1992). Sf9 cells were used to seed 96 well plates at 2×10^4 cells/well and the plates were incubated for 1 hour to allow the cells to attach. A ten-fold dilution series of the virus in Grace's complete medium was made. The dilutions made ranged from 10^{-1} to 10^{-12} . Once the cells had attached the 10^{-2} to 10^{-12} were used to infect the wells. The wells were infected with 50 μ l virus/well, and 8 wells were used per dilution. A single column of wells was not infected with the virus and these wells were used as a negative control. The plates were then incubated at 27°C for 10 days. After 5 days of incubation the cells were fed with a drop of Grace's complete medium. After 10 days of incubation the wells were scored for virus by evaluating the cytopathic effect.

3.4 Virus Amplification

Virus stocks were made for both FBHaSV virus and bacmid vector virus as follows:

Passage 1 Virus Stocks: 35 mm 6 well plates were seeded with Sf9 cells at a density of 1×10^6 cells/well and incubated at room temperature for 1 hour to allow the cells to attach. Following incubation the Grace's complete insect medium was removed from the cells, and the cells were infected with 0.5ml of plaque purified virus in Grace's complete insect medium. The cells were gently agitated at room temperature for 1 hour. Following incubation 1.5ml of Grace's complete insect medium was added to the infected cells and the cells were incubated at 27°C for 4 days. After 4 days the supernatant was removed and transferred to a sterile Eppendorf tube. The supernatant was microfuged at 2000 rpm for 5 minutes in a Heraeus microfuge to pellet cells and debris. The supernatant was stored at 4°C and used to generate Passage 2 stocks.

Passage 2 Virus Stocks: 2 x T75 (75cm²) Tissue Culture flasks that had 80% cell confluency were used. The 15ml's of Grace's complete insect medium used to grow the cells was removed and replaced with 8ml's of Grace's complete

insect medium. 250 μ l of passage 1 virus stock was added directly to the medium and the flasks incubated at room temperature with gentle agitation for 2 hours. Each flask was fed with 7ml of Grace's complete insect medium and incubated at 27°C for 4 days. The 15ml supernatant was transferred to a sterile Beckman JA20 centrifuge tube and centrifuged at 2000 rpm for 10 minutes in a Beckman JA20 rotor to pellet the cells and debris. 1ml aliquots of the supernatant were made and stored at 4°C. These aliquots were used to generate Passage 3 stocks.

Passage 3 Virus Stocks: 2xT75 flasks were prepared in the same manner as for the passage 2 virus stocks. The cells were infected with 250 μ l of the passage 2 virus stock and incubated at room temperature for 2 hours with gentle agitation. The cells were fed with 9 ml's of Grace's complete insect medium and incubated at 27°C for 4 days. After 4 days of incubation the supernatant was transferred to a sterile Beckman JA20 centrifuge tube and centrifuged at 2000 rpm for 10 minutes in a Beckman JA20 rotor to pellet the cells and debris. The supernatant was stored at 4°C and was used to infect insect cells.

The cells and debris pellet of the passage 3 virus stocks was resuspended in 50 μ l cracking buffer (62.5mM Tris-HCl pH 6.8, 5% Sodium Dodecyl Sulphate (SDS), 5% v/v β -mercapto-ethanol, 10% v/v glycerol, 2.5% bromophenol blue). 20 μ l of the resuspended pellet and 20 μ l supernatant sample (10 μ l of the passage 3 virus stock mixed with 10 μ l of cracking buffer) were separated by SDS-PAGE and analysed by Western Blot analysis. The Roche Low Range Protein Molecular Weight Marker was used as the molecular weight marker. The SDS-PAGE gel with a 7.5% resolving gel [3.84ml 40% Acrylamide: bis-Acrylamide (19:1), 7.5ml 1M Tris pH 8.7, 8.96ml dddH₂O, 200 μ l 10% SDS, 200 μ l 10% Ammonium Persulphate (APS), 20 μ l TEMED] and a stacking gel of 5.2% [1.3ml 40% Acrylamide: bis-Acrylamide (19:1), 1.3ml Tris pH 6.8, 7.5 ml dddH₂O, 100 μ l 10% SDS, 50 μ l 105 APS, 10 μ l TEMED]. The SDS-

polyacrylamide gel was electrophoresed at 150-200v for up to 1 hour in 1x Q Running Buffer pH 8.3 [28.8g Glycine, 6g Tris, 2g SDS, made to 1L in dddH₂O] using the BioRad Gel Electrophoresis Apparatus. The gel was then electroblotted onto Hybond C nylon membrane (Amersham) in 1xTransfer buffer [14.8g Glycine, 3.03g Tris, 200ml Methanol, made to 1L in dddH₂O] using the BioRad Gel Transfer Apparatus at 250mA for 1 hour (Bjerrum and Heegaard, 1988).

For Western Blot analysis the nylon membranes were incubated in BLOTTO [5% non-fat milk powder dissolved in TBS Tween (100ml 1M Tris pH 7.5, 30ml 5M NaCl, 500 μ l Tween 20, made to 1L in dddH₂O)] overnight at room temperature with gentle rocking. The membranes were washed (1 x 15 minutes and 4 x 5 minutes) in TBS-Tween, and incubated for 2 hours in 1^o polyclonal anti-HaSV antibody (obtained from A. Dinsmore, Syngenta) diluted 1:3000 in 1% BSA dissolved in TBS-Tween. The membranes were washed (1 x 15 minutes and 4 x 5 minutes) in TBS-Tween, and incubated for 90 minutes in 2^o anti-mouse and rabbit antibodies labelled with peroxidase (BM Chemiluminescence Western Blotting Kit, Roche) diluted as per manufacturer's instructions in 1% BSA dissolved in TBS-Tween. The membranes were washed (1 x 15 minutes and 4 x 5minutes) in TBS-Tween and prepared for development as described in the BM Chemiluminescence Western Blotting Kit, Roche. The membranes were exposed to AGFA CP-BU medical X-ray film in an autocassette with intensifying screen for 5 minutes. The film was developed using the AGFA Film development kit and analysed.

The virus stocks generated in this study were subsequently used for all future expression studies and capsid production experiments.

3.5 Baculoviral Expression of Recombinant HaSV in *Spodoptera frugiperda* cells

Unless otherwise stated the protocol used for the infection of Sf9 cells with FBHaSV and analysis of the infection products was as described by Canady *et al.* (2000).

Determination of the Amount of Viral Inoculum Required for Infections at an Multiplicity of Infection of 5 and 10 using the Plaquing Technique

Sf9 cells were infected as monolayers in T75 Tissue Culture flasks. Flasks that showed 80% cell confluence were calculated to have 3×10^7 cells/flask. The flasks were infected with the recombinant FBHaSV at an multiplicity of infection (MOI) of 5 and 10. The amount of viral inoculum required for infection at the desired MOIs was initially calculated using the virus titre for FBHaSV calculated by the plaquing technique. For infections at an MOI of 5 the viral inoculum required was calculated as outlined in the Bac to Bac Manual, GIBCO BRL.

$$\begin{aligned} \text{Inoculum required (ml)} &= \frac{\text{desired MOI (pfu/ml)} \times \text{total number of cells}}{\text{titre of viral inoculum (pfu/ml)}} \\ &= \frac{5 \times (3 \times 10^7)}{8.5 \times 10^8} \\ &= \frac{15 \times 10^7}{8.5 \times 10^8} \\ &= 0.176 \text{ ml} \end{aligned}$$

176 μ l of FBHaSV virus was used to infect T75 flasks of Sf9 cells (3×10^7 cells/flask) at an MOI of 5. For an MOI of 10, 352 μ l of FBHaSV virus was used to infect T75 flasks of Sf9 cells (3×10^7 cells/flask). The flasks infected at an MOI of 5 and 10 were harvested 5 days post-infection and lysed with 0.5% (v/v) Nonidet P40 (NP40, Roche), a non-ionic detergent that does not dissociate virions (Gallagher and Rueckert, 1988). The cell lysate was centrifuged at 5000rpm in a Beckman JA20 rotor for 10 minutes to pellet the cell debris. RNase A was added to the supernatant to a final concentration of 10 μ g/ml and incubated at 27°C for 30 minutes. The cell lysate supernatant was stored at 4°C.

Determination of the Amount of Viral Inoculum Required for Infections at an MOI of 5 and 10 using the End-point Dilution Method

Following the determination of the FBHaSV virus titre using the end-point dilution assay, the amount of viral inoculum required for the infection of Sf9 cells in T75 flasks at an MOI of 5 and 10 was recalculated:

$$\begin{aligned}\text{Viral Inoculum required (ml)} &= \frac{\text{desired MOI (pfu/ml)} \times \text{total number of cells}}{\text{titre of viral inoculum (pfu/ml)}} \\ &= \frac{5 \times (3 \times 10^7)}{2.3 \times 10^{10}} \\ &= \frac{15 \times 10^7}{2.3 \times 10^{10}} \\ &= 0.007\text{ml}\end{aligned}$$

7 μ l of FBHaSV virus was used to infect T75 flasks of Sf9 cells (3×10^7 cells/flask) at an MOI of 5. For an MOI of 10, 14 μ l of FBHaSV virus was used to infect T75 flasks of Sf9 cells (3×10^7 cells/flask). The infected cells were harvested 4 and 5 days postinfection, and lysed with 0.5% (v/v) NP40. The cell lysate was centrifuged at 5 000rpm in a Beckman JA20 rotor for 10 minutes at 4°C to pellet the cell debris. RNase A was added to the supernatant to a final concentration of 10 μ g/ml and incubated at 27°C for 30 minutes. The cell lysate supernatant was stored at 4°C

VLP Purification

The cell lysate supernatant of the VLP preparations from Sf99 cell infected at an MOI of 5 and 10 using viral inoculum calculated by the plaquing technique was centrifuged through a 2ml 30% sucrose cushion made in buffer A (250mM NaCl, 50mM Tris pH7.5), in a Beckman SW41 rotor at 27 000rpm for 3 hours at 4°C. The sucrose pellets were resuspended overnight in 2ml buffer A. The resuspended sucrose pellets were centrifuged through a 10-40% continuous sucrose gradient made in buffer A and poured using a BioRad gradient maker. The gradients were centrifuged in a Beckman SW41 rotor at 30 000rpm for 2.5 hours at 4°C. 400 μ l fractions of the sucrose gradient were collected on an ISCO gradient fractionator. Consecutive fractions were pooled to obtain 800 μ l

fractions and the refractive indices (RI's) of the 800 μ l fractions were determined using a refractometer. The RI values were used to calculate the concentration of sucrose in each fraction. 10 μ l of each fraction was mixed with 10 μ l of cracking buffer (62.5mM Tris-HCl pH 6.8, 5% SDS, 5% v/v β -mercapto- ethanol, 10% v/v glycerol, 2.5% bromophenol blue), and separated by SDS-PAGE and analysed by Western Blot analysis.

The cell lysate supernatant of the VLP preparations from Sf99 cell infected at an MOI of 5 and 10 using viral inoculum calculated by the end-point dilution method was centrifuged through a 4ml 30% sucrose cushion made in buffer A, at 25 000rpm in a Beckman SW28 rotor for 5.5 hours at 11°C. The sucrose pellet was resuspended overnight in 1.5ml of buffer A (Taylor *et al.*, 2002). The resuspended sucrose pellets were loaded on a 10-40% sucrose step gradient prepared in buffer A, and centrifuged in a Beckman SW41 rotor at 40 000rpm for 1.25 hours at 11°C (Taylor *et al.*, 2002). 400 μ l fractions of the sucrose gradient were collected using an ISCO gradient fractionator. Consecutive fractions were pooled to make 800 μ l fractions. 10 μ l of the fractions was mixed with 10 μ l of cracking buffer, separated by SDS-PAGE and analysed by Western Blot analysis. The RI value of each of the 800 μ l fractions was determined using a refractometer. The refractive indices were used to determine the concentration of sucrose in each fraction.

SDS-PAGE separation of the 10-40% sucrose gradient fractions was carried out as follows: Roche Low Range Protein Molecular Weight Marker was used for analysis. Polyacrylamide gels with a 7.5% resolving gel and a stacking gel of 5.2% , were electrophoresed using the BioRad Gel Electrophoresis Apparatus at 150-200v for up to 1 hour in 1x Q Running Buffer pH 8.3 . The gel was then electroblotted onto Hybond C nylon membrane (Amersham) in 1xTransfer buffer using the BioRad Gel Transfer Apparatus at 250mA for 1 hour (Bjerrum and Heegaard, 1988).



For Western Blot analysis the nylon membranes were incubated in BLOTTO [5% non-fat milk powder dissolved in TBS Tween] overnight at room temperature with gentle rocking. The membranes were washed (1 x 15 minutes and 4 x 5 minutes) in TBS-Tween, and incubated for 2 hours in 1° polyclonal anti-HaSV antibody (obtained from A. Dinsmore, Syngenta) diluted 1:3000 in 1% BSA dissolved in TBS-Tween. The membranes were washed (1 x 15 minutes and 4 x 5 minutes) in TBS-Tween, and incubated for 90 minutes in 2° anti-mouse and anti-rabbit antibodies labelled with peroxidase (BM Chemiluminescence Western Blotting Kit, Roche) diluted as per manufacturer's instructions in 1% BSA dissolved in TBS-Tween. The membranes were washed (1 x 15 minutes and 4 x 5 minutes) in TBS-Tween and prepared for development as described in the BM Chemiluminescence Western Blotting Kit, Roche. The membranes were exposed to AGFA CP-BU medical X-ray film in an autocassette with an intensifying screen for a maximum of 5 minutes. The film was developed using the AGFA Film development kit and analysed.

The VLP preparations from Sf9 cells infected at an MOI of 5 determined using the virus titre calculated by the plaquing technique were centrifuged in a 30-60% continuous caesium chloride gradient at 30 000 rpm in a Beckman SW41 rotor for 18 hours at 11°C (Venter, 2002). A 1.5ml band of capsid protein was extracted approximately halfway through the gradient and the refractive index value of the band determined using a refractometer. The refractive index value of the band of capsid protein was used to determine the buoyant density of the VLPs.

3.6 RNA Isolations and Analysis

A modified method detailed in Agrawal and Johnson (1995), was used to determine whether or not the VLPs expressed in FBHaSV infected Sf9 cells encapsidated capsid protein mRNA. VLP preparations that had undergone spontaneous maturation were used. 100µl of the VLP preparation was used for RNA extraction and 50µl of wild-type HaSV at a concentration of 10^{11} virus

particles/ml was used as a positive control. Equal amounts of sample and phenol/TE (pH 4.5), were vortexed and microfuged at 13 000rpm for 2 minutes in a Heraeus microfuge. The aqueous layer was extracted with an equal volume of chloroform: isoamyl alcohol (24:1) by vortexing and microfuged as above. The aqueous layer was then removed and the chloroform: isoamyl alcohol extraction repeated. 0.1 volume of 3M sodium acetate and 2.5 volumes of 95% ethanol were added to the aqueous layer and the samples incubated at -20°C for at least 4 hours to precipitate the RNA. The samples were centrifuged at 13 000rpm for 10 minutes at 4°C to pellet the RNA. The RNA pellet was air-dried and resuspended in 10µl DEPC treated water.

1µl (in a total volume of 10µl) of the extracted RNA was used for RT-PCR using the Titan One Tube RT-PCR System (Roche). The primers used for the RT-PCR were HR236F3 (GTAGCGAACGTAGAGAA) and AV9 (CGTTGTGGCGGCAGGTGA) that bind within the HaSV P71 ORF to produce a 478 base pair fragment. 25µl reactions were set-up according to the manufacturers specifications. The samples were boiled for 1 minute prior to the addition of the reverse transcriptase enzyme mix. pAV3 a multi-copy yeast expression vector that contains the HaSV *p71* ORF was used as a positive control to ensure that the PCR conditions of the RT-PCR were optimal for the particular primers used. The products of the RT-PCR were analysed on a 1.2% agarose gel. 10µl of each 25µl reaction was loaded onto the gel. The RT-PCR protocol used is outlined in Table 3.2.

Table 3.2 RT-PCR Protocol for the Analysis of Viral RNA

Temperature (°C)	Time	No. of Cycles
60	30 minutes	1
94	2 minutes	1
94	10 seconds	10
55	30 seconds	
68	2 minutes	
94	10 seconds	30
55	30 seconds	
68	2 minutes + 5 seconds per cycle	
68	7 minutes	1

Amplification reactions were also performed using only *Taq* polymerase (Roche) under RT-PCR conditions to confirm that RNA and not DNA was being used as a template in the RT-PCR reactions.

3.7 Transmission Electron Microscopy (TEM) Analysis

For electron microscopic analysis, VLP preparations were absorbed onto carbon-coated grids. The grids were stained with 2% uranyl acetate and visualised in a JEM100CX transmission electron microscope.

3.8 Acid Maturation of Procapsids

Acid maturation of procapsid preparations was done by diluting the immature capsids either 1:10 or 1:5 in buffer B [70mM sodium acetate pH 5.0] (Canady *et al.*, 2000). 1ml acid maturation reaction samples were set up for each dilution. The diluted samples were incubated either at room temperature or on ice for 5 or 10 hours, or overnight to determine the best incubation time for maturation. 200 μ l of each acid maturation sample was precipitated by adding 24% Trichloro-acetic acid (TCA) to a final concentration of 6%, and the samples incubated on ice for 1 hour. The samples were then centrifuged at 13 000rpm for 10 minutes at 4°C and the supernatant removed

with a Pasteur pipette. 200 μ l of ice cold acetone was added to the TCA pellets, and the samples were incubated on ice for 15 minutes. The samples were then microfuged at 13 000rpm for 10 minutes at 4°C in a Heraeus microfuge and the supernatant removed with a Pasteur pipette. The pellets were air-dried for 10 minutes and the protein resuspended in 20 μ l of cracking buffer. The samples were separated by SDS-PAGE and analysed by Western Blot analysis as described above.

3.9 Encapsidation of a FITC Labelled Peptide by Recombinant HaSV VLPs

Recombinant HaSV VLPs were produced and purified as described above for VLP preparations produced and purified from Sf9 cells infected at an MOI of 5 and harvested 4 days postinfection using viral inoculum determined by the end-point dilution method.

The exogenous particle used to load the HaSV procapsids was a Tyrosine-Valine-Alanine-Aspartic acid-Hydroxyl peptide labelled with fluorescein isothiocyanate (FITC-YVAD, C₄₂H₄₁N₅O₁₃S) (BACHEM). FITC is a reagent that is normally used for fluorescent labelling. The peptide was resuspended in 0.2M NaHCO₃ according to the manufacturers specifications. Prior to attempting the loading experiments the ability of the spectrofluorometer (Fluorescence Spectrophotometer F-2500 Hitachi) to detect FITC-YVAD was calibrated. The samples used for the FITC-YVAD standard curve were further diluted in buffer A (used for resuspending the VLP preparations) as this was the buffer in which the loading experiments were to be performed. FITC-YVAD concentrations ranging from 10 μ mole to 0.1 μ mole were used to create the standard curve. The transmittance of FITC at an excitation wavelength of 490nm and an emission wavelength of 520nm was determined. FITC-YVAD concentrations above 1.0 μ mole were found to be above the range that could be detected by the spectrofluorometer, and FITC-YVAD concentrations ranging from 1.0-0.1 μ mole were analysed. The peak area for the various concentrations of FITC-YVAD was used as the differentiating factor (Zhang *et al.*, 2001). The experiments and

controls conducted to determine whether FITC-YVAD was encapsidated by FBHaSV VLPs are listed in Table 3.3.

Table 3.3 Experiments and Controls Conducted in the determination of FITC-YVAD Encapsidation by FBHaSV VLPs

<i>Sample No</i>	<i>PROCAPSIDS</i>	<i>FITC-YVAD</i>	<i>Buffer B</i>
1	+ ^a	- ^b	-
2	+	-	+
3	+	+	-
4	+	+	+
5	-	+	-

a + solutions added to the samples

b – solutions not added to the samples

400µl fractions of each gradient were collected using an ISCO gradient fractionator. Consecutive fractions were pooled to make 800µl fractions. The refractive index (RI) value of each fraction was determined using a refractometer. The RI values were used to determine the buoyant density of each fraction. The fractions that had a buoyant density similar to that calculated for FBHaSV VLPs and above were analysed further. 200µl of each fraction with a buoyant density similar to that calculated for FBHaSV and above were acetone precipitated. Acetone precipitation was carried out as follows: 300µl of 1% SDS and 1ml acetone were added to the samples and the samples incubated at 37°C for 1 hour. 10µg/ml bovine serum albumin (Roche), was added to the samples as a carrier, and the samples incubated at room temperature at room temperature for 30 minutes. The samples were microfuged at 13 000rpm in a Heraeus microfuge for 5 minutes. The supernatant was removed and the samples air-dried at 37°C for a maximum of 30 minutes. The protein pellets were resuspended in 20µl cracking buffer, separated by SDS-PAGE and analysed by Western blot analysis as described above.

The transmittance of each fraction at an excitation wavelength of 490nm and an emission wavelength of 520nm was determined using a spectrofluorometer. The concentration of FITC-YVAD in each fraction was determined using a FITC-YVAD concentration vs. peak area standard curve.

CHAPTER 4

Results

4.1 Construction of Recombinant Baculovirus Expressing HaSV Capsid Precursor Protein

Construction of Recombinant Bacmid

Of the four colonies screened by restriction mapping, two appeared to contain the HaSV *p71* fragment and one recombinant was selected for further restriction mapping. The presence of the correct DNA fragment was confirmed by determining the nucleotide sequence of the 5' end of the *p71* ORF. The Kozak sequence in this construct, GGATCCACAATGGAGAT, was similar to the baculovirus consensus sequence, Table 2.1, with A found at position -3 relative to the ATG at positions +1, +2, and +3. The length of the 5' untranslated leader sequence was however not optimal as it was 59 nucleotides long. mRNAs of baculoviruses usually have leader sequences that are short, and leader sequences that are longer than 30 nucleotides may interfere with the expression of the heterologous gene (O'Reilly, 1992).

The recombinant bacmid DNA isolated following transformation into *E. coli* DH10Bac cells was analysed by PCR amplification using pucF and pucR primers that bind within the *lacZ* α peptide to determine if the correct insert had been recombined into the bacmid DNA. If no recombination had occurred between the bacmid DNA and the donor plasmid the primers used for PCR amplification would bind within the bacmid and amplify a 300 base pair (bp) fragment. If pFASTBAC1 with no insert had been recombined into the bacmid DNA then the primers would bind within the bacmid, and amplification of a PCR product of approximately 2 300bp was expected. However if recombination had occurred between the insert ligated into pFASTBAC1 and the bacmid DNA, the expected size of the PCR product would be 4 339bp. The selected recombinant bacmid DNA isolate in (Figure 4.1 lane 2) yielded a PCR product of the size (4.3Kb) expected if recombination had occurred between pFBHaSV and the

bacmid DNA. A band of approximately 300 bp was also detected in all the samples and this band was due to binding of the primers within the bacmid DNA. Non-specific binding of the primers used for PCR amplification within the bacmid DNA was also detected in all the samples. The recombinant plasmid giving the 4.3kb PCR amplification product was used to generate recombinant virus stocks.

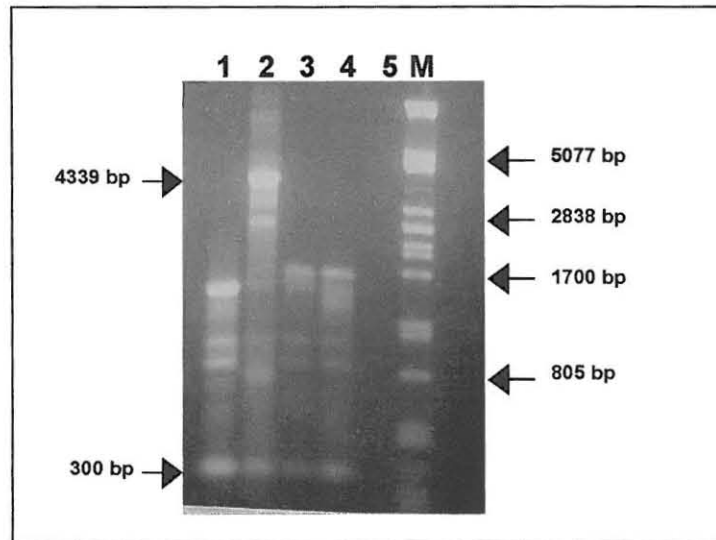


Figure 4.1 Agarose gel electrophoresis of PCR products of possible recombinant bacmid DNA, FBHaSV, isolates. Lanes 1-4. Bacmid DNA isolated from white *E. coli* DH10Bac transformants; **Lane 5.** No DNA control sample; **Lane M.** Molecular weight marker λ Pst I

4.2 Transfection of Insect cells

Establishment of Virus Stocks

The virus titre of the passage three virus stocks was initially determined using the plaquing technique. For the FBHaSV virus stocks 85 plaques were counted in the 10^{-7} dilution well. The virus titre for FBHaSV was calculated to be 8.5×10^8 plaque forming units (pfu)/ ml. The virus titre of the control virus was determined using the 10^{-8} dilution well where 10 plaques were counted. The virus titre of the control virus was calculated to be 1×10^9 pfu/ml. This method was however found to be highly unreliable as the plaques were unevenly distributed over the dilution series and it was also difficult to discern which areas of clear zones

following staining with Neutral Red were due to plaque formation and which areas were due to poor staining technique.

50% Tissue Culture Infectious Dose (TCID₅₀) Assay

Using the TCID₅₀ assay the infectivity of HaSV virus was scored by comparing the cells in the non-infected wells, the negative controls, with the cells in the infected wells and determining which of the infected wells showed signs of cytopathic effect caused by viral infection of the cells. The results obtained using this method are listed in Table 4.1.

Table 4.1 Infectivity of FBHaSV as scored using the TCID₅₀ Assay

Dilution	10 ⁻⁸	10 ⁻⁹	10 ⁻¹⁰	10 ⁻¹¹
No. "+"	8	4	2	0
No. "-"	0	4	6	8
Total "+"	14	6	2	0
Total "-"	0	4	6	8
% "+"	100	60	16	0

The dilution that would have given 50% infection was then determined, and was found to lie between 10⁻⁹ and 10⁻¹⁰. This dilution was calculated by linear interpolation between the infection rates observed at these dilutions.

The proportionate distance (PD) of a 50% response from the response above 50% was calculated:

$$\begin{aligned}
 1. \text{ PD} &= [(\% \text{ above } 50\%) - 50\%] / [(\% \text{ above } 50\%) - (\% \text{ below } 50\%)] \\
 &= (60 - 50) / (60 - 16) \\
 &= 10 / 44 \\
 &= 0.23
 \end{aligned}$$

The dose that would have given a 50% response (TCID₅₀) was calculated:

$$\begin{aligned}
 2. \text{ PD} \times \log \text{ dilution factor} &= 0.23 \times -1 \\
 &= -0.23
 \end{aligned}$$

$$\begin{aligned}
 3. \log 50\% \text{ end-point or TCID}_{50} &= \log (\text{dilution above } 50\% \text{ end-point}) + "2" \\
 &= \log [10^{-9} + (-0.23)] \\
 &= 9.23
 \end{aligned}$$

$$4. \text{ TCID}_{50} = 10^{-9.23}$$

$$\begin{aligned}
 5. \text{ Virus titre for FBHaSV} &= 1/ \text{TCID}_{50} \text{ in infectious doses/ unit of inoculum} \\
 &= 3.4 \times 10^{10}/\text{ml}
 \end{aligned}$$

The virus titre determined in infectious doses/ unit of inoculum was converted to plaque forming units (pfu)/ unit of inoculum using the Poisson distribution. It was understood that the proportion (p) of cultures remaining uninfected at any given dose was $e^{-\mu}$, where μ is the mean concentration of infectious particles at that dose. The TCID_{50} was the dose at which 50% of the cultures became infected, i.e. $p = 0.5$. Therefore $0.5 = e^{-\mu}$, thus implying that μ , the mean concentration of infectious units at that dose = 0.69 (O'Reilly *et al.*, 1992).

$$\begin{aligned}
 6. \text{ pfu/ unit of inoculum} &= \text{TCID}_{50} \times 0.69 \\
 &= 3.4 \times 10^{10} \times 0.69 \\
 &= 2.3 \times 10^{10} \text{ pfu/ml}
 \end{aligned}$$

4.3 Baculoviral Expression of Recombinant HaSV in *Spodoptera frugiperda* Cells

Virus passage 3 stocks were analysed for the presence of HaSV capsid protein. It was essential to determine that the virus stocks were capable of infecting the *Spodoptera frugiperda* cells and that infection resulted in the expression of HaSV capsid protein as the virus stocks were to be used for all infections requiring the expression of HaSV capsid protein in the insect cells.

The soluble and insoluble fractions of the virus passage 3 stocks were analysed by Western blot to determine: (1) The amount of HaSV capsid protein that was being expressed. (2) What fraction of the expressed protein remained soluble as insoluble protein could not be utilised for further experiments. If a higher fraction of the expressed capsid protein was insoluble than was soluble, mechanisms for assisting in the post-translation processing of the expressed protein would have been required (Ailor and Betenbaugh, 1999).

Western blot analysis of the pellets (insoluble fractions) and the viral inoculum supernatant (soluble fractions) of the passage 3 virus stocks made from the

recombinant bacmid DNA, FBHaSV, and the vector DNA, control (Figure 4.2) indicated that HaSV capsid protein was being expressed only in the cells infected with FBHaSV. The lack of detection of any protein in the control samples indicated that the primary antibodies used did not cross-react with any of the insect cell and vector protein.

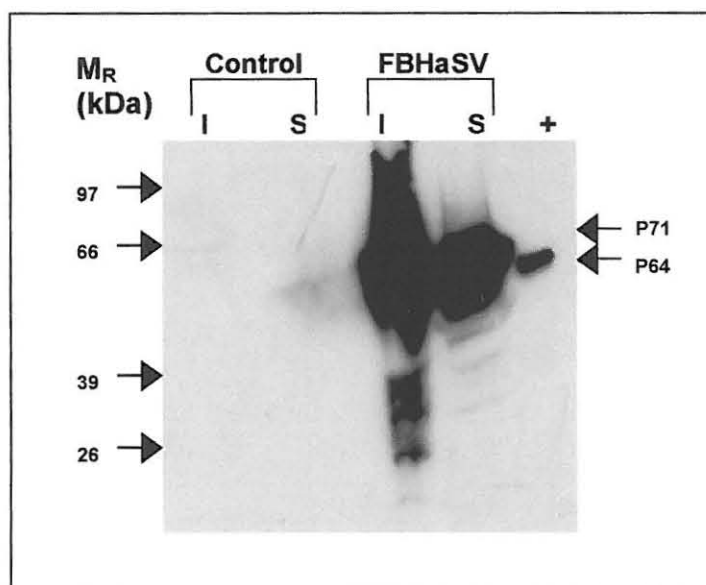


Figure 4.2 Western blot analysis of soluble and insoluble fractions of passage 3 virus stocks from Sf9 cells. + 1ng HaSV positive control; I. Insoluble fractions following centrifugation; S. Soluble fractions following centrifugation. M_R. Protein Molecular Weight marker. The X-Ray film was exposed for 2 minutes

Viral protein was detected in both soluble and insoluble fractions of FBHaSV. The expressed protein appeared to be mature capsid protein (P64) as it comigrated with the HaSV positive control that contains mature capsid protein. More protein could be detected in the insoluble fractions than in the soluble fractions. This was however most probably due to the pellets being resuspended in a volume lower than that of the soluble fractions. The concentration of protein that was insoluble was found to be lower than that of the soluble protein when the volumes that both samples were resuspended in was taken into account.

Effect of Varying Multiplicity's of Infection (MOI) on HaSV Capsid Protein Expression

Recombinant gene expression using the baculovirus expression system usually results the in host cells cellular machinery being completely deteriorated several days postinfection (Ailor and Betenbaugh, 1999). One of the objectives of this project was to express large enough quantities of pure HaSV procapsids that could be used in *in vitro* loading experiments. Agrawal and Johnson (1995) found that the method used in virus purification affected VLP yield. The pH at which the VLPs are harvested has been found to have an effect on the morphology of the expressed VLPs, with procapsids being found when infected cells are harvested at neutral pH (Canady *et al.*, 2000; Taylor *et al.*, 2002). The objective of these experiments was therefore to determine the MOI at which the insect cells should be infected so as to get maximum expression of soluble precursor capsid protein prior to the host cells post-translation processing machinery being totally deteriorated by the expressed virus.

Due to an error in the initial calculation of the virus titre of the passage 3 virus stocks the MOI of the recombinant virus stocks was underestimated. As a result the initial experiments were conducted at an MOI of 250 and 125. *Spodoptera frugiperda* cells infected at an MOI of 250 and 125 were infected with 352 μ l and 176 μ l viral inoculum respectively. The effects of the infection of *Spodoptera frugiperda* cells at an MOI 125 and 250 on procapsid production were analysed and compared. The effects of the number of days the cells were harvested postinfection on procapsid production were also analysed.

The 10%-40% sucrose gradient profile of the VLP preparations from *Sf9* cells infected with recombinant baculovirus at an MOI of 250 and harvested 5 days post-infection indicated that immature capsid protein (P71) was present in all the fractions with its highest concentrations being detected at sucrose concentrations ranging from 12%-17% (Figure 4.3, Panel A lanes 5-7, Panel C, Fractions 5-7). Mature capsid protein (P64) was detected in sucrose concentrations higher than 28% with the highest concentration of p64 being

detected at 33% sucrose (Figure 4.3 Panel B lanes 10-12 and 14, Panel C Fractions 10-12 and 14).

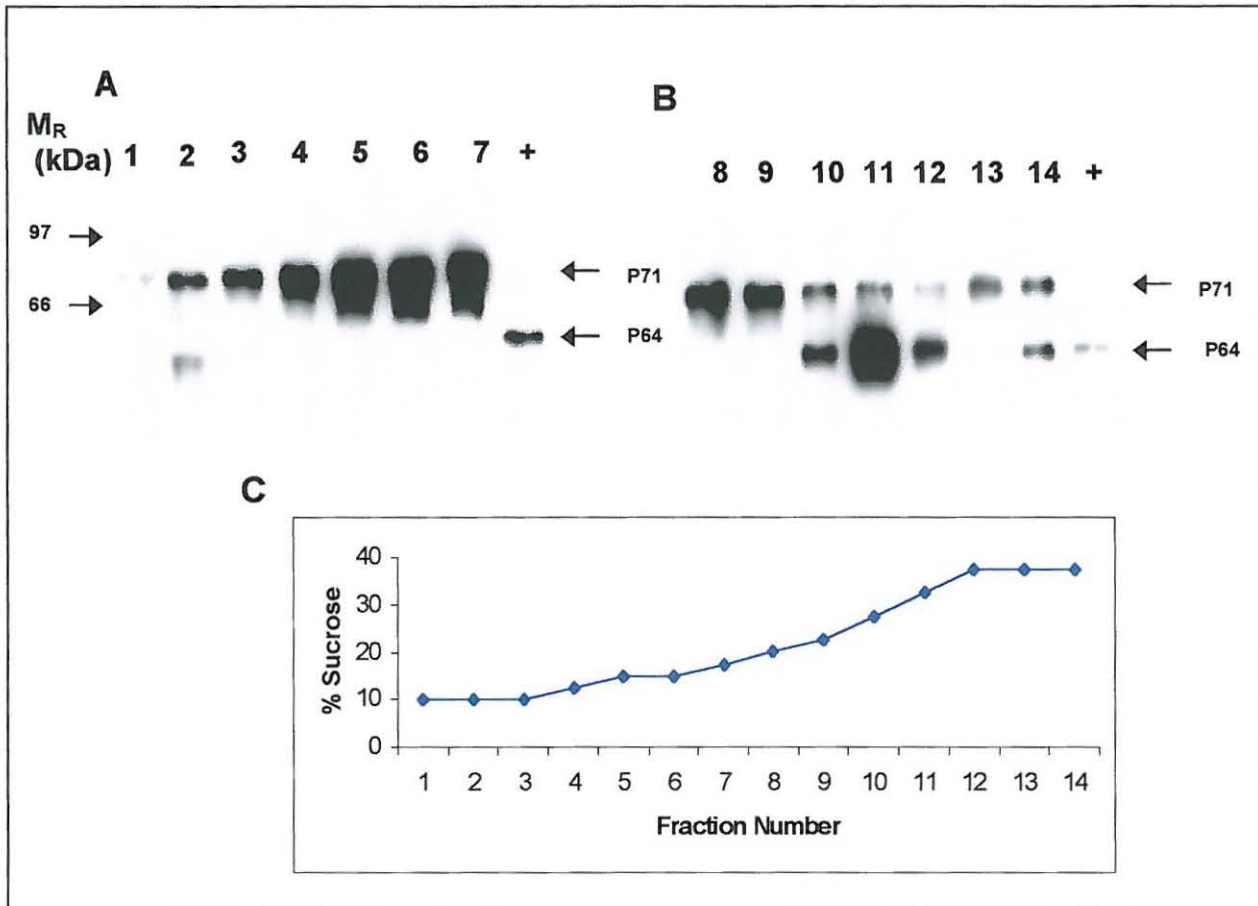


Figure 4.3 Sucrose gradient centrifugation of VLPs expressed in Sf9 cells infected with FBHaSV at an MOI of 250 and harvested 5 days postinfection. M_R, Molecular weight marker. Panels A and B Western blot analysis of the fractions collected across a 10-40% sucrose gradient. Lanes 1-14 represents the fraction number of each sample. 10 μl of each fraction was loaded onto the SDS-polyacrylamide gel. +, 1 ng HaSV was used as a positive control. P71 and P64 represent precursor capsid protein and mature capsid protein respectively. The X-ray film was exposed for 5 minutes. Panel C Profile of the sucrose concentrations of the fractions in A and B.

The sucrose gradient profile of the VLP preparations from Sf9 cells infected with FBHaSV virus at an MOI of 125 and harvested 5 days postinfection was very similar to the profile of VLP preparations from insect cells infected at an MOI of 250 and harvested 5 days postinfection (data not shown). The number of days

(4 or 5 days) postinfection that the infected cells were harvested also had no effect on HaSV capsid protein expression.

The VLPs produced in *Sf9* cells infected at an MOI of 125 were also purified by centrifugation through a 30-60% caesium chloride gradient. A band of virus protein was extracted from the caesium chloride gradient. The buoyant density of VLPs in this band of protein was calculated and found to be 1.27g/ml.

Sf9 cells were then infected at an MOI of 10 and 5 with 14 μ l and 7 μ l of viral inoculum respectively. The infected cells were harvested 4 and 5 days postinfection to determine the optimal time span in which to express maximum amounts of procapsid VLPs.

The 10-40% sucrose gradient profile of the VLP preparations from *Sf9* cells harvested 5 days post-infection and infected at an MOI of 10 indicated that both P71 and p64 were expressed (Figure 4.4 Panels A and B). P64 was detected only in the fractions with a maximum sucrose concentration of 10.5% (Figure 4.4, Panel A lanes 1-4, and Panel C). In the fractions with a sucrose concentration ranging from 11-22% no capsid protein could be detected (Figure 4.4, Panels A and B lanes 5-10, and Panel C). P71 was detected in the fractions that had a sucrose concentration ranging from 25-39% with the highest concentration of immature capsid protein detected at a sucrose concentration of 30% (Figure 4.4 Panels A and lanes 1-4 and 11-15, and Panel C). The 10-40% sucrose gradient profile of VLP preparations from FBHaSV infected *Sf9* cells infected at an MOI of 10 and harvested 4 days post-infection was very similar to that of the 5 days post-infection harvests, data not shown.

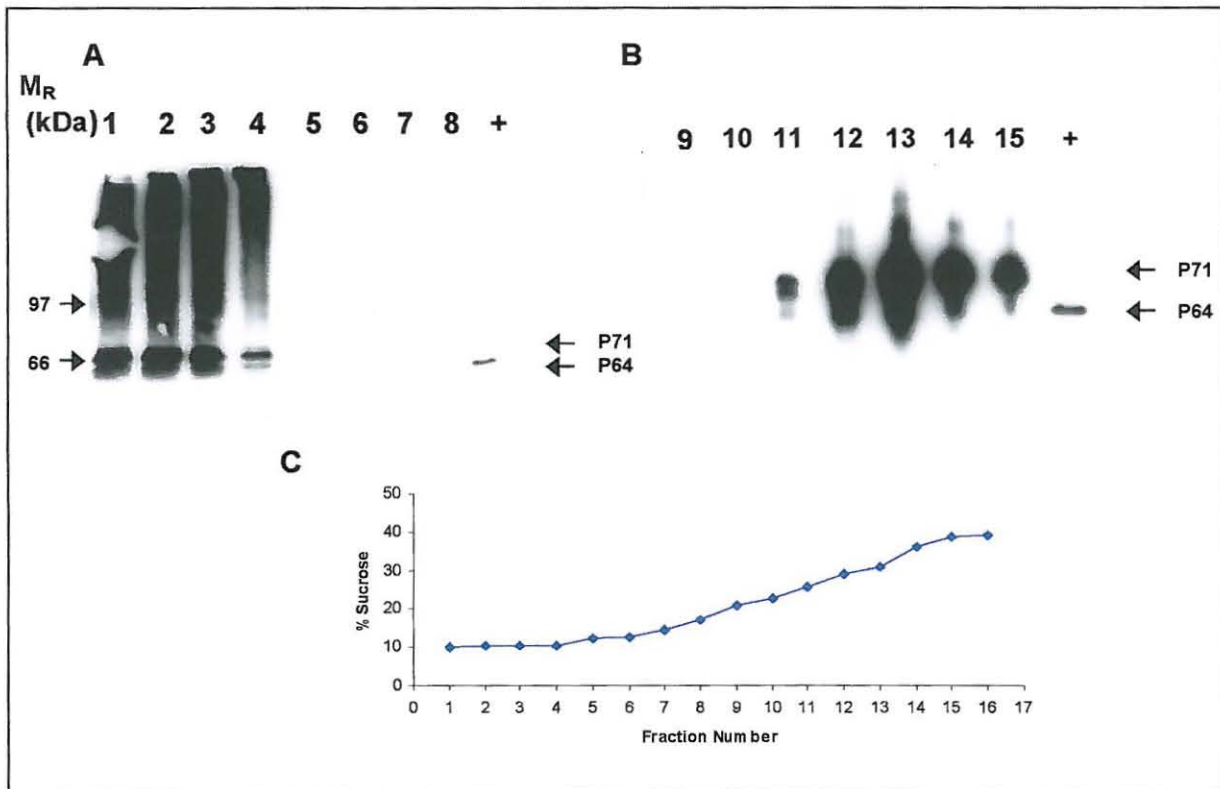


Figure 4.4 Sucrose gradient centrifugation of VLPs expressed in Sf9 cells infected with FBHaSV at an MOI of 10 and harvested 5 days postinfection. M_R. Molecular weight marker. **Panels A and B** Western blot analysis of the fractions collected across a 10-40% sucrose gradient. **Lanes 1-15** represent the fraction number of each sample +. 1ng HaSV was used as a positive control. **P71 and P64** represent precursor capsid protein and mature capsid protein respectively The X-ray film was exposed for 2 minutes. **Panel C** Profile of the sucrose concentrations of the fractions in **A** and **B**.

The 10-40% sucrose gradient profile of the VLP preparations from Sf9 cells harvested 5 days post-infection and infected at an MOI of 5 indicated that both P71 and P64 was being expressed (Figure 4.5, Panels A and B). Very faint bands of P64 could only be detected in the fractions with a sucrose concentration ranging from 10-15%(Figure 4.5, Panel A, lanes 1-3). P71 was detected in all the fractions with the highest concentration of this protein detected at a sucrose concentration of 39% (Figure 4.5, Panels A and B, lanes 6-16, Panel C).

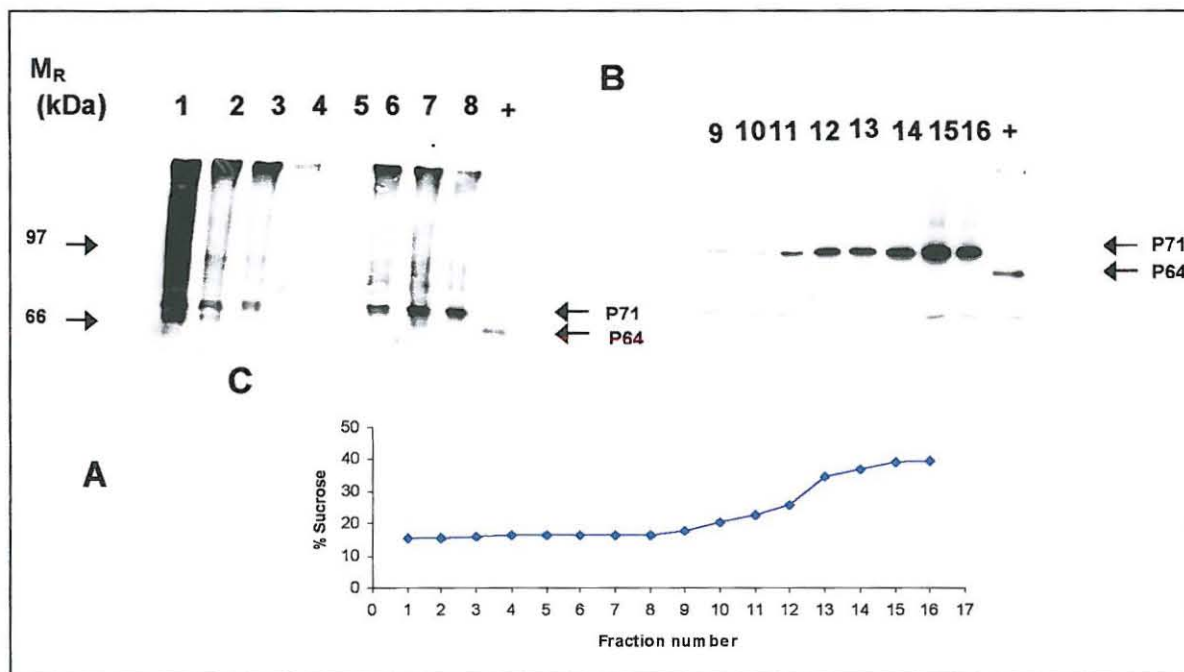


Figure 4.5 Sucrose gradient centrifugation of VLPs expressed in Sf9 cells infected with FBHaSV at an MOI of 5 and harvested 5 days postinfection. M_R Molecular weight marker Panels A and B Western blot analysis of the fractions collected across a 10-40% sucrose gradient. Lanes 1-16 represent the fraction number of each sample. +. 1 ng HaSV was used as a positive control. P71 and P64 represent precursor capsid protein and mature capsid protein respectively. The X-ray film was exposed for 2 minutes. Panel C Profile of the sucrose concentrations of the fractions in A and B.

Western blot analysis of the 10-40% sucrose gradient profile of the VLP preparations generated in Sf9 cells infected with FBHaSV virus at an MOI of 5 and harvested 4 days post-infection showed predominantly the presence of P71 (Figure 4.6, Panels A and B). P64 was detected in fractions that had a sucrose concentration that ranged from 10-12% (Figure 4.6, Panel A lanes 1-2). P71 was detected in all the fractions with the highest concentration detected at a sucrose concentration of 36-37% (Figure 4.6, Panels A and B).

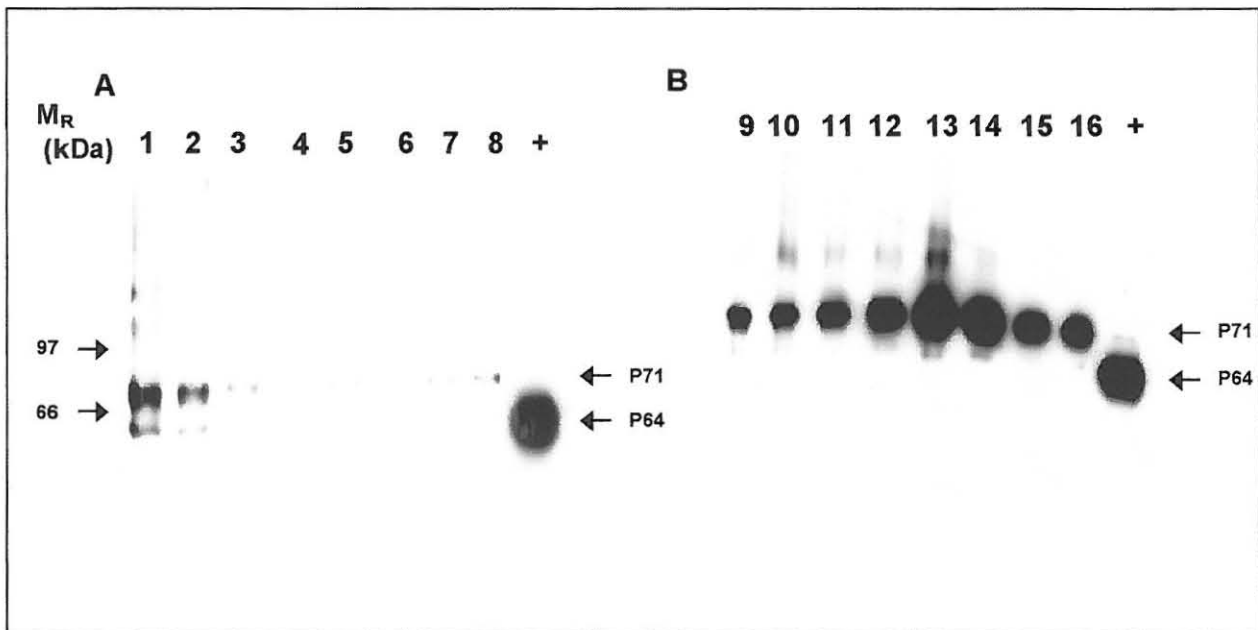


Figure 4.6 Sucrose gradient centrifugation of VLPs expressed in *Sf9* cells infected with FBHaSV at an MOI of 5 and harvested 4 days postinfection. M_R , Molecular weight marker. Panels A and B Western blot analysis of the fractions collected across a 10-40% sucrose gradient. Lanes 1-16: fraction number of each sucrose gradient sample. +, 1ng HaSV was used as a positive control. P71 and P64 represent precursor and mature capsid proteins respectively.

The infection of cells at an MOI of 250 and 125 resulted in the production of capsids that spontaneously underwent autoproteolytic maturation cleavage. Infection at these MOIs was therefore not suitable for maximum procapsid production. For optimum production of HaSV procapsids *Sf9* cells infected at an

MOI of 5 and harvested 4 days postinfection appeared to produce the best results. The VLPs produced in cells infected at this MOI were mostly procapsids with negligible amounts of spontaneous maturation cleavage occurring. Infection of *Sf9* cells at an MOI of 5 and harvest 4 days postinfection was used for all experiments that required maximum procapsid production.

Transmission Electron Microscopy Analysis

VLP preparations from *Sf9* cells infected at an MOI of 250 were analysed by transmission electron microscopy to determine the presence of VLPs. Fraction

11 in (Figure 4.3, Panel B) was used for the transmission electron microscopic examination. This fraction was selected for electron microscopic examination, as it was the fraction in which the highest concentration of a protein that co-migrated with mature capsid protein was detected. Autoproteolytic maturation cleavage stabilises VLPs (Zlotnick *et al.*, 1994). VLPs that had undergone autoproteolytic maturation cleavage were therefore analysed by TEM as these VLPs would be more stable than the procapsids and they were also more likely to morphologically resemble wild-type HaSV. The transmission electron microscopic examination of Fraction 11 revealed particles of approximately 40nm that were morphologically similar to wild-type HaSV (Figure 4.7, Panel B vs. Panel A respectively). The VLPs also appeared to be electron dense suggesting that they may have encapsidated RNA (Figure 4.7 Panel B).

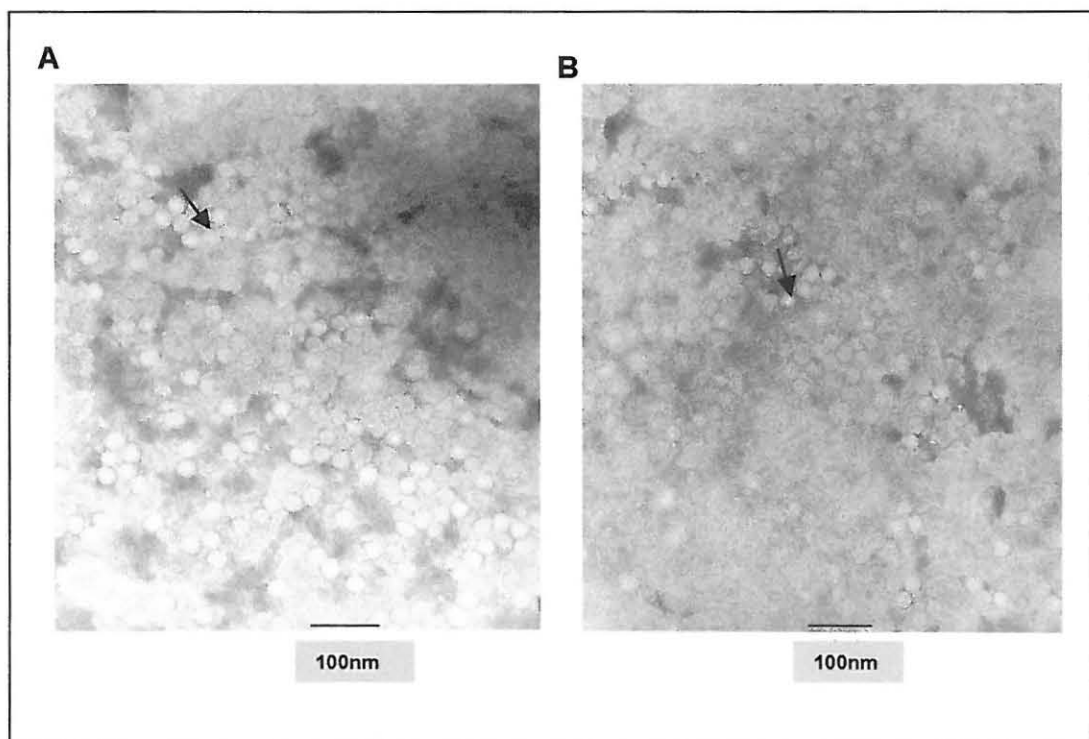


Figure 4.7 Transmission electron microscopy analysis of HaSV VLPs from *Spodoptera frugiperda* 9 cells infected with FBHaSV. **Panel A** Electron micrograph of wild-type HaSV. The arrow indicates virus particles. **Panel B** Electron Micrograph of HaSV VLPs derived from *Sf9* cells infected with FBHaSV. The arrow indicates VLPs

RNA Isolation and Analysis

$N_{\omega}V$ VLPs produced in *Spodoptera frugiperda* cells specifically and selectively encapsidate their capsid protein mRNA as they assemble. The assembled VLPs also undergo spontaneous autoproteolytic maturation (Agrawal and Johnson, 1995). VLP preparations from Sf9 cells infected at an MOI of 250 were used for RNA extractions. These VLPs were used as they underwent post-assembly spontaneous maturation (Figure 4.3, Panel B), and they also appeared electron dense suggesting that they had encapsidated RNA (Figure 4.7, Panel B). The RNA encapsidated by the VLPs was analysed to determine if capsid protein mRNA had been encapsidated.

RT-PCR and PCR analysis of isolated wild-type HaSV RNA gave the expected results of a 478 bp fragment in the lane with the RT-PCR products and no product in the PCR reactions lane (Figure 4.8, Panel B lanes 2 and 3) respectively. The RT-PCR and PCR products of RNA extracted from the VLP preparations also gave results similar to those of the wild-type HaSV RNA. A 478 bp fragment was identified in the lane containing the RT-PCR products and no product was detected in the lane containing the PCR samples (Figure 4.8, Panel B lanes 4 and 5) respectively. pAV3 was amplified under the same conditions as the wild-type HaSV and FBHaSV RNA using *Taq* polymerase instead of the Reverse transcriptase enzyme mix used in the RT-PCR kit. The amplification of pAV3 was used as a positive control for the PCR conditions of the RT-PCR, and a product of 478 bp was amplified (Figure 4.8, Panel B lane 6).

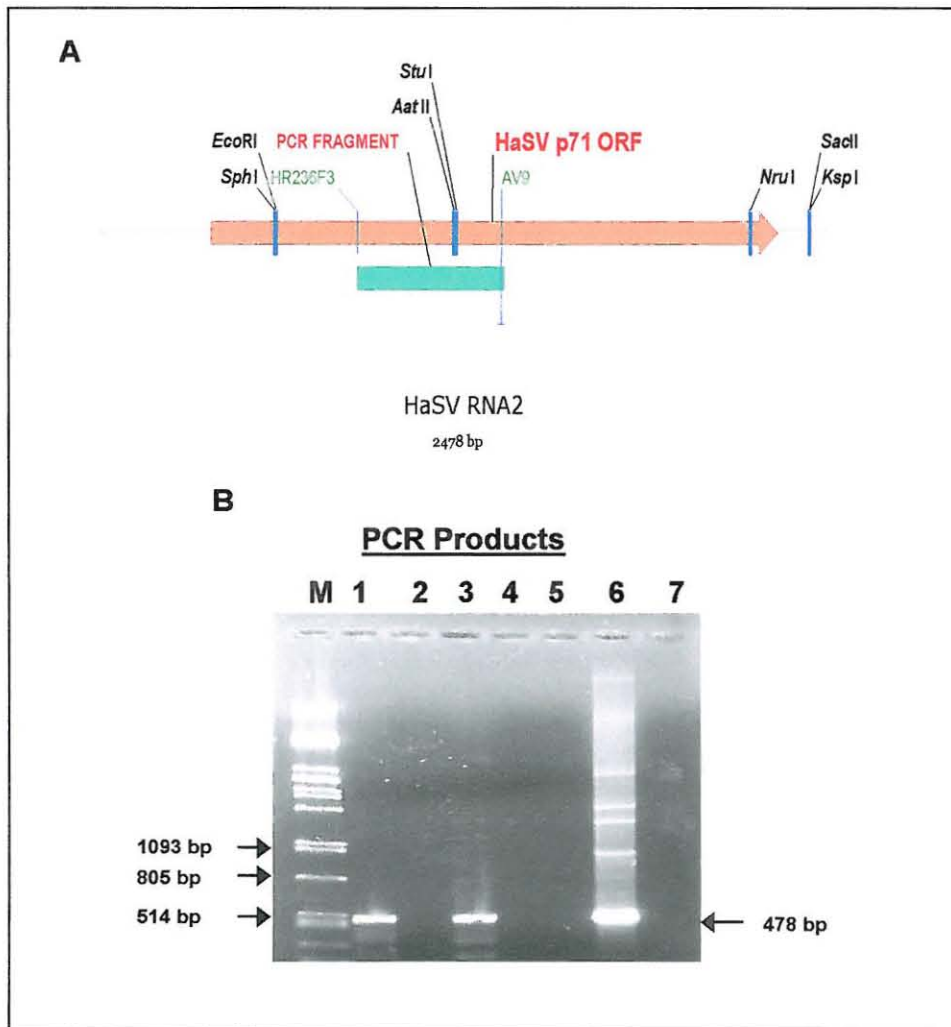


Figure 4.8 Panel A. A schematic representation of HaSV RNA2. An orange arrow indicates the p71 ORF. The positions of the PCR primers are indicated. The size of the RT-PCR product relative to the p71 ORF indicated by a green rectangle below the orange arrow that indicates the p71 ORF. **Panel B. Agarose gel electrophoresis of RT-PCR products of RNA extracted from wild-type HaSV and HaSV VLPs produced in Sf9 cells.** Panel B: M. *λPst I* molecular weight marker. Lane 1. Wild-type RNA analysed by RT-PCR. Lane 2. Wild-type RNA analysed by PCR. Lane 3. VLP RNA analysed by RT-PCR. Lane 4. VLP RNA analysed by PCR. Lane 5. H₂O negative control analysed by RT-PCR. Lane 6 pAV3 analysed by PCR. Lane 7. H₂O negative control analysed by PCR.

4.4. Encapsidation of Exogenous Molecules by FBHaSV Capsids

N₀V procapsids are porous VLPs at neutral pH that have the same protein composition as the solid shell mature capsids (Canady *et al.*, 2000). Lowering of the procapsid pH from neutral to pH 5.0 results in a conformational transition of

the procapsids to a solid shell capsid (Canady *et al.*, 2001; Taylor *et al.*, 2002). Once the solid shell structure has been achieved the capsid proteins undergo irreversible autoproteolytic maturation cleavage, thus resulting in the capsids being "locked" in the mature capsid conformation, (Canady *et al.*, 2001).

N ω V's pH dependent structural changes are similar to those observed in *Cowpea chlorotic mottle virus* (CCMV) where the virus undergoes reversible swelling at pH values higher than 6.5 to form a porous capsid. When the pH of the viruses is lowered they undergo a structural change and form solid shell capsids (Douglas and Young, 1998). CCMV's pH dependent ability to open and close pores on its surface has been used to reversibly encapsidate inorganic minerals and an organic polymer within its capsid. N ω V procapsids could be used in a manner similar to that used for CCMVs to encapsidate exogenous molecules that would be locked within the VLP capsid once autoproteolytic maturation cleavage had been induced.

Acid Maturation

Due to the similarities at sequence level between the *Nudaurelia* ω -like viruses (Hanzlik *et al.*, 1995), it was understood HaSVs procapsids would also have porous capsid shells that could be induced to form solid capsid shells that undergo autoproteolytic maturation cleavage by the lowering of the procapsid pH. If the HaSV VLPs underwent autoproteolytic maturation cleavage of their precursor capsid protein when their pH was lowered from neutral to pH 5.0, mature capsid protein (P64) would be detected in VLP preparations that previously only contained precursor capsid protein (P71). If HaSV procapsid protein was able to undergo pH dependent autoproteolytic maturation cleavage, then the HaSV VLPs too could possibly be utilised in a manner similar to that of CCMV to encapsidate exogenous molecules.

HaSV VLPs produced in Sf9 cells infected at an MOI of 10 and 5 and harvested 4 days post-infection were used as these samples contained precursor capsid protein with negligible amounts of mature capsid protein. The VLPs were

purified by centrifugation through a 30% sucrose cushion. The acid maturation samples were initially diluted 1:5 and 1:10 in buffer B [70mM sodium acetate (pH 5.0)] and incubated for 5 hours at room temperature and on ice. Acid maturation appeared to give the best results when the VLPs expressed from cells infected at an MOI of 5 were diluted 1:5 in buffer B and incubated at room temperature. The same sample diluted 1:10 in buffer B also acid matured, but not as much maturation was detected as in the 1:5 dilution sample (Figure 4.9 Panels A and B lane 3). Data for undiluted sample controls, although not indicated in Figure 4.9, was based on data obtained from similar experiments performed, also not indicated.

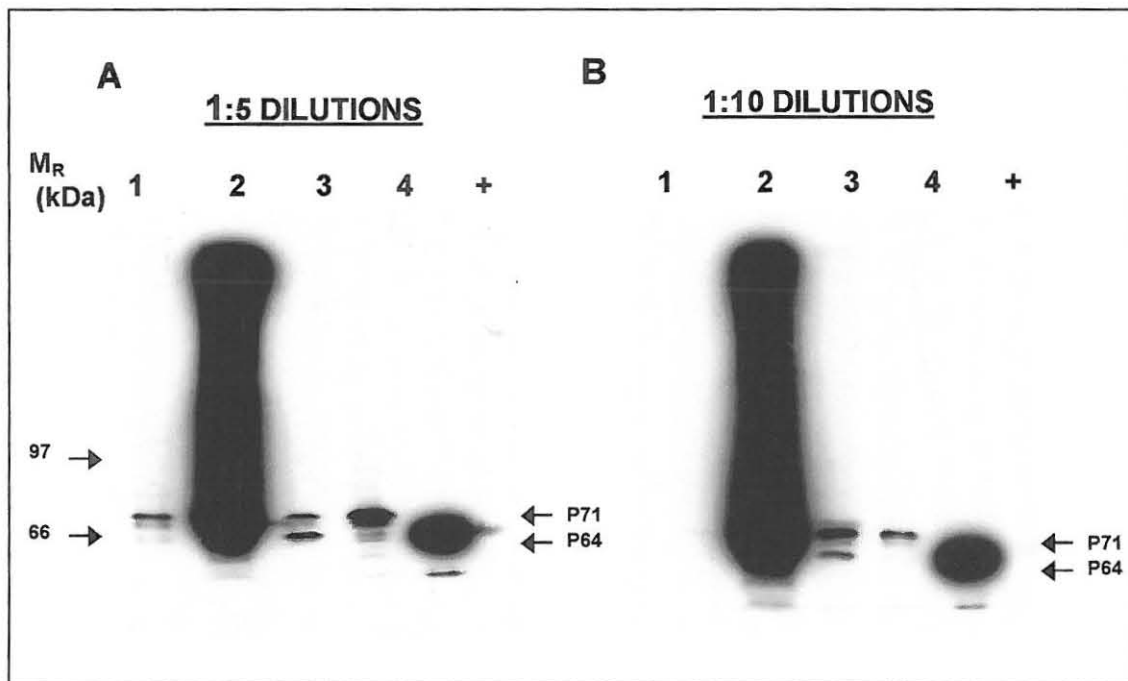


Figure 4.9 Western Blot analysis of acid matured HaSV capsid protein diluted 1:5 (Panel A) and 1:10 (Panel B) in buffer B. + 1ng HaSV. M_R . Molecular weight marker. **Panels A and B:** Lane 1. MOI 10 samples incubated at room temperature (RT). Lane 2. MOI 10 samples incubated on ice. Lane 3 MOI 5 samples incubated at RT. Lane 4. MOI 5 samples incubated on ice. **P71 and P64** indicate the positions of precursor and mature capsid protein respectively. The X-ray film was exposed for 5 minutes

The VLP preparations from cells infected at an MOI of 10 and incubated at room temperature showed very little maturation when the samples were diluted 1:5 in buffer B and no protein could be detected in the lane with the 1:10 dilution (Figure 4.9, Panels A and B lane 1). It was difficult to discern if the samples incubated on ice had undergone autoproteolytic maturation cleavage as the protein samples had formed smears (Figure 4.9, Panels A and B lane 2).

Dilution of the VLP preparations 1:5 in buffer B gave the best acid maturation results. The 1:5 dilutions in buffer B were therefore repeated and samples were incubated for 5 hours or 10 hours or overnight. The incubation time was increased because even though the conformational transition from procapsid to capsid occurs within milliseconds, autoproteolytic maturation cleavage is delayed and has a half-life of several hours (Canady *et al.*, 2001). An increase in incubation time was therefore expected to result in an increase in the amount of P71 that was converted to P64 as the time scale increased. The samples were incubated at room temperature and on ice to determine if time would have an effect on acid maturation on ice.

No maturation was detected in the samples that were acid matured and incubated on ice (Figure 4.10, lanes 3-5). Very faint bands of protein, both P71 and P64 could be detected in the samples incubated overnight at room temperature (Figure 4.8, lane 6). No protein was detected in the sample incubated at room temperature for 10 hours (Figure 4.10, lane 7). P71 and P64 could be detected in the sample incubated at room temperature for 5 hours, (Figure 4.10, lane 8) however not all the protein had matured.

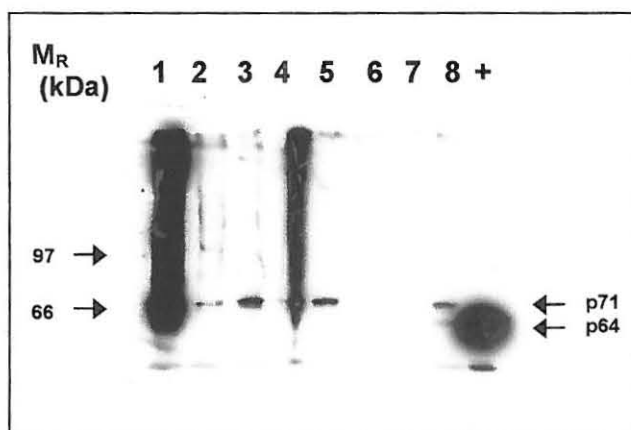


Figure 4.10 Western Blot analysis of acid matured HaSV capsid protein diluted 1:5 in buffer B. M_R . Molecular weight marker. **Lane 1.** Unmatured sample. **Lane 2.** 1:10 dilution of the unmaturation sample. **Lane 3.** Matured sample incubated 5 hours on ice. **Lane 4.** Matured sample incubated 10 hours on ice. **Lane 5.** Matured sample incubated overnight on ice. **Lane 6.** Matured sample incubated overnight at room temperature (RT). **Lane 7.** Matured sample incubated for 10 hours at RT. **Lane 8.** Matured sample incubated at RT for 5 hours. The X-ray film was exposed for 5 minutes

The lack of increase in the rate of autoproteolytic maturation cleavage of the FBHaSV VLPs with an increase in incubation time was probably due to not all the precursor capsid protein assembling into capsids, and therefore not all the detected precursor protein would undergo acid maturation. Lowering the pH of procapsids has been postulated to protonate acidic residues and reduce electrostatic repulsion thus allowing the protein subunits to compact and form the solid shell of the capsid has been postulated (Zlotnick *et al.*, 1994). The rate of autoproteolytic maturation cleavage of the precursor capsid protein would therefore decrease with an increase in the stability of the procapsid (Gallagher and Reuckert, 1988; Zlotnick *et al.*, 1994). The acidic residues of the capsids that did assemble were probably protonated at a relatively fast rate thus resulting in an increase in the energy barrier for proteolysis fairly quickly. A fast increase in the energy barrier for proteolysis would therefore result in a decreased rate of autoproteolytic maturation cleavage. Based on the results obtained in Figure 4.10, the produced FBHaSV VLPs have an autoproteolytic maturation half-life of not more than 5 hours, with the rate of maturation

decreasing after 5 hours of incubation. Autoproteolytic maturation cleavage kinetics are energy driven (Zlotnick *et al.*, 1994). Incubation of the acid maturation samples on ice would therefore inhibit or slow down the rate of maturation. Acid maturation of FBHaSV VLPs was therefore executed at room temperature so as not to slow down the cleavage kinetics and for no longer than 5 hours as the half-life for acid maturation of FBHaSV VLPs appeared to be no longer than 5 hours. Not all the expressed procapsid protein underwent acid maturation implying that some of the protein might have been aggregated protein.

FITC-YVAD Encapsidation by Recombinant HaSV VLPs

VLPs from *Spodoptera frugiperda* 9 cells infected at an MOI of 5 and harvested 4 days postinfection were centrifuged through a 30% sucrose cushion and the sucrose pellets resuspended overnight in buffer A [250mM sodium chloride and 50mM Tris (pH 7.5)].

Western blot analysis of the VLP preparations from *Sf9* cells infected at an MOI of 5 and harvested 4 days postinfection indicated that no autoproteolytic maturation cleavage had occurred as the capsid protein was still in its precursor form (Figure 4.11). The VLP preparation in (Figure 4.11, lane 2) was used in the FITC-YVAD encapsidation experiments, as it appeared to contain the most precursor capsid protein.

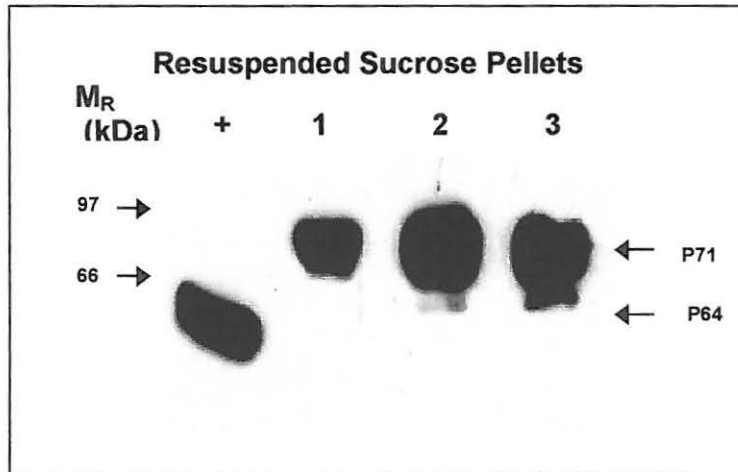


Figure 4.11 Resuspended sucrose pellets used in the encapsidation of FITC. + 1ng HaSV was used as a positive control. Lanes 1-3 Different sucrose pellets resuspended in buffer A. 10 μ l of each sucrose pellet suspension from a total volume of 1.5ml was loaded on the SDS polyacrylamide gel. The X-ray film was exposed for 5 minutes

1ng of HasV in the positive control contains 10⁹vp/ml (Venter, 2001). The protein signal of the VLP preparation in (Figure 4.11, lane 2) was appeared three times more intense as the 1ng HaSV positive control on the X-ray film. Based on this observation, the VLP preparation in (Figure 4.9, lane 2) therefore contained 3x10⁹vp/ml. 10 μ l out of 1.5 ml of the VLP preparation had been separated by SDS-PAGE and analysed by Western blot analysis and there were therefore 4.5x10¹¹vp/ml in the 1.5ml sample used in the FITC-YVAD encapsidation experiments. 400 μ l of the VLP preparation was used in each of the FITC-YVAD encapsidation experimental reactions and the control reactions outlined in Table 3.3, except for the sample 1 controls where 300 μ l of the VLP preparation was used. The 400 μ l reactions each therefore contained 1.2x10¹¹vp/ml and the 300 μ l reaction contained 9x10¹⁰vp/ml. 1 μ mole of FITC-YVAD was added per virus particle as this was the maximum amount of FITC-YVAD that could be detected by the spectrofluorometer as determined by the FITC-YVAD concentration vs. peak area standard curve.

The various samples outlined in Table 3.3 were incubated at room temperature for 24 hours. The samples to be acid matured were diluted 1:5 in buffer B and incubated at room temperature for 5 hours. The FITC-YVAD encapsidation samples as well as the controls were then centrifuged through a 30-60% caesium chloride gradient. The refractive indices of 30, 40, 50, and 60% control caesium chloride were determined using a refractometer. The buoyant densities at each of the different concentrations of caesium chloride were obtained from Dawson *et al* (1986). The refractive index values and the buoyant densities of the control caesium chloride samples were used to construct a refractive index vs. buoyant density standard curve. The caesium chloride refractive index vs. buoyant density standard curve used to calculate the buoyant densities of the FITC-YVAD encapsidation experimental reactions and control reactions had a R^2 value of 0.9914.

The caesium chloride gradient fractions of FITC-YVAD encapsidation experimental and control samples with a buoyant density equal to and above 1.27g/ml were analysed by Western blot. These fractions were selected for analysis as the buoyant density of FBHaSV VLPs was calculated to be 1.27g/ml.

10 μ l of each 800 μ l caesium chloride gradient was analysed by Western blot. Western blot analysis of the procapsid control fractions with a buoyant density above 1.27g/ml indicated that the maximum buoyant density at which HaSV precursor capsid protein could be detected was 1.36g/ml. Most of the HasV precursor protein was detected at a buoyant density of 1.27g/ml (Figure 4.12, Panel A and C Fraction 4)

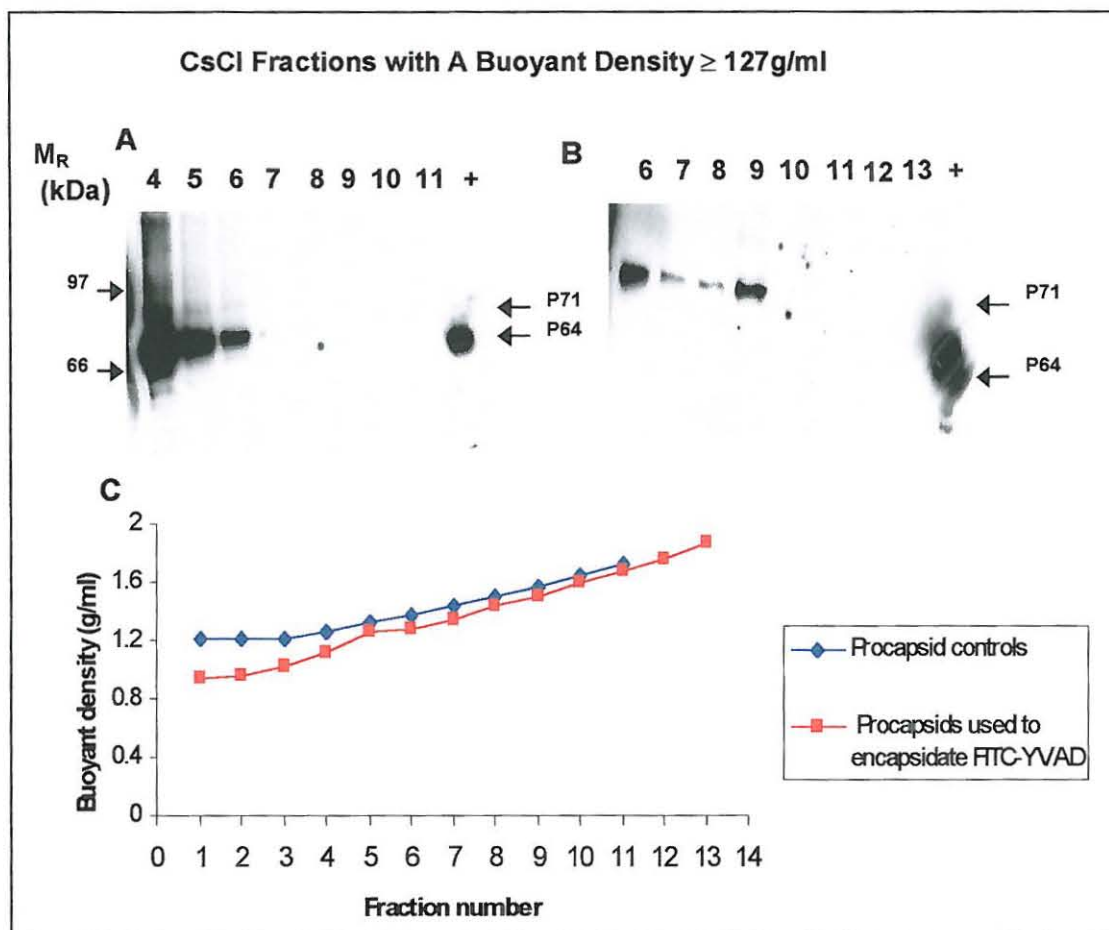


Figure 4.12 Western blot analysis of caesium chloride (CsCl) gradient fractions of FBHaSV VLPs and FBHaSV VLPs used in the encapsidation of FITC. M_R Molecular weight marker. + 1ng HaSV was used as a positive control. **Panel A.** Western blot analysis of procapsid control fractions with a buoyant density ≥ 1.27 g/ml collected across a 30-60% caesium chloride gradient. The fraction numbers are indicated above each lane. **Panel B.** Western blot analysis of acid matured VLPs used in the encapsidation of FITC with a buoyant density ≥ 1.27 g/ml collected across a 30-60% caesium chloride gradient. The fraction numbers are indicated above each fraction. **P71 and P64** indicate the positions of precursor and mature capsid protein. The X-ray film was exposed for 5 minutes. **Panel C.** Profile of the buoyant densities of the fractions in A and B.

FBHaSV VLPs used in the encapsidation of FITC-YVAD and acid matured were also analysed by Western blot. Fractions with a buoyant density ≥ 1.27 g/ml were analysed. Western blot analysis of these fractions indicated that HaSV capsid protein could be detected at buoyant densities up to and including 1.5g/ml (Figure 4.12, Panel B and C). The concentration of HaSV capsid protein also appeared to be equivalent at buoyant densities of 1.281g/ml and 1.5g/ml

(Figure 4.12, Panel B and C). Western blot analysis of the FITC-YVAD loaded acid matured fractions also indicated that the procapsids had not undergone maturation. No HaSV capsid protein could be detected by Western blot analysis of the acid matured procapsid controls and therefore no correlation could be made between the buoyant densities of the acid matured VLPs used in the encapsidation of FITC-YVAD and acid matured VLPs used as controls.

Various known FITC-YVAD concentrations were analysed using a spectrofluorometer and the reading obtained used to create a standard curve. The spectrofluorometer readings for the various FITC-YVAD concentrations are outlined in (Table 4.2). The peak area of the graph obtained for each FITC-YVAD concentration was used to create a standard curve.

Table 4.2 Spectrofluorometer readings of various FITC-YVAD concentrations used to create peak area vs. FITC-YVAD concentration standard curve

FITC (µmoles)	Excitation Start (nm)	Excitation Apex (nm)	Emission (nm)	Peak Height	Peak Area (nm)	Peak Valley (nm)
0.1	490	497.5	600	151.3	4047.907	600
0.25	490	497	600	330.3	8003.981	600
0.5	490	498.5	600	681.5	15601.279	600
0.75	490	498.5	600	947.3	21729.820	600
1.0	490	497.5	600	1353	30867.649	600

The peak area and concentration of the various FITC-YVAD samples were used to create a peak area vs. FITC-YVAD concentration standard curve (Figure 4.13). The FITC-YVAD encapsidation experimental and control caesium chloride fractions were analysed using a spectrofluorometer to determine the peak area of the FITC-YVAD excitation and emission wavelength graphs for each fraction. The FITC-YVAD concentration in each fraction was determined using an area of peak vs. FITC-YVAD concentration standard curve with a R^2 value of 0.9961 (Figure 4.13).

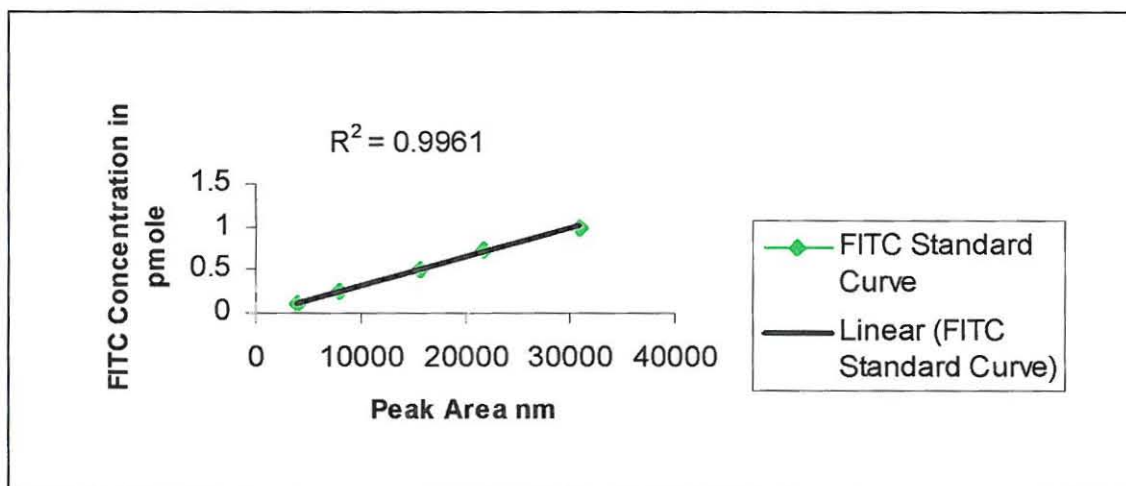


Figure 4.13 Standard curve used to calculate FITC concentrations in various FITC containing samples. The R^2 value of the graph is indicated. The peak area values for the graphs of the various FITC concentrations were determined using a spectrofluorometer and are outlined in Table 4.2

The concentration of FITC-YVAD profile in the VLP preparations used in the encapsidation of FITC-YVAD but not treated with buffer B was similar to that of the FITC control (Figure 4.14). The FITC-YVAD concentration profile of the buffer B treated VLP preparations used in the encapsidation of FITC-YVAD showed a marked decrease in the concentration of FITC when compared to that of the FITC-YVAD control (Figure 4.14). The concentration of FITC-YVAD in the VLP preparation fractions that had a buoyant density $\geq 1.27\text{g/ml}$ was less than $0.1\mu\text{mole}$. The FITC-YVAD control fractions with a buoyant density $\geq 1.27\text{g/ml}$ also had FITC-YVAD concentration levels less than $0.1\mu\text{mole}$.

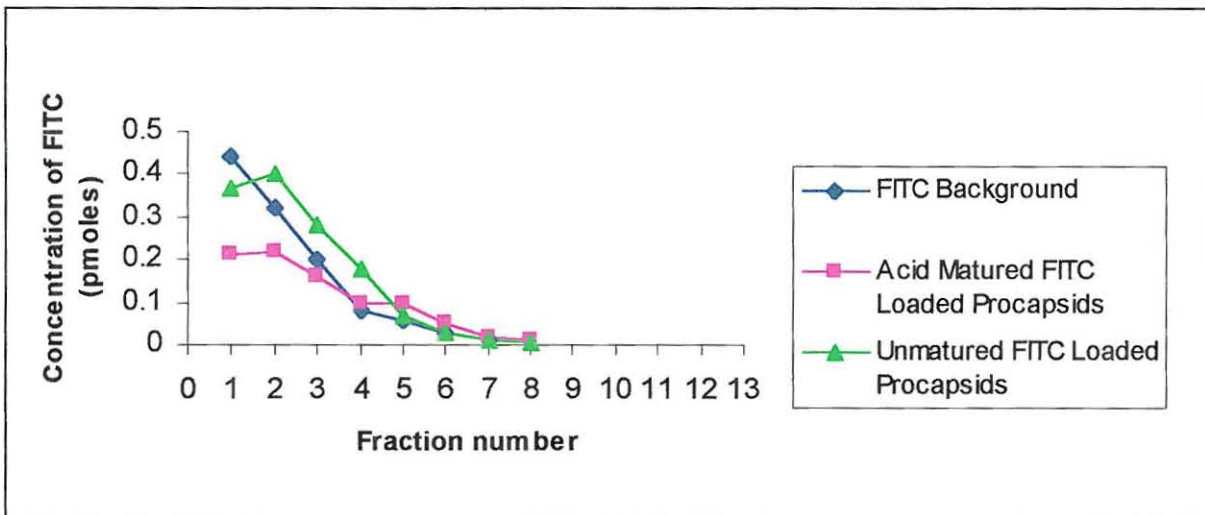


Figure 4.14 FITC peptide concentration profiles of VLP preparations as determined using a spectrofluorometer. The VLP preparations were mixed with FITC peptide and incubated for 24 hours prior to centrifugation through a 30-60% caesium chloride gradient. The transmittance of FITC peptide at an excitation wavelength of 490nm and an emission wavelength of 520nm was determined.

A repetition of the FITC-YVAD encapsidation experimental reactions and controls reactions yielded no results that correlated with the results that were obtained above. No HaSV capsid protein could be detected by Western blot analysis in any of the fractions with a buoyant density of 1.27g/ml and above.

CHAPTER 5

Discussion

The main objective of this project was to express the HaSV coat protein in insect cells using a baculovirus expression system. The expressed precursor coat protein was expected to assemble into VLPs based on similar observations for N_ωV coat protein expressed in a baculovirus expression system (Agrawal and Johnson, 1995). The assembled VLPs would either undergo spontaneous autoproteolytic maturation or remain in their procapsid form. This was based on conflicting results obtained when the N_ωV coat protein was expressed in a baculovirus expression system. Agrawal and Johnson (1995) found that when the N_ωV coat protein was expressed in a baculovirus expression system, the expressed N_ωV precursor coat protein spontaneously underwent autoproteolytic maturation cleavage. However when Canady *et al.* (2000) expressed the N_ωV coat protein under similar conditions they found that at neutral pH the expressed precursor coat protein did not undergo spontaneous maturation and maturation had to be induced by lowering the pH of the procapsids to pH 5.0. The differences in the results obtained by Agrawal and Johnson (1995) and Canady *et al.* (2000) were as a result of both groups using different N_ωV cDNAs (Glover, 2002). The assembled HaSV VLPs were also to be analysed for the encapsidation of their coat protein mRNA.

HaSV procapsids that did not undergo spontaneous autoproteolytic maturation cleavage were required for the encapsidation of an exogenous molecule within the capsid. The encapsidated molecule would then be locked within the capsid by the induction of autoproteolytic maturation cleavage. Autoproteolytic maturation cleavage irreversibly locks the capsid shell in its mature conformation (Canady *et al.*, 2001; Taylor *et al.*, 2002).

5.1 Construction and Isolation Recombinant Plasmids

pFBHaSV a baculovirus transfer vector that contains the HaSV *p71* ORF was constructed and transformed into *E. coli* DH10Bac cells where recombination of the HaSV *P71* ORF into bacmid DNA occurred. Recombination was confirmed by PCR analysis of DNA extracted from the *E. coli* DH10Bac cells. The PCR primers used in the PCR amplification reaction showed nonspecific binding within the bacmid DNA resulting in bands of non-specific PCR product. The nonspecific binding of the primers was likely due to the fact that the *lacZ* α region that flanks the points of recombination within the recombinant baculovirus shuttle vector (bacmid) came from a pUC-based plasmid. The primers used in the PCR amplification reaction were pUC primers. Some of the plasmids used in the construction of the bacmid were also pUC plasmids (Luckow *et al.*, 1993). The PCR primers would then also bind to regions that showed similarities to their sequence within the regions of the pUC plasmids that were used to construct the bacmid. Increasing the length of the primers used to include sequences that are not common with pUC plasmids could have decreased the degree of nonspecific binding. The annealing temperature of the PCR cycle could have been increased thus also decreasing the rate of nonspecific binding of the primers. The use of primers that bound within the region recombined into the bacmid would have also decreased the rate nonspecific PCR products. However since the presence of the 4.3kb PCR product indicating the integration of the *p71* ORF fragment into the bacmid was clearly visible, the PCR reaction was not optimised. The recombinant bacmid DNA, FBHaSV, and bacmid DNA were used to transfect *Spodoptera frugiperda* 9 cells.

The 5' end of the *p71* ORF was sequenced to confirm that the context of the translation initiation codon was the same as the consensus sequence of highly expressed AcMNPV proteins (O'Reilly *et al.*, 1992; Venter, 2001). The context of the initiation codon was such that A was found at position -3 and G at position +4 with the AUG at positions +1, +2 and +3 respectively. The context of the translation initiation codon is important in preventing leaky scanning

(Gale *et al.*, 2000). If the context of the translation initiation codon is such that the preinitiation complex recognises the translation initiation codon as a weak codon, it scans past it and initiates translation at a downstream initiation codon with a consensus context for translation initiation (Kozak, 1999; Gale *et al.*, 2000). mRNAs of baculoviruses have short untranslated leader sequences that are no longer than 30 bases (O'Reilly *et al.*, 1992). Agrawal and Johnson (1995), found that when the untranslated leader sequence of N_ωV capsid protein ORF was 90 bases long, no detectable levels of capsid protein was expressed in a baculovirus expression system. Decreasing of the length of the leader sequence to 22 bases resulted in the expression of capsid protein that was detectable (Agrawal and Johnson, 1995). The untranslated leader sequence of the *p71* ORF in pFBHaSV was 59 bases long, however genes with untranslated leader sequences of up to 60 bases have been expressed using the baculovirus expression system (O'Reilly *et al.*, 1992). The length of the untranslated leader sequence within a range of 17-80 bases may increase the efficiency of translation (Kozak, 1999). The *p71* ORF contains a stem loop structure that starts at position 1130 (Hanzlik *et al.*, 1995). The position of secondary structures in relation to the initiation codon may have a positive or negative effect on mRNA translation (Kozak, 1999). The secondary structure contained within the *p71* ORF is too far downstream of the initiation codon to affect it positively, however its position may still enable it to inhibit ribosomal scanning (Kozak, 1999; Gale *et al.*, 2000). The translation of the HaSV capsid protein mRNA however did not seem to be affected by the presence of the stem loop structure, as capsid protein subunits that were still capable of assembling were expressed.

Several methods may be utilised to transfect recombinant DNA into insect cells. These methods include the use of the liposome technique where a low copy number of vector is introduced to the cells and a greater number of cells receive the construct (Luque and O'Reilly, 1999). Another method that may be used is calcium phosphate mediated transfection, however this method requires large amounts of DNA (O'Reilly *et al.*, 1992). The liposome technique was used to

transfect Sf9 cells with recombinant FBHaSV DNA and control bacmid DNA. The supernatants obtained following the transfection of *Spodoptera frugiperda* 9 cells with FBHaSV were used to infect Sf9 cells and recombinant and nonrecombinant bacmid virus plaque purified. Plaque purification was not necessary (Luckow *et al.*, 1993), but a single round of plaque purification was done to ensure that no cross-contamination between the recombinant virus and the nonrecombinant parental virus had occurred. Plaque purification is conducted to ensure that no cross contamination occurs between the parental virus and the recombinant virus when recombination is carried out within the insect cells (O'Reilly 1992). However with the Bac to Bac[®] Baculovirus system recombination takes place within *E. coli* cells and not within insect cells thus negating the need for plaque purification (Luckow *et al.*, 1993). The nonrecombinant parental virus was plaque purified as it was used as a negative control for all experiments conducted with FBHaSV.

Following plaque purification the virus was amplified and virus stocks made. Passage 3 virus stocks were used because virus passages higher than 5 made in cell culture may lead to the accumulation of variants within the stock (Luque and O'Reilly, 1999). The titres of passage 3 virus stocks were determined for both FBHaSV and bacmid DNA using plaquing techniques. This technique however proved unreliable in determining the titres of the virus due to difficulties experienced in identifying the occlusion negative plaques and also due to the plaques not being evenly distributed over the dilution series range. The poor distribution of the plaques over the dilution series range may have been due to poor amplification of the recombinant virus, or due to poor transfection results. The poor transfection results may have been due to insufficient DNA or poor quality of the DNA used. The quality of the DNA may be improved by utilising DNA for transfection within 48 hours of its extraction from *E. coli* DH10Bac cells (Luckow *et al.*, 1993).

Due to problems encountered with the plaquing technique the TCID₅₀ assay was used to calculate the virus titre of the passage three stocks as it had been previously found to give virus titre results similar to those calculated using the plaquing technique (Roberts, 1985). The TCID₅₀ assay is the dilution of virus inoculum that would be required to infect 50% of multiple cultures (O'Reilly *et al.*, 1992). The TCID₅₀ assay proved to be more reliable than the plaquing technique as it did not involve the identification of occlusion negative plaques. The TCID₅₀ assay involves the identification of infected cells by the presence of cytopathic effects (O'Reilly *et al.*, 1992). The TCID₅₀ assay has been found to be just as reliable as the plaquing technique under conditions where the problems encountered with the plaquing technique have been resolved. The TCID₅₀ assay also has an advantage over the plaquing technique, in that differentiation between occlusion negative plaques caused by recombinant virus and occlusion positive plaques caused by parental virus is not necessary (O'Reilly *et al.*, 1992).

The virus titre in infectious doses/ unit of inoculum as calculated using the TCID₅₀ assay was used to calculate the virus titre in plaque forming units (pfu's)/ unit of inoculum. The titre was calculated in pfu's/ unit of inoculum as the amount of viral inoculum required for specific multiplicity's of infection is calculated in pfu's/ unit of inoculum. When the FBHaSV virus titre, calculated according to the plaquing technique, was compared to that calculated according the end-point dilution, it was found that the virus titre calculated using the TCID₅₀ assay was at least 1 log higher than the virus titre calculated using the plaquing technique. Based on the virus titre calculated by the TCID₅₀ assay it was determined that cells infected with viral inoculum calculated using virus titre determined by the plaquing technique were infected at MOIs of 250 and 125 instead of 10 and 5 respectively. The virus titre that was calculated by the TCID₅₀ assay was then used to calculate the viral inoculum for all infections carried out.

Viral inoculum required for infection at an MOI of 5 and 10 was 7 μ l and 14 μ l respectively. Agrawal and Johnson (1995) used 1ml of viral inoculum to infect insect cells at an MOI of 5-10. The volume of viral inoculum required for infection at desired MOIs is dependent on virus titre. A low virus titre necessitates the use of high volumes of virus inoculum for infection at low MOIs (O'Reilly *et al.*, 1992). A low virus titre might be as a result of low virus amplification which in turn is affected by the cell passage number and the type of cell line that is being utilised (O'Reilly *et al.*, 1992). The method of transfection also affects the efficiency and levels of recombinant virus stocks with the liposome technique being the most reliable (Luque and O'Reilly, 1999).

5.2 Baculoviral Expression of Recombinant HaSV VLPs in *Spodoptera frugiperda* cells

The MOI at which cells are infected, affects the rate at which the host's cellular resources are utilised (Nolan and Shatzman, 1998). The virus shuts down the host's cellular metabolism to maximise viral exploitation of the cell's resources (Ailor and Betenbaugh, 1999). When cells are infected at an MOI of 5-10, the metabolic activity of the infected cells normally ceases within 72 hours postinfection (O'Reilly *et al.*, 1992; Agrawal and Johnson 1995). The use of a strong baculoviral promoter such as the *polyhedrin* promoter results in the expression of high levels of proteins (O'Reilly *et al.*, 1992). The high levels of protein being expressed require processing prior to their secretion from the cell (Ailor and Betenbaugh, 1999). When the host's cellular metabolism is shut down, the secretory pathway is no longer able to provide for the folding, assembly and postranslation modification of proteins. The expressed protein may then accumulate as aggregates (Nolan and Shatzman, 1998). Once the virus particles have utilised all of the host's available resources, the virus particles are released from the dying cells (O'Reilly, 1992). The infection of insect cells at a low MOI means that a low number of infectious particles are introduced into the cells. The cellular resources are therefore utilised at a low rate thus decreasing the chances of the expression of misfolded proteins (Nolan and Shatzman 1998).

The infection of cells at an MOI of 250 and 125 bombards the cells with infectious particles. The host cellular resources are therefore utilised at a fast rate resulting in metabolic activity ceasing early. The quick loss of the host's metabolic activity therefore results in an accumulation of protein that has not been properly processed by the secretory pathway (Nolan and Shatzman, 1998). When Sf9 cells were infected at an MOI of 250 or 125 P71 was detected in all the fractions of the 10-40% sucrose gradient. The presence of P71 in all the fractions was possibly as a consequence of the virus particle being unstable, as the structure of the procapsid has compromised stability. Canady *et al.* (2000) visualised N ω V procapsids under EM and found that the procapsid structure was fragile, with the stability of the VLP being increased by lowering the particle pH from neutral to 5.0. The P71 would therefore be in constant transition between the assembled and disassembled states (T. Hanzlik, personal communication).

Some of the P71 expressed in insect cells infected at an MOI of 250 and 125 into VLPs that underwent spontaneous autoproteolytic maturation cleavage that was made evident by the detection of P64 in fractions with a sucrose concentration higher than 28%. Autoproteolytic maturation cleavage is a process that is dependent on the assembly of virus particles and is not known to occur in unassembled subunits (Gallagher and Rueckert, 1988). The detection of P64 in some of the sucrose gradient fractions therefore implied that the expressed precursor capsid protein subunits had undergone assembly that would have facilitated the occurrence of spontaneous autoproteolytic maturation cleavage. Spontaneous maturation cleavage of capsid protein expressed in baculovirus expression systems has been previously described for nodaviruses and N ω V (Zlotnick *et al.*, 1994; Agrawal and Johnson, 1995). The spontaneous autoproteolytic maturation cleavage of precursor capsid protein is facilitated by the release of the virus particles from dying cells (Agrawal and Johnson, 1995). The infection of Sf9 cells at an MOI of 250 and 125 would have therefore provided the conditions for the spontaneous maturation to occur, as the use of

the host's cellular resources by the infectious particles would have led to the cells dying at a fast rate.

The detection of both P71 and P64 in some of the fractions was due to the immature capsids having the same buoyant density as the mature capsids. The presence of both immature and mature capsid proteins in some of the fractions was possibly due to autoproteolytic maturation not having gone to completion. The kinetics of autoproteolytic maturation cleavage are consistent with a reaction that slows down at a rate that is proportional to the number of cleavages that occur (Zlotnick *et al.*, 1994). Mature capsid protein may therefore be found mixed with immature capsid protein (Schneemann and Marshall, 1998; Canady *et al.*, 2001). The capsids that have undergone autoproteolytic maturation are also stable and do not undergo the transitions in their conformation that is evident in the procapsids. This is due to autoproteolytic maturation being irreversible and also stabilising the structure of the mature capsid (Canady *et al.*, 2000 and 2001; Taylor *et al.*, 2002).

The assembly of P71 into mature capsids was also made evident by the observation of VLPs that were morphologically indistinguishable from wild-type HaSV by TEM. The assembly of FHV and N_oV capsid protein into VLPs that are morphologically indistinguishable from wild-type virus when their capsid proteins have been expressed in baculovirus systems has also been previously described (Schneemann *et al.*, 1993; Agrawal and Johnson, 1995).

The expression of VLPs in Sf9 cells infected at an MOI of 10 or 5 yielded only P71 in fractions with a sucrose concentration of 25% and above across a 10-40% sucrose gradient. The absence of any detectable P64 in these fractions suggested that the expressed protein had not undergone assembly. The presence of P64 in fractions lower than 25% suggested that the protein had aggregated. This was due to the fact that capsids have a smaller diameter than procapsids and would therefore be expected to migrate further than the procapsids in a 10-40% sucrose gradient (Canady *et al.*, 2000; Taylor *et al.*, 2002). Autoproteolytic maturation cleavage of nodaviral VLPs is dependent

virus particle assembly (Gallagher and Rueckert, 1988). Due to the high degree of similarity between the *Nodaviridae* and *Tetraviridae* autoproteolytic cleavage process (Munshi *et al.*, 1996), particle assembly might also play a role in the autoproteolytic maturation of tetraviral particles.

Lowering of the FBHaSV procapsids pH to 5.0 was able to induce them to undergo autoproteolytic maturation cleavage. Assembled precursor capsid protein subunits rapidly undergo the structural changes from the procapsid to the capsid that allow for autoproteolytic maturation to occur when their pH is lowered (Canady *et al.*, 2000 and 2001; Taylor *et al.*, 2002). The ability of the HaSV precursor capsid protein to undergo autoproteolytic maturation cleavage therefore implied that the precursor capsid protein subunits had assembled into procapsids. These assembled procapsids would then undergo the transitional conformational changes that are required for autoproteolytic maturation cleavage to occur.

Acid maturation of the FBHaSV VLPs however did not result in the autoproteolytic maturation cleavage occurring in all the procapsids. The lack of complete autoproteolytic maturation cleavage might have been due to some of the protein being detected by Western blot analysis being aggregated protein. The inability of all the expressed precursor capsid protein to undergo autoproteolytic maturation *in vitro* was similar to what was observed when the HaSV capsid protein was expressed in yeast cells when their pH was lowered to 5.0 (Venter, 2001). Very little of the yeast expressed precursor capsid protein underwent acid induced autoproteolytic maturation cleavage (Venter 2001). An increase in the incubation time of the acid treated procapsids did not lead to all the precursor capsid protein undergoing autoproteolytic maturation cleavage. Acid induced autoproteolytic maturation cleavage occurs at a much slower rate than spontaneous maturation (Canady *et al.*, 2001; Taylor *et al.*, 2002). However the absence of any further detectable maturation cleavage occurring after 5 hours of incubation implied that all the energy required for proteolysis had been utilised (Zlotnick *et al.*, 1994). Maturation slows down at a rate that is

proportional to the utilisation of the energy required for proteolysis (Gallagher and Rueckert, 1988; Zlotnick *et al.*, 1994). The inability of all the expressed precursor capsid protein to undergo maturation might have been as a result of not all the expressed precursor capsid protein undergoing assembly, as autoproteolytic maturation cleavage is an assembly dependent process (Gallagher and Rueckert, 1988).

The infection of insect cells with a low concentration of infectious particles leads to the host's cellular resources being utilised at a slower rate than when the cells are infected at a high concentration of infectious particles. The rate of cell lysis of the cells infected at a lower rate of infection is also lower. When Sf 9 cells are infected at a low concentration of FBHaSV infectious particles the expressed P71 does not undergo spontaneous maturation while infection at a high concentration of infectious particles leads to the occurrence of spontaneous autoproteolytic maturation cleavage. Cells infected at a low concentration of infectious particles would also be expected to express more protein that has been properly processed by the insect cells secretory pathway as cessation of metabolic activity occurs at a lower rate than cells infected at a high concentration of infectious particles (Nolan and Shatzman, 1998). The protein expressed in insect cells infected at a high concentration of infectious particles was also expected to therefore accumulate as aggregates (Ailor and Betenbaugh, 1999). This was however not observed as infection at a high concentration of infectious particles yielded a high concentration of protein that remained soluble and spontaneously underwent autoproteolytic maturation indicating that it had been properly processed.

5.3 FITC-YVAD Encapsidation by Recombinant HaSV VLPs

Viral vectors have been developed mainly for use as delivery vehicles for genetic material (Nolan and Shatzman, 1998). However Douglas and Young (1998) have shown that it is possible to encapsidate exogenous molecules within a capsid shell by the use of pH dependent opening and gating of pores in the CCMV capsid. Their ability to encapsidate exogenous molecules within

capsids therefore implied that any virus particle that contained pores in its capsid that could be opened and gated in a manner that could be controlled was eligible for use as a delivery vector for exogenous molecules.

Native viruses are protein assemblies that act as host containers for the storage and transport of genetic material (Douglas and Young, 1998). Purified coat protein subunits of many viruses may be assembled *in vitro* into empty virus particles (Smith, 1995). However the precursor capsid proteins of N ω V and FHV assemble into capsids that encapsidate RNA (Schneemann *et al.*, 1993; Agrawal and Johnson, 1995). FHV VLPs encapsidate both their capsid protein mRNA and cellular mRNA while N ω V VLPs specifically and selectively encapsidate their capsid protein mRNA (Schneemann *et al.*, 1993; Agrawal and Johnson, 1995). FBHaSV VLPs were found to encapsidate their mRNA and the ability of the VLPs to encapsidate cellular mRNA was not analysed. It was however unlikely that the FBHaSV VLPs encapsidated cellular mRNA as N ω V VLPs only encapsidated their capsid protein mRNA, and the *Nuduarelia* ω -like viruses are highly similar both structurally and sequentially (Hanzlik *et al.*, 1993 and 1995).

Due to problems encountered with the gradient maker used to pour the sucrose gradients, sucrose gradients that gave reproducible could no longer be poured. Venter (2001) had utilised both sucrose and caesium chloride gradients to successfully separate procapsids from capsids. Caesium chloride gradients were therefore utilised for determining the buoyant densities of the VLPs utilised in the encapsidation experiments

The buoyant density of the FBHaSV VLPs was found to be 1.27g/ml. The buoyant density of wild-type HaSV was found to be 1.296g/ml (Hanzlik *et al.*, 1993). This difference in the buoyant densities of the wild-type HaSV and the FBHaSV VLPs was likely due to the VLPs encapsidating only capsid protein mRNA while wild-type HaSV encapsidates both RNA1 and RNA2 (Hanzlik *et al.*, 1993). The maximum buoyant density at which the FBHaSV VLPs could be

detected was 1.36g/ml with the highest concentration of VLPs found at 1.27g/ml.

Prior to attempting any encapsidation experiments it was established that the FBHaSV VLPs that were produced in Sf9 cells, were procapsids that could be induced to undergo autoproteolytic maturation cleavage. The presence of procapsids was determined by induction the precursor capsid protein to undergo autoproteolytic maturation by lowering the particle pH from neutral to 5.0. NoV particles undergo transitional conformational changes from procapsids to capsids that are required for autoproteolytic maturation cleavage to occur (Canady *et al*, 2000, 2001; Taylor *et al.*, 2002). Observation of the VLP preparations under EM would have also confirmed the presence of procapsids. The use of acid maturation as an indicator of procapsid assembly was also as a result of data obtained by Venter (2001) for HaSV VLPs produced in yeast. Venter (2001), found that only those procapsids that had assembled were able to undergo acid maturation. The ability of the procapsids to undergo autoproteolytic maturation cleavage was important as once the procapsids had encapsidated the exogenous molecule maturation cleavage would be utilised to irreversibly trap the loaded molecule within the capsid. Once VLPs had encapsidated the exogenous molecule their buoyant densities were expected to increase with the increase being attributed to the encapsidated molecule. The increase in the buoyant density of the VLPs that had encapsidated the FITC labelled peptide would have been similar to the shift to the right in the absorbance spectrum of CCMV particles that had been used to encapsidate an anionic organic polymer (Douglas and Young, 1998).

The acid matured FBHaSV VLPs used in the encapsidation of the FITC labelled peptide had a maximum buoyant density of 1.5g/ml. This increase in the buoyant density at which the FBHaSV VLPs could be detected implied that the FITC labelled peptide had been encapsidated by the VLPs. This data could however not be supported by the detection of FITC-YVAD concentrations in these fractions that was higher than that detected in the control samples used in

the elimination of FITC-YVAD that had not been encapsidated but was in the solution (background FITC-YVAD).

This absence of any detectable concentrations of FITC-YVAD in the VLPs used in the encapsidation of the FITC labelled peptide may have been due to the FITC being quenched by the acid utilised in the maturation of the VLPs. FITC is pH-sensitive and its fluorescence is significantly reduced below pH 7.0 (<http://www.probes.com>; 2002). This deduction was however still not supported by the detection of FITC-YVAD concentrations similar to those detected in the background FITC-YVAD fractions with similar buoyant densities. The effect of the acidic buffer utilised in the acid maturation of the VLPs on the FITC labelled peptide may have been determined by the treatment of the FITC labelled peptide with the acidic buffer under conditions that were the same as those used in the acid maturation of the VLPs

5.4 Conclusion and Future Work

The expression of the HaSV capsid protein ORF in *Sf9* cells using a baculovirus vector resulted in the expression of HaSV precursor protein that assembled into procapsids. Infection of *Sf9* cells with a high concentration of infectious particles results in the assembled procapsids spontaneously undergoing autoproteolytic maturation cleavage. The mature capsids are morphologically indistinguishable from wild-type HaSV and encapsidate their capsid protein mRNA.

When the *Sf9* cells are infected at low concentration of infectious particles, the procapsids do not undergo spontaneous autoproteolytic maturation. Maturation cleavage can however be induced by acid treatment of the procapsids. Only a low fraction of the procapsids could be induced to undergo autoproteolytic maturation cleavage regardless of the incubation time. Acid maturation of the procapsids gave inconsistent results and would therefore need to be optimised if the HaSV particles are to be utilised as delivery vectors for exogenous molecules to prohibit uncontrolled ingress and egress of the molecules from the VLPs. Buffers with a high salt concentration have a stabilising effect on the

procapsids (Taylor *et al.*, 2002). Increasing the stability of the VLPs may lead to an increase in the yield of procapsids that are able to undergo acid induced maturation and also increase the consistency at which maturation occurs. Future work will therefore include the induction of autoproteolytic maturation cleavage utilising buffers that have a high salt concentration.

Future work will also include the investigation of the ability of different insect cell lines to produce HaSV VLPs. Different cell lines may express varying amounts of capsid protein. The ability of the secretory pathways of different cell lines to process the expressed protein may affect the amount of expressed protein that remains soluble. For HaSV VLPs to be utilised as delivery vehicles, a large quantity of precursor capsid protein that may assemble into procapsids is required as the procapsids are utilised to load the exogenous molecules.

The ability of the HaSV procapsids to encapsidate exogenous molecules was implied by an increase in the buoyant density of the VLPs that were mixed with the exogenous molecule. The increase in the buoyant densities of these VLPs could however not be substantiated with a detectable increase in the concentration of the exogenous molecule when compared with control samples at similar buoyant densities. Acid quenches the FITC isomer I used to label the peptide encapsidated by the HaSV VLPs. The encapsidation experiments will therefore be repeated utilising peptides labelled with derivatives of FITC that are not quenched at acidic pH, as induction of autoproteolytic maturation cleavage of the procapsids is done in an acidic buffer.

REFERENCES

1. Agrawal, D. K., and Johnson, J. E., 1992, *Sequence analysis of the capsid protein of Nudaurelia capensis ω virus, an insect virus with T=4 icosahedral symmetry*. *Virology* **190**: 806-814
2. Agrawal, D. K., and Johnson, J. E., 1995, *Assembly of the T=4 Nudaurelia capensis ω virus capsid protein, post-translational cleavage, and specific encapsidation of its mRNA in a baculovirus expression system*. *Virology* **207**: 89-97
3. Ailor, E., and Betenbaugh, M. J., 1999, *Modifying secretion and post-translational processing in insect cells*. *Current Opinion in Biotechnology* **10**: 142-145
4. Bac-to-Bac[®] Baculovirus Instruction Manual, GIBCO BRL
5. Ball, L. A., 1992, *Cellular expression of a functional nodavirus RNA replicon from Vaccinia virus vectors*. *Journal of Virology* **66**: 2335-2345
6. Ball, A., 1995, *Requirements for the self-directed replication of Flock House virus RNA1*. *Journal of Virology* **69**: 720-727
7. Ball, L. A., and Johnson, K. L., 1998, *Nodaviruses*. *The Insect Viruses*, Miller, L. K., and Ball, L. A., ed., Plenum Press, New York, 269-299
8. Baker, T. S., Olson, N. H., and Fuller, S.D., 1999, *Adding the Third Dimension to Virus Life cycles: Three-Dimensional Reconstruction of Icosahedral Viruses Cryo-Electron Micrographs*. *Microbiology and Molecular Biology Reviews* **63**: 862-922

9. Berger, B., Shor, P. W., Tucker-Kellogg, L., and King, J., 1994, *Local rule-based theory of virus shell assembly*. Proceedings of the National Academy of Science USA **91**: 7732-7736
10. Berghammer, H., and Auer, B., 1993, *'Easypreps: fast and easy plasmid minipreparation for analysis of recombinant clones in E. coli*. Biotechniques **14**: 527-528
11. Bjerrum, O., and Heegaard, H., 1988, *Immunoblotting- general principles and procedures*. CRC Handbook of Immunoblotting of Proteins Volume1: Technical Descriptions. CRC Press Inc., Florida
12. Canady, M. A., Tihova, M., Hanzlik, T.N., Johnson, J. E., and Yeager, M., 2000, *Large conformational changes in the maturation of a simple RNA virus, Nudaurelia capensis ω virus (N ω V)*. Journal of Molecular Biology **299**: 573-584
13. Canady, M. A., Tsuruta, H., and Johnson, J. E., 2001, *Analysis of rapid, large-scale protein quaternary structural changes: time-resolved X-ray solution scattering of Nudaurelia capensis ω virus (N ω V) maturation*. Journal of Molecular Biology **311**: 803-814
14. Casjens, S., 1985, *An introduction to virus structure and assembly*. Virus Structure and Assembly, Casjens, S. ed. Jones and Bartlett Publishers, Inc. California
15. Cheng, R. H., Reddy, V. S., Olson, N. H., Fisher, a. J., Baker, T. S., and Johnson, J. E., 1994, *Functional implications of quasi-equivalence in a T=3 icosahedral animal virus established by cryo-electron microscopy and X-ray crystallography*. Structure **2**: 271-282

16. Christain, P., and Scotti, P. D., 1998, *The Picorna-like viruses of Lepidopterans*. The Insect Viruses, Miller, L. K., and Ball, L. A., ed., Plenum Press, New York, 269-299
17. Dawson, R. M. C, Elliot, D. C., Elliot, W. H., and Jones, K. M, 1986, *Data for biochemical research*, 3rd ed. Clarendon Press, Oxford, 545-547
18. Douglas, T., and Young, M., 1998, *Host-guest encapsulation of materials assembled by virus protein cages*. *Nature* **393**: 152-155
19. Frolov, I., Hoffman, T. A., Pragai, B. M., Dryga, S. A., Huang, H. V., Schlesinger, S., and Rice, C. M., 1996, *Alphavirus-based expression vectors: strategies and applications*. *Proceedings of the National Academy of Science USA* **93**: 11371-11377
20. Gale, M., Tan, S., and Katze., M., 2000, *Translation control of viral gene expression in eukaryotes*. *Microbiology and Molecular Biology Reviews* **64**: 239-280
21. Gallagher, T. M. and Rueckert, R. R., 1988, *Assembly-dependent maturation cleavage in provirions of a small icosahedral insect ribovirus*. *Journal of Virology* **62**: 3399-3406
22. Glover, L., 2002, *Development of a baculovirus expression system for Nudaurelia capensis ω virus*. Honours Thesis, Rhodes University, South Africa
23. Gorbalenya, A.E., Pringle, F. M., Zeddarn, J., Luke, B. T., Cameron, C. E., Kalmakoff, J., Hanzlik, T. N., Gordon, K. H. J., and Ward, V. K., 2002, *The palm subdomain-based active site is Internally permuted in viral RNA-dependent RNA polymerases of an ancient lineage*. *Journal of Molecular Biology* **324**: 47-62

24. Gordon, K. H. J., Johnson, K. N., and Hanzlik, T. N., 1995, *The larger genomic RNA of Helicoverpa armigera Stunt Tetravirus encodes the viral RNA polymerase and has a novel 3'-terminal tRNA-like structure*. *Virology* **208**: 84-98
25. Gordon, K. H. J., and Hanzlik, T. N., 1998, *Tetraviruses*. The Insect Viruses, Miller, L. K., and Ball, L. A., ed., Plenum Press, New York
26. Gordon, K. H. J., Williams, M. R., Hendry, D. A., and Hanzlik, T. N., 1999, *Sequence of the genomic RNA of Nudaurelia β virus (Tetraviridae) defines a novel virus genome organization*. *Virology* **258**: 42-53
27. Gordon, K. H. J., Lincoln, M., Larkin, P., and Hanzlik, T. N., 2001, *Non-replicative assembly of an insect virus in plant cells*. *Virology* **288**: 36-50
28. Growth and maintenance of insect cell lines, Invitrogen
29. Hanzlik, T. N., Dorrian, S. J., Gordon, K. H. J., and Christian, P., 1993, *A novel small RNA virus isolated from the cotton bollworm Helicoverpa armigera*. *Journal of General Virology* **74**: 1805-1810
30. Hanzlik, T. N., Dorrian, S. J., Johnson, K. N., Brooks, E. M., and Gordon, K. H. J., 1995, *Sequence of RNA2 of the Helicoverpa armigera stunt virus (Tetraviridae) and Bacterial Expression of its Gene*. *Journal of General Virology* **76**: 799-811
31. Hanzlik, T. N., and Gordon, K. H. J., 1997, *The Tetraviridae*. *Advances in Virus Research* **48**: 101-168
32. Hanzlik, T. N., and Gordon, K. H. J., 1999, *Tetraviruses (Tetraviridae)*. *Encyclopaedia of Virology* 2nd Ed., Granoff, A., and Webster, R. G., ed., Academic Press, New York

33. Hendry, D., Hodgson, V., Clark, R., and Newman, J., 1985, *Small RNA viruses co-infecting the Pine Emperor moth (Nudaurelia cytherea capensis)*. Journal of General Virology **66**: 627-632
34. Hendry, D. A., 1991, *Nodaviridae of invertebrates*. Viruses of Invertebrates, Kurstak, E., ed., Marcel Dekker, New York, 277-285
35. Hendry, D., and Agrawal, D., 1994, *Tetraviruses*. Encyclopaedia of Virology. Granoff, A., and Webster, R. G., ed., Academic Press, New York
36. Houk, K. N., Nakamura, K., Sheu, C., and Keating, A. E., 1996, *Gating as a control element in constrictive binding and guest release by hemicarcerands*. Science **273**: 627-629
37. <http://www.probes.com>, 2002
38. Johnson, J. E., 1996, *Functional implications of protein-protein interactions in icosahedral viruses*. Proceedings of the National Academy of Science **93**: 27-33
39. Johnson, J. E., and Chiu, W., 2000, *Structures of virus and virus-like particles*. Current Opinion in Structural Biology **10**: 229-235
40. Juckes, I. R. M., 1979, *Comparison of some biophysical properties of the Nudaurelia β and ϵ viruses*. Journal of General Virology **42**: 89-94
41. Kost, T. A., and Condreay, J. P., 1999, *Recombinant baculoviruses as expression vectors for insect cells and mammalian cells*. Current Opinion in Biotechnology **10**: 428-433
42. Kozak, M., 1991, *Structural features in eukaryotic mRNAs that modulate the initiation of translation*. Journal of Biological Chemistry **266**: 19867-19870

43. Liljas, L., 1999, *Virus assembly*. *Current Opinion in Structural Biology* **9**: 129-134
44. Luckow, V., Lee, S., Barry, G., and Olins, P., 1993, *Efficient generation of infectious recombinant baculoviruses by site-specific transposon-mediated insertion of foreign genes into a baculovirus propagated in Escherichia coli*. *Journal of Virology* **67**: 4566-4579
45. Luque, T., and O'Reilly, D. R., 1999, *Generation of baculovirus expression vectors*. *Molecular Biotechnology* **13**: 153-163
46. Miller, L. K., and Ball, L. A., eds, 1998, *The insect viruses*, Plenum Press, New York, 269-299
47. Miller, D., O'Reilly, D., and Dall, D., 1999, *Insect pest control by viruses*. *Encyclopaedia of Virology 2nd Ed.*, Granoff, A., and Webster, R. G., ed., Academic Press, New York, **3**: 843-849
48. Morton, C. L., and Potter, P. M., 2000, *Comparison of Escherichia coli, Saccharomyces cerevisiae, Pichia pastoris, Spodoptera frugiperda, and COS7 cells for recombinant gene expression*. *Molecular Biotechnology* **16**: 193-202
49. Munshi, S., Liljas L., Cavarelli, J., Bomu, W., McKinney, B., Reddy, V., and Johnson, J. E., 1996, *The 2.8Å Structure of a T=4 animal virus and its implications for membrane translocation of RNA*. *Journal of Molecular Biology* **261**: 1-10
50. Nolan, G. P., and Shatzman, A. R., 1998, *Expression vectors and delivery systems*. *Current Opinion in Biotechnology* **9**: 447-450

51. Oliviera, A. C., Gomes, A. M. O., Almeida, F. C. L., Mohana-Borges, R., Valente, A. P., Reddy, V. S., Johnson, J. E., and Silva, J. L., 2000, *Virus maturation targets the protein capsid to concerted disassembly and unfolding*. The Journal of Biological Chemistry **275**: 16037-16043
52. O'Reilly, D. R., Miller, L. K., and Luckow, V. A., 1992, *Baculovirus expression vectors, a laboratory manual*. W. H. Freeman and Company, New York
53. Pfeifer, T. A., 1998, *Expression of heterologous proteins in stable insect cell culture*. Current Opinion in Biotechnology **9**: 518-521
54. Price, B. D., Rueckert, R. R., and Ahlquist, P. *Complete replication of an animal virus and maintenance of expression vectors derived from it in Saccharomyces cerevisiae*. Proceedings of the National Academy of Science USA **93**: 9465-9470
55. Pringle, F., Gordon, K. H. J., Hanzlik, T. N., Kalmakoff, J., Scotti, P., and Ward, S., 1999, *A novel expression strategy for Thosea asigna virus (Tetraviridae)*. Journal of General Virology **80**: 1855-1863
56. Reddy, V. S., Giesing, H.A., Kumar, A., Post, C. B., Brooks, C. L. 3rd, and Johnson, J. E., 1998, *Energetics of quasi-equivalence: computational analysis of protein-protein interactions in icosahedral viruses*. Biophysical Journal **74**: 546-558
57. Roberts, P. L., 1985, *Infectivity assays for the Autographa californica nuclear polyhedrosis virus using Spodoptera littoralis cells*. Journal of Virological Methods **10**: 1-10
58. Robinson, I. K., and Harrison, S. C., 1982, *Structure of the expanded state of Tomato bushy stunt virus*. Nature **297**: 563-568

59. Rossmann, M. G., and Erickson, J. W., 1985, *Structure and assembly of icosahedral shells*. Virus Structure and Assembly, Casjens, S. ed. Jones and Bartlett Publishers, Inc. California
60. Sambrook, J., Fritsch, E. F., Maniatis, T., 1989. *Molecular cloning, a laboratory manual*, 2nd Ed. Cold Spring Harbour Laboratory Press, New York
61. Schneemann, A., and Marshall, D., 1998, *Specific encapsidation of nodavirus RNAs is mediated through the C terminus of capsid precursor protein alpha*. Journal of Virology **72**: 8738-8746
62. Schneemann, A., Dasgupta, R., Johnson, J. E., and Rueckert, R., 1993, *Use of recombinant baculoviruses in synthesis of morphologically distinct virus like particles of Flock House virus, nodavirus*. Journal of Virology. **67**: 2756-2763
63. Schneemann, A., Zhong, W., Gallagher, T. M., and Rueckert R. R., 1992, *Maturation cleavage required for infectivity of a nodavirus*. Journal of Virology **66**: 6728-6734
64. Smith, A. E., 1995, *Viral vectors in gene therapy*. Annual Review of Microbiology **49**: 807-838
65. Speir, J. A., Munshi, S., Wang, G., Baker, T., and Johnson, J. E., 1995, *Structure of the native and swollen forms of Cowpea chlorotic mottle virus determined by X-ray crystallography and cryo-electron microscopy*. Structure **3**: 63-78
66. Taylor, D. J., Krishna, N. K., Canady, M. A., Schneemann, A., and Johnson, J. E., 2002, *Large-scale, pH dependent, quaternary structure changes in an RNA virus capsid are reversible in the absence of subunit autoproteolysis*. Journal of Virology **76**: 9972-9980

67. Tortora, G. J., Funke, B. E., and Case, C. L., 1995, *Microbiology, An Introduction*, 5th ed. The Benjamin/ Cummings Publishing Company, New York
68. van Regenmortel, M.H.V., Fauquet, C.M., Bishop, D.H.L., Carstens, E.B., Estes, M.K., Lemon, S.M., Maniloff, J., Mayo, M.A., McGeoch, D.J., Pringle, C.R. and Wickner, R.B., 2000, *Virus taxonomy. Seventh report of the International Committee on Taxonomy of Viruses*. Academic Press, New York
69. Venter, A. P. 2001, *Heterologous expression of the Helicoverpa armigera stunt virus in Saccharomyces cerevisiae*. PhD Thesis, Rhodes University, South Africa.
70. Zhang, D., Fu, M., Ma, W., and Chen, D., 2001, *Fluorescent Determination of Noradrenaline and Dopamine Derived With Cy₅ in Capillary Electrophoresis*. *Analytical Sciences* **17**: 1331-1333
71. Zlotnick, A., Reddy, V. S., Dasgupta, R., Schneemann, A., Ray, W. J. Jr., Rueckert, R. R., and Johnson, J. E., 1994, *Capsid assembly in a family of animal viruses primes an autoproteolytic maturation that depends on a single aspartic acid residue*. *The Journal of Biological Chemistry* **269**: 13680-13684

